

E77-10056

CR-144497

GEOLOGIC INVESTIGATIONS IN THE
BASIN AND RANGE OF NEVADA
USING SKYLAB/EREP DATA

"Made available under NASA sponsorship
in the interest of early and wide dis-
semination of Earth Resources Survey
Program information and without liability
for any use made thereof."

FINAL REPORT

JUNE 1975

CONTRACT NO. NAS 9-13274

(E77-10056) GEOLOGIC INVESTIGATIONS IN THE
BASIN AND RANGE OF NEVADA USING SKYLAB/EREP
DATA Final Report (Nevada Univ.) 169 p
HC A08/MF A01

N77-14555

CSSL 08B

Unclass

G3/43 00056

JACK G. QUADE

DENNIS T. TREXLER

Mackay School of Mines
University of Nevada, Reno
Reno, Nevada 89507

Original photography may be purchased from:
EROS Data Center
10th and Dakota Avenue
Sioux Falls, SD 57198

ORIGINAL CONTAINS
COLOR ILLUSTRATIONS

prepared for
PRINCIPAL INVESTIGATIONS MANAGEMENT OFFICE
NATIONAL AERONAUTICS AND SPACE ADMINISTRATION
LYNDON B. JOHNSON SPACE CENTER
HOUSTON, TEXAS 77958

Acknowledgments

We would like to express our gratitude to many colleagues who aided in preparation of this report. Thanks are due to Dr. Wilton Melhorn and Mr. James Frater of Purdue University who prepared the geomorphic analysis of Skylab data. To Mr. Pat Walker, who aided in the structural interpretation and preparation of figures, we are indebted. We would also like to acknowledge Dr. Alan Ryall of the Mackay School of Mines Seismological Laboratory for providing the computer listing of earthquake epicenters in western Nevada and eastern California.

The technical and administrative assistance provided by Dr. David Amsbury of the Principal Investigations Management Office at JSC throughout the duration of this contract is greatly appreciated.

TABLE OF CONTENTS

ACKNOWLEDGMENTS	i
TABLE OF CONTENTS	ii
LIST OF FIGURES	iii
LIST OF TABLES	vi
AIRCRAFT AND SKYLAB DATA PRODUCTS	1
GEOMORPHOLOGY	3
Location and Physical Description of Area	3
Geological Setting	3
Vegetation, Climate, and Land Use	5
Basic Data Products	6
Analytical Procedure	7
General Statement	8
Skylab Frame 2	9
Skylab Frame 3	11
Conclusion	16
Geomorphic Reconnaissance Using S-19' & Frames 1 and 4	17
References Cited	21
FAULT STUDIES NORTH-CENTRAL NEVADA	22
Analytical Procedure	23
Frenchie Creek Quadrangle Area #3	25
Battle Mountain Airport Area #1	26
Trout Creek Area #2	31
Conclusions	33
References Cited	37

RECONNAISSANCE FAULT MAPPING WEST-CENTRAL NEVADA	38
Analytical Procedure	38
S-190A Analysis	39
Summary	40
S-190B Analysis	41
The Gabbs Valley Anticline	42
Summary	47
References Cited	49
COMPARISON OF EARTHQUAKE EPICENTERS TO FAULTS AS MAPPED FROM S-190A DATA	50
Regional Seismic Patterns	50
Faulting and Seismic Activity in the Mina Area	51
References	54
RELATIONSHIP OF METAL MINING DISTRICT TO STRUCTURAL INTERPRETATION OF S-190A	55
A Possible Ore Deposit	56
References	59
LITHOLOGIC MAPPING	60
Multispectral Test Site Description	60
Photographic Data Products	60
Geologic Photomapping	61
Usefulness of S-190B Photographs for Geologic Mapping in Areas of Complex Lithologies	63
Mina NW, 7.5-minute Quadrangle, Nevada	64
INTERPRETATION OF S-192 DATA PRODUCTS	67
APPENDIX A	

List of Figures

1. NASA Aircraft photographic coverage of central Nevada.
2. SL-2 S-190A (Track 6 and 20) Photography of Nevada.
3. SL-3 S-190A photography of Nevada.
4. SL-3 S-190B photography of Nevada.
5. SL-3 S-190B (Track 20) photograph frame index.
6. S-190B frames indexed to 1:250,000 Ams topographic maps.
7. SL-3 S-190B frame 2, geomorphic interpretation of Winnemucca area.
8. SL-3 S-190B frame 3, geomorphic interpretation of Battle Mountain area.
9. U-2 underflight photography, geomorphic interpretation west of Battle Mountain.
10. U-2 underflight photography, geomorphic interpretation of Buffalo Valley.
11. Portion of SL-3 frame 3, geomorphology near Battle Mountain.
12. U-2 underflight photography, geomorphology of Sheep Creek Range.
13. U-2 underflight photography, geomorphology of Argenta Rim.
14. SL-3 S-190B frame 1, geomorphology of the Black Rock Desert.
15. SL-3 S-190B frame 4, geomorphology of Diamond Valley.
16. SL-3 S-190B frame 3, structural map and areas 1, 7 and 3.
17. Crescent Valley Quadrangle (1:62,500) with probable or doubtful faults.
18. U-2 underflight photography, 1:110,000 scale of area #1.
19. U-2 underflight photography 1:30,000 scale of area #1.
20. U-2 underflight photography, 1:110,000 scale of area #2.

21. Looking south in area #2 of prominent fault scarp.
22. Looking southeast in area #2 of two different faults.
23. SL-3 S-190A frame 56, structures and earthquake centers.
24. SL-3 S-190A frame 57, structures and earthquake centers.
25. SL-3 S-190B, frame 12, structures of Walker Lake area.
26. SL-3 S-190B, frame 13, structures of Mina area.
27. SL-3 S-190B, structures and S-192 site locations.
28. SL-3 S-190B, Gabbs Valley Anticline midday.
29. RB-57, underflight, Gabbs Valley Anticline midday.
30. SL-3 S-190A, photography, Gabbs Valley Anticline, M.S. site.
31. Groundbased photography of N.W. dipping beds.
32. Groundbased photography of fault scarp and E. dipping beds.
33. Groundbased photography of the multispectral test site.
34. Geologic interpretation from S-190B, SL-3, track #59.
35. A portion of the geologic map of Esmeralda County, Nevada.
36. The geologic map of the multispectral test site from RC-8 color
ektachrome.
37. RB-57 photograph of the multispectral test site (AMPS system).
38. Geologic map of multispectral test site from AMPS color ektachrome.
39. Geologic interpretation map of S-190B, frames 12 and 13.
40. Geologic map prepared from U.S.G.S. map GQ-45, Mina Quadrangle,
Nevada.
41. Explanation of geologic map (Figure 39).
42. Differentiation of cultivated and uncultivated fields.

43. Differentiation between snow and clouds using different bands.
44. Field operating mode of spectrometer.
45. Site locations used during spectral reflectance studies.
46. Spectral reflectance curves from Crow Springs Mining District.

List of Tables

1. Index list of symbols for geomorphic landforms.
2. Index list of symbols for mountains and valleys, geomorphology.
3. Index list of symbols for SL-3 frame 1, geomorphology.
4. Index list of symbols for SL-3 frame 4, geomorphology.
5. Numerical key for frames 1 through 4, geomorphology.
6. Metal mining district index.
7. Sites S-192 effectiveness comparison.
8. Band usefulness S-192.
9. Lithology band identification S-192.
10. Comparison of various bands in discerning drainage patterns.

AIRCRAFT AND SKYLAB DATA PRODUCTS

Three PB-57 missions were flown on behalf of this investigation. None of the missions were pre-SL-2. The first mission was flown on June 5, 1973. This mission did not cover all of the pre-selected test sites because prior permission to enter restricted airspace over the northern portion of the Nevada Test Site was not obtained. Mission 249 on August 29, 1973 was a pickup mission to obtain photography of the area missed on mission 239. Figure 1 shows the maximum area of coverage of RB-57 RC-8 photography for the three missions.

Mission 249 on September 13 was flown concurrent with Skylab fly-by of ground track 59. Sixty percent forelap was not obtained with the AMPS camera system because of limited magazine capacity. The RC-8 cameras were loaded with B & W infrared and color infrared when they should have contained color Ektachrome and high resolution B & W (S-022 film).

Skylab imagery was obtained over portions of Nevada during SL-2; May 30 and 3 June. Only the S-190A camera system was operating during these passes and abundant clouds covered a large portion of the ~~area~~ ^{frames,} (see figure 2). S-192 imagery was obtained during both passes but only quicklook data of Channels 2, 7 and 11 were received by the Principle Investigator.

During SL-3, three passes were made over the test site. Figures 3 and 4 show the S-190A and S-190B photo coverage, respectively. The first pass was on August 11, 1973 at approximately 0827 local time. At this time the sun angle was approximately 28 degrees. The S-190A system

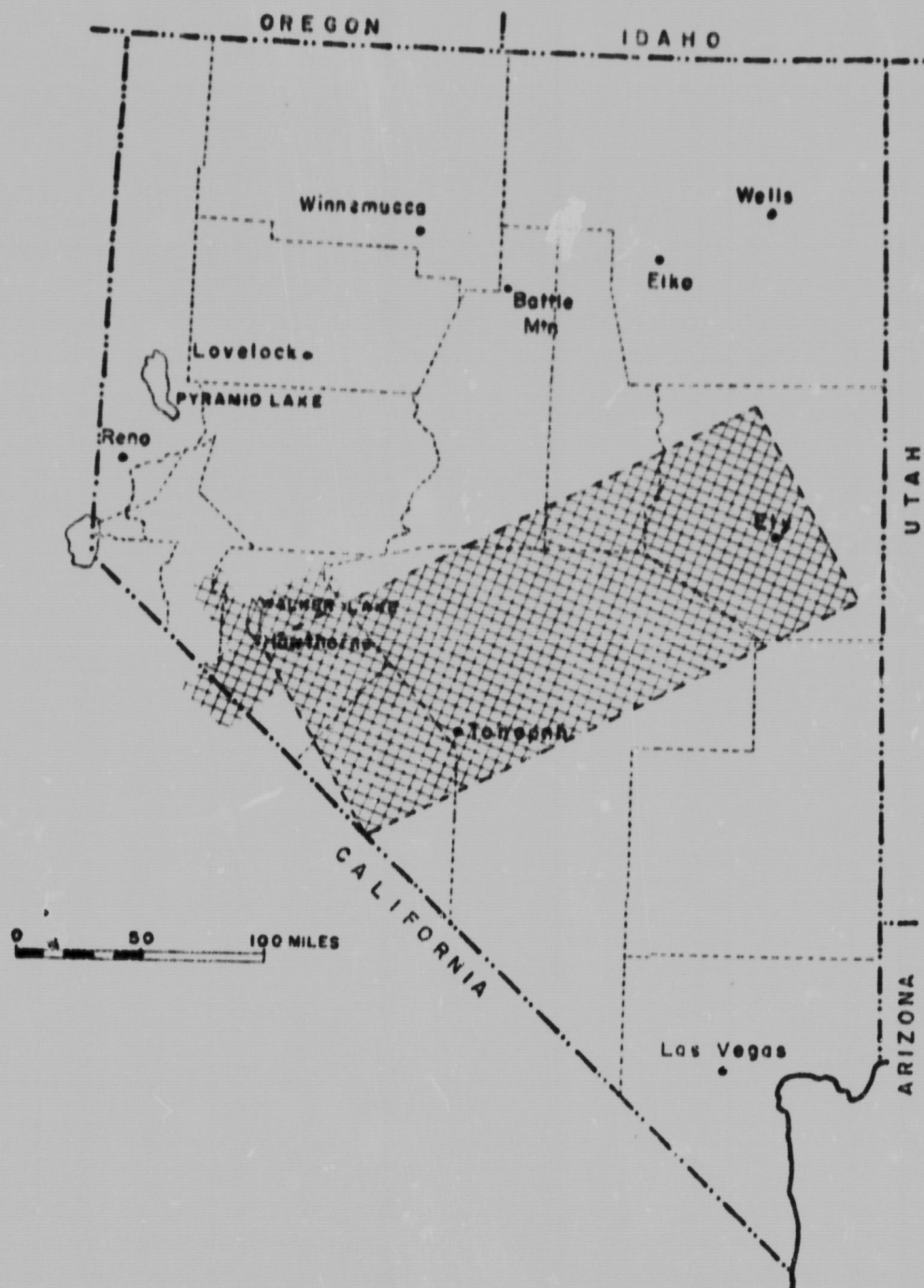


Figure 1. Area of aircraft photographic coverage of central Nevada.

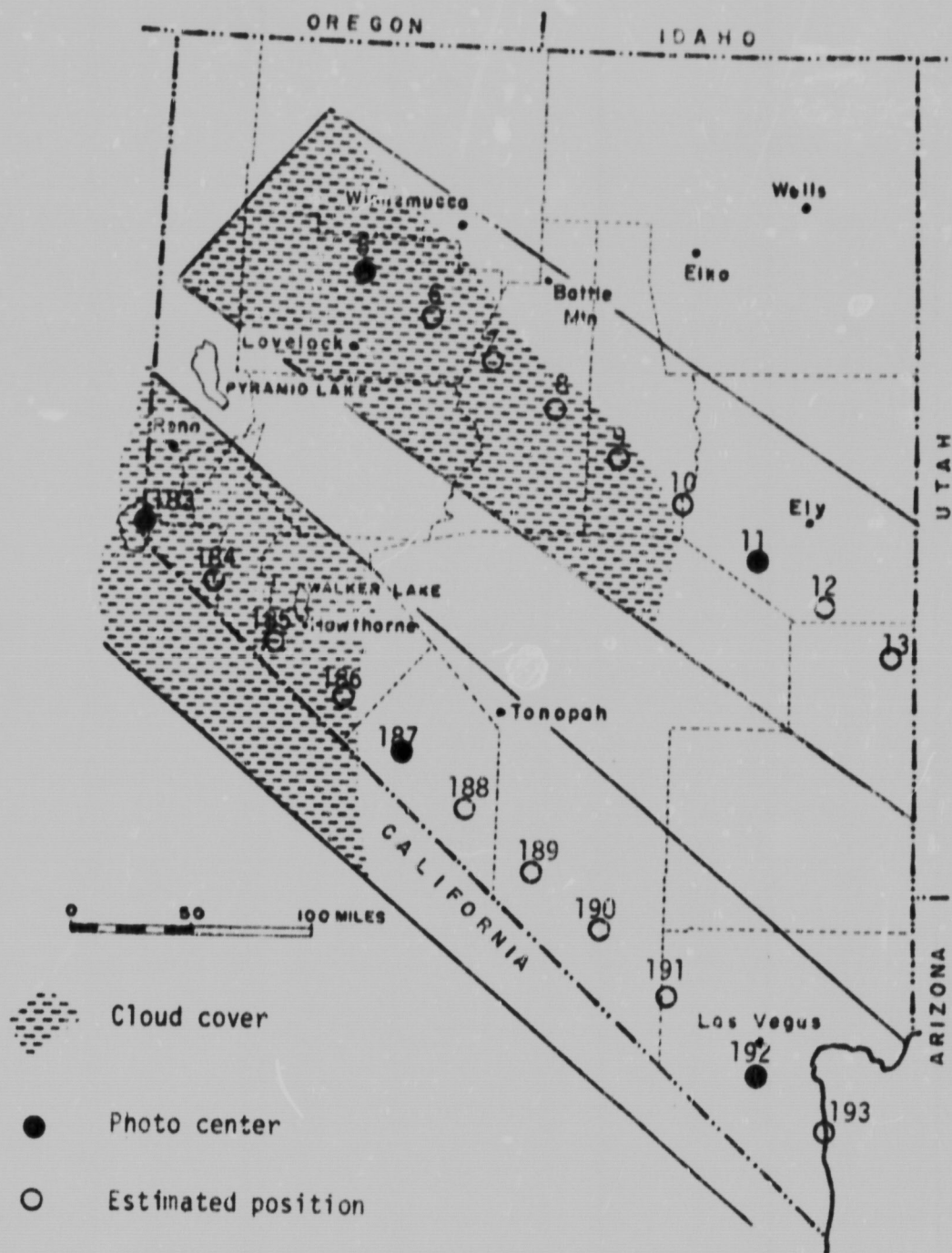


Figure 2. SL-2 S-190A photography of Nevada showing ground tracks 6 and 20, (rolls 1-6).

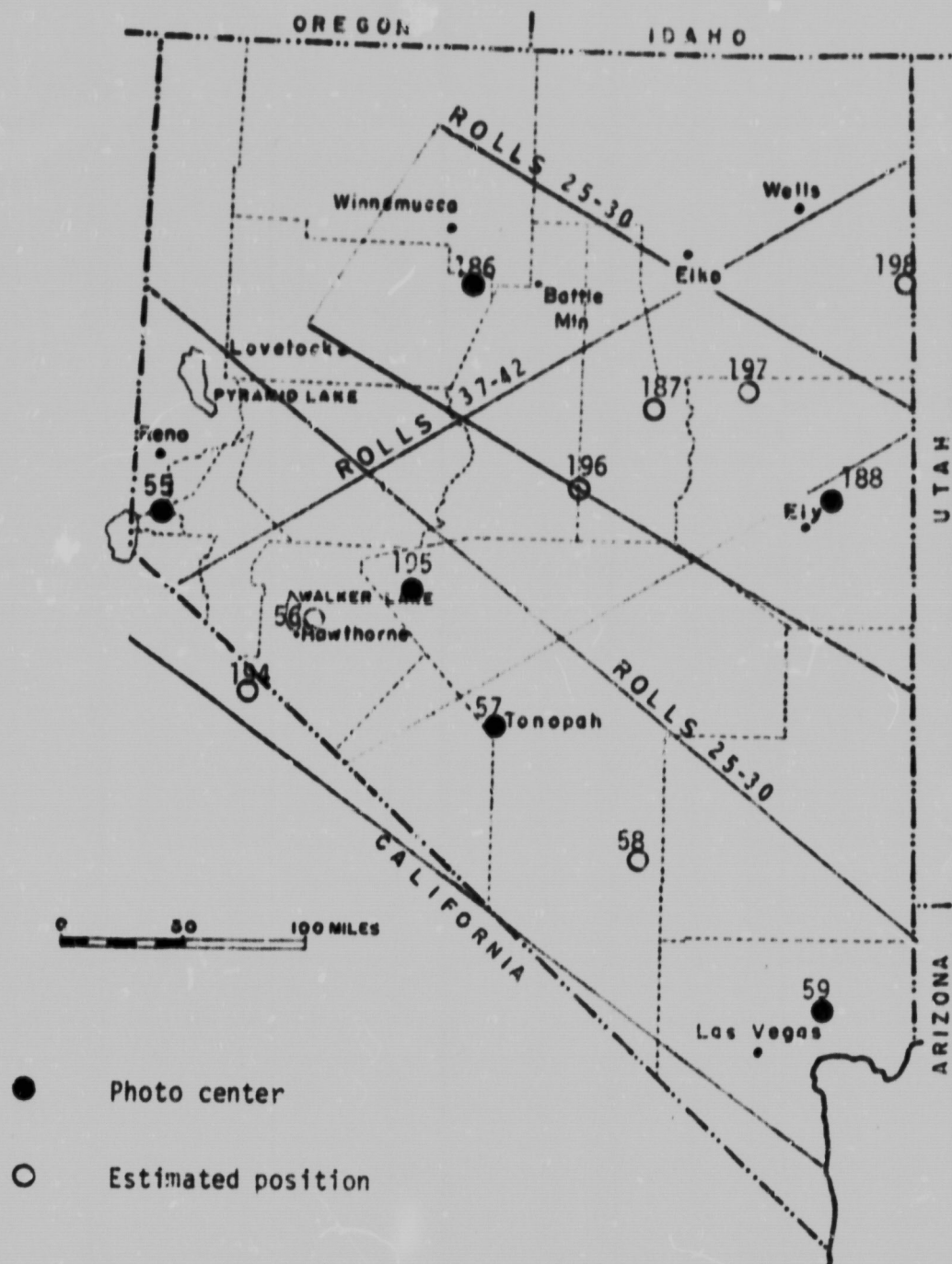


Figure 3. SL-3 S-190A photography of Nevada.

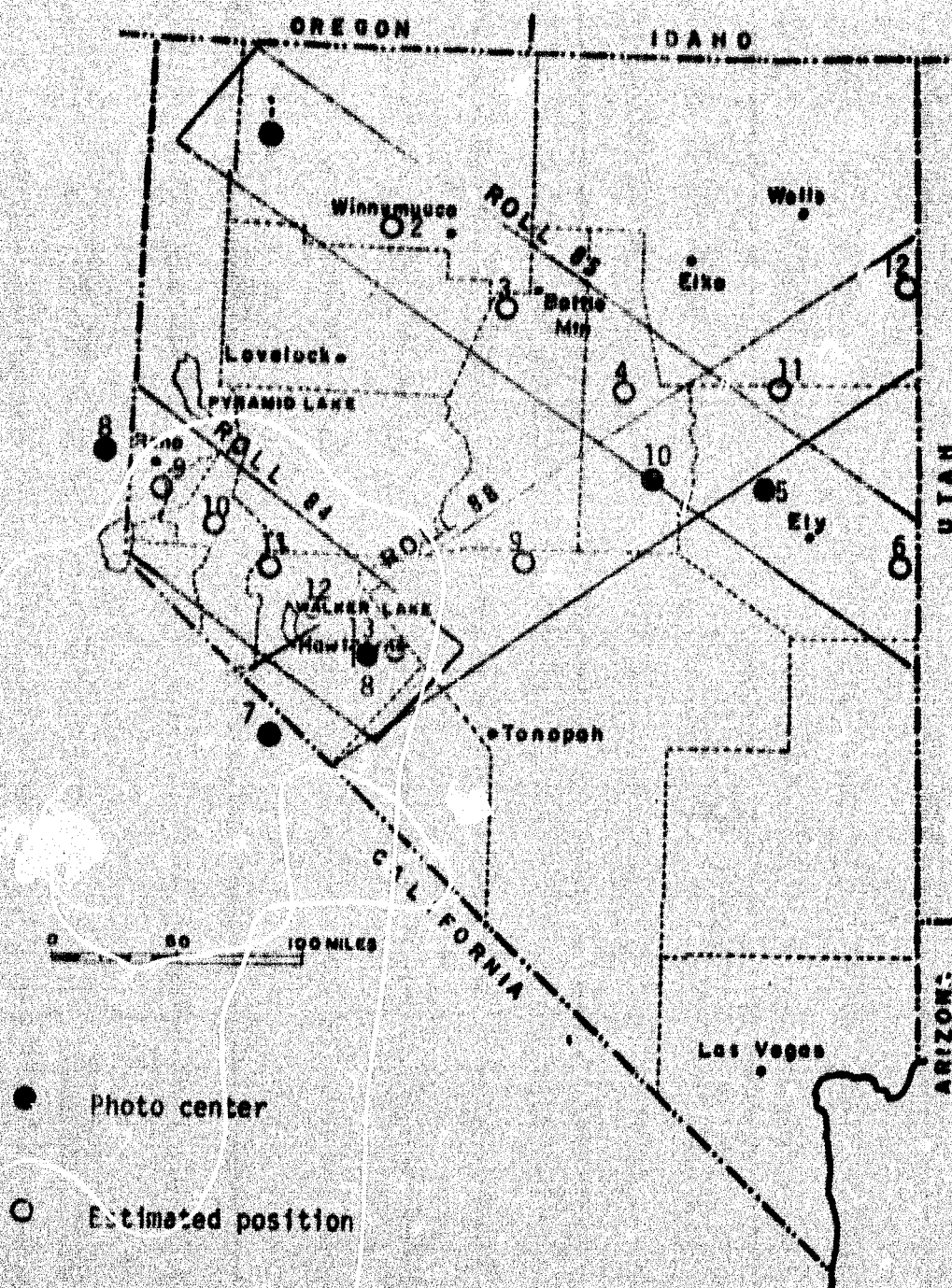


Figure 4. SL-3 S-190B photography of Nevada.

did not produce stereo-overlap and the S-190B camera, which had 60 percent forelap was shut-off over the southern one-half of the state. The second pass was on August 12, 1973 along ground track 20 at approximately

Both the S-190A and S-190B systems did not produce 60 percent forelap photography. The high resolution black and white film in the S-190B camera produced some of the most useful data for structural interpretation because of the low sun-angle. The third pass was on September 13, 1973 along ground track 59. During this pass neither camera system produced 60% forelap.

REPRODUCIBILITY OF THE
ORIGINAL PAGE IS POOR

GEOGRAPHY

Location and Physical Description of Area

The study area in northwestern and central Nevada covers a part of the western sector of the Great Basin (Figure 5). This semi-arid region is characterized by a series of north-south trending mountain ranges separated by long, smoothly sloping alluvial aprons or bajadas leading down to intermontane basins or playas occupying the lowest parts of these basins. The entire area is one of internal drainage without egress to the sea. Runoff, mostly snowmelt, collects in a few permanent saline or alkaline lakes or in dozens of ephemeral playas. Hydrographically the Great Basin is a complex of intermontane salinas, most of which are dry most of the year. (Sheldon, 1966). The only significant perennial stream in the area studied is Humboldt River, which flows westward and terminates in Humboldt Sink. Lesser streams are Quinn River and Reese River.

The average local relief is between 5,000 and 6,000 ft. The valleys are generally slightly more than 4,000 ft. in altitude, and the highest peaks approach 10,000 feet.

Geological Setting

The region is part of a dominantly volcanic province and there are widespread exposures of Tertiary flows, ashfall deposits, and volcanic lacustrine sediments. Locally, Paleozoic sandstones and carbonates are exposed because of pre-volcanic topography or post-volcanic erosion. There are also rather limited outcrops of Tertiary

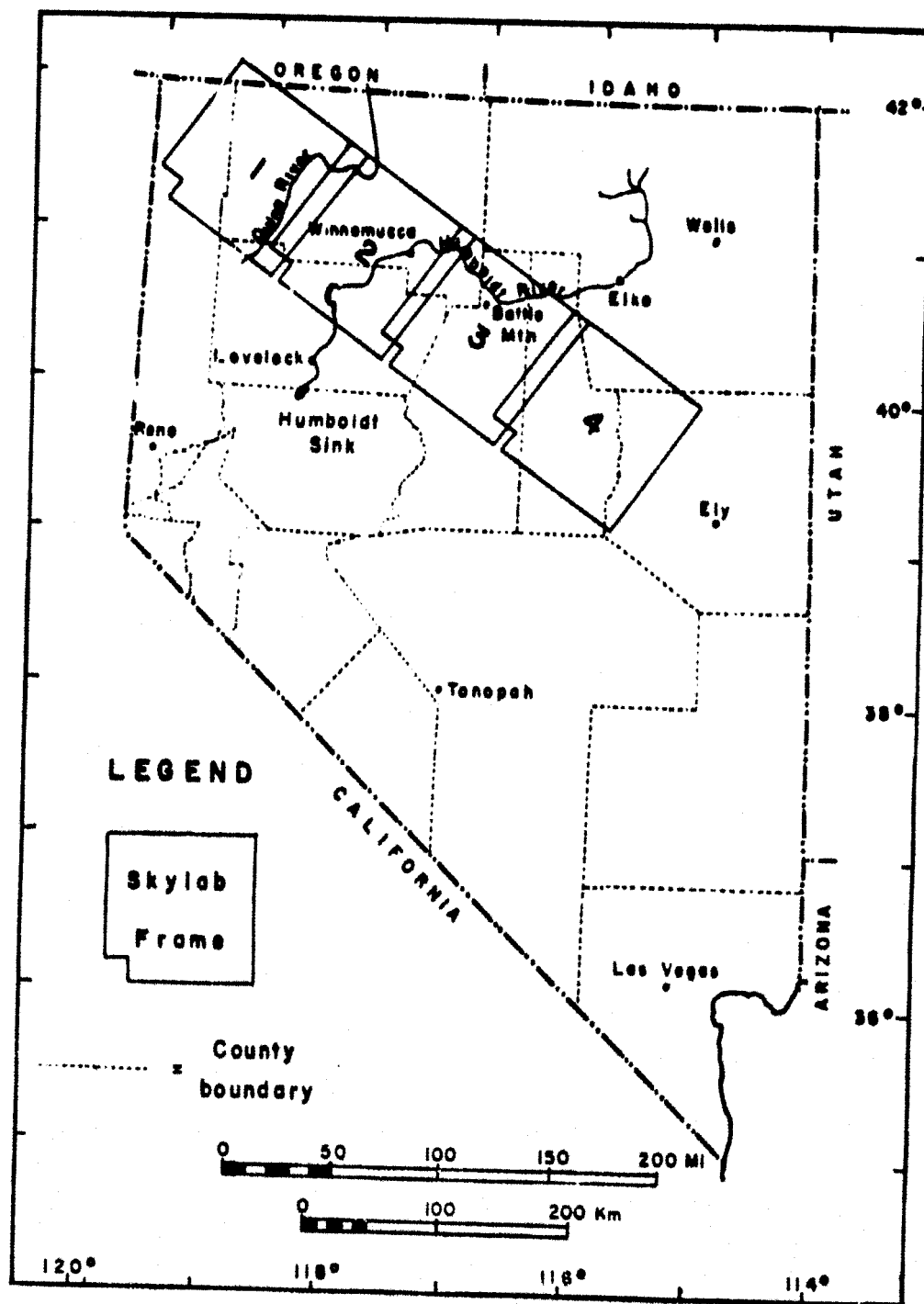


Figure 5. Index map of Nevada showing the location of S-190B frames 1-4, roll 85, on Track 20 August 12, 1973.

granitic intrusions. The basins are infilled mostly with Pleistocene and Holocene alluvial, colluvial, or lacustrine deposits of varying thicknesses. Small areas of glacial deposits may be present around a few high peaks, but these have never been mapped in detail and are not distinguishable on SKYLAB photography of the region. No glacial deposits are definitely identified in the study area covered by the underflight photography.

Vegetation, Climate, and Land Use

Climatic data are sparse but total precipitation ranges from about 4 in/yr in the basins to a maximum of about 16 to 20 in/yr on the high peaks, as estimated from known moisture requirements of various Western tree cover types.

Great Basin sagebrush (Artemisia) is ubiquitous, especially in the basins and on lower slopes of the ranges. Along Humboldt River, particularly downstream from Battle Mountain, there is some intermixture with saltbush (Atriplex), greasewood (Sarcobatus) and saltcedar, along with various low shrubs and grasses. Increasing altitude and moisture is marked by change to juniper-pinyon woodland (Juniperus and Pinus), but stands are generally thin and scattered. The volcanic plateaus of High Rock and Sheep Creek are sagebrush steppe of Artemisia and wheatgrass (Agropyron). Limited mahogany and oak scrub stands (Cercocarpus and Quercus) are scattered across the Shoshone and northern Toiyabe ranges. The highest peaks are above timber line and have a thin cover of grasses approximating a subalpine assemblage. Where water is perennially available in canyons, cottonwood, box elder, and multiflora rose are common. The dunes and playa area west of Winnemucca is bare desert.

Nowhere is vegetation thick enough to obscure geomorphic or geological details as seen on SKYLAB or underflight photography. Land use has been, is, and will continue to be dominated by mining, open-range grazing, and limited irrigation of potatoes, legumes, hay, and alfalfa.

Basic Data Products

Basic data products used in the geomorphic interpretation consist of four cloud-free, black-and-white SKYLAB photographs (numbered 85-001 to 85-004, and here after referred to as frames 1 through 4). U-2 underflight (low sun-angle) photography was obtained at a flight altitude of 65,000 ft. MSL in October, 1974. The SKYLAB frames were obtained on August 11, 1973 by the 18 in. focal length S-190B camera. Original data were second generation 4.5 in. x 4.5 in. black and white diapositives on a scale of 1:936,000. The 17.5 in. x 17.5 in. black-and-white enlarged prints analyzed were made from internegatives of the original data: and thus are fourth generation products on a scale of approximately 1:250,000.

Underflight data were available in two scales and formats, 1:120,000 (9 in. x 9 in.) and 1:30,000 (9 in. x 18 in.). The 9 in. x 9 in. photography was taken by a 6 in. focal length RC-10 camera and the 9 in. x 18 in. photography was taken with a 24 in. focal length HR-732R camera. The resultant 1:120,000 scale and 1:30,000 scale, respectively, assumes a mean terrain elevation of 5,000 ft. Both sets of underflight data were available for most of the same area covered by the U. S. Geological Survey, Winnemucca 2° topographic map. Therefore the detailed analysis described in this paper was restricted to SKYLAB frame 3 most of which lies within the boundaries of the Winnemucca sheet (Figure 6).

The enlarged scale of the SKYLAB frames used closely approximates the 1:250,000 scale of the 2° topographic maps. Use of three different photographic scales in conjunction with these topographic maps allowed detailed analysis in some key areas. Ground control consisted primarily of the topographic maps and published county geologic maps, although

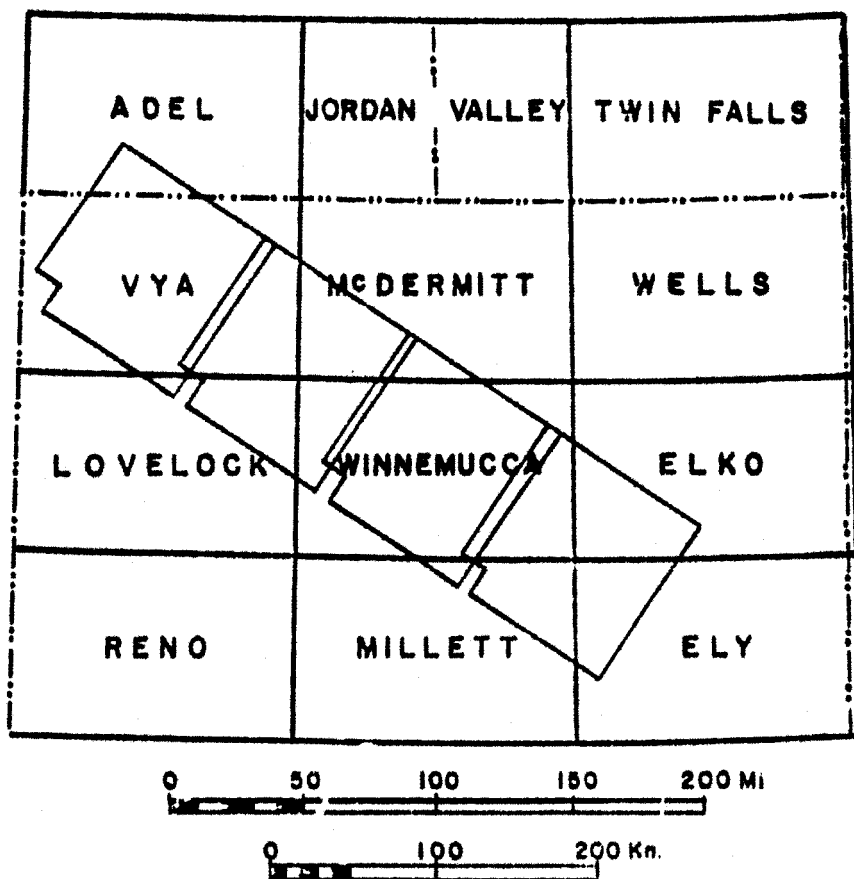


Figure 6. Index map showing the location of S-1908 frames 1-4, roll 85 on 1:250,000 AMS topographic maps.

limited ground truth was available. Some larger scale topographic maps were available and were used where better detail was needed to delineate interesting geomorphic features.

It must be noted that the SKYLAB frames are perspective photographs and because of the Earth's curvature distortion increases outward from the center point of the frame. For the reconnaissance mapping undertaken, however, this problem is relatively unimportant. Scalar approximation between topographic maps and photographs is ample for the correlative work of topographic elevation and strandline occurrence described in a subsequent section.

Analytical Procedure

Mylar overlays were fitted over each of the four SKYLAB frames, and letters were used to label mountain ranges and basins as identified from the topographic sheets. This was done for orientation and to facilitate written description of the area. Geomorphic analysis and interpretation of landforms was then completed. A number was assigned to each landform and written on the mylar overlay instead of the landform name in order to avoid cluttering. Landforms were numbered as identified, hence there is no specific ordering scheme. Continuity was established by labeling similar landforms with the same number on all four frames. For example, landslides were assigned "1" on frame 1, thus a "1" on any of the four frames indicates some type of landslide. The key for each frame includes all landforms to each mountain range and valley, and also any supplemental notations made during the mapping.

Aerial photographic terrain analysis of each SKYLAB frame was initially accomplished by: 1) tonal variation indicating surface or near surface ground conditions, 2) recognition of topography as deduced

from shadow effects, drainage patterns, and topographic base maps, 3) drainage patterns indicating the type of parent rock and soil materials which in turn influences amount and type of runoff, 4) vegetation and land use, 5) landform association with surrounding features or 6) any combination of these factors. An impression of ~~stereoscopic~~ ^{stereophics} may be obtained if B & W diapositives at the original scale are viewed through a binocular microscope.

However, these products were not in hand for use in this study, and no stereoscopic analysis was possible on the SKYLAB products in the form used because there is virtually no overlap. Therefore photographic interpretation was necessarily limited to simple pattern and textural recognition and the relationship of a given feature to its surroundings. After this initial analysis, the U-2 photography which covered parts of the Winnemucca topographic sheet was used for detailed analysis of parts of SKYLAB frame 3 (Figure 6). Stereoscopic vision is possible with both scales of U-2 photography and thus added the valuable third dimension to the interpretation. Thus underflight data were used to enhance landforms already mapped and to locate landforms previously unrecognized.

General Statement

Geomorphic mapping was completed for all four SKYLAB frames, but owing to repetition of landform types or families, the need for brevity, and availability of underflight coverage for only one SKYLAB frame (Frame 3), only SKYLAB frames 2 and 3 are discussed herein. Most landforms mapped in the study area are represented on these frames and a discussion of scalar problems in interpretation can be undertaken from the two frames selected.

Comparison of results for the three different scales used (1:250,000, 1:120,000 and 1:30,000) is interesting. The lack of stereoscopic capability from the enlarged SKYLAB photography is unfortunate, but this problem is remedied by resort to underflight data. SKYLAB's synoptic view of the Earth's surface provides an insight unique to this scale. In fact, large structural and geomorphic features never before seen on this scale stand out clearly, whereas only small, discrete parts of these features could be studied from previous photographs and thus the relationships and distribution of major features had not been recognized.

Conversely, owing to the small scale of the original SKYLAB photography, resolution elements are necessarily large. Because SKYLAB photography is of such high quality, however, enlargement up to 4 diameters is possible with excellent results if precision equipment is used. Enlargement capability restores much detail lost on the small-scale original photographs. However, with enlargement some interpretative insight still is lacking because of no stereoscopic coverage.

SKYLAB Frame 2

SKYLAB frame 2 (Figure 7) is an example of the 1:250,000 scale photography used. This frame is exemplified by typical Basin and Range topography. The only perennial rivers, the Quinn and the Humboldt, traverse this area. Except for these two rivers intermontane, closed-basin drainage is typical. Many geomorphological and cultural features can be discerned. Agricultural areas, with conspicuous rectangular fields and center-stand irrigation systems are obvious in the valleys. Major roads are traced as they follow along valleys or cut across a mountain pass. Abandoned strandlines formed by Pleistocene lakes, a large band

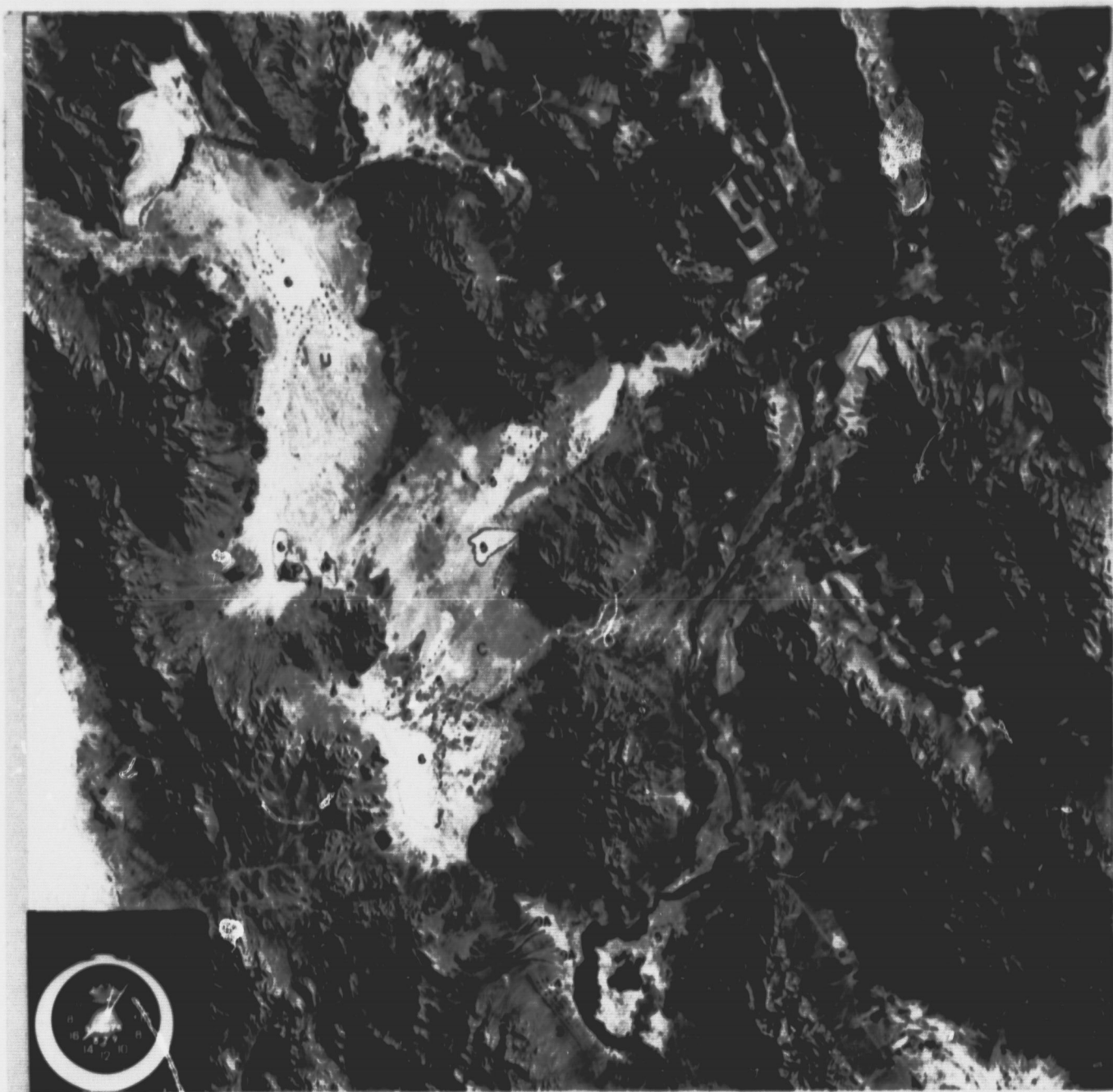


Figure 7. SKYLAB S-190B frame 2, roll 85, scale 1:602,000. Overlay provides geomorphic interpretation. Numbers and letters identified in tables 1 and 2.

REPRODUCIBILITY OF THE
ORIGINAL PAGE IS POOR

Table 1 - List of symbols for landforms.

Landform number	Name	Present on SKYLAB	
		frame 2	frame 3
1	landslide		x
2	louderback	x	x
3	wave cut bench	x	
4	strandlines	x	x
5	dunes	x	
6	playa	x	x
6a	playa lake		x
			x
7	fault-line trace	x	x
7a	fault trace	x	x
8	bajada	x	x
8a	pediment	x	x
9	alluvial fan	x	x
9a	compound fan	x	x
10	spring/seepage area	x	
11	perennial lake	x	
11a	Rye Patch Reservoir	x	
12	intermittent lake	x	
12a	Pitt-Taylor Reservoir	x	
15	urban area	x	x
15a	Winnemucca	x	
15b	Battle Mountain		x
17	plateau		x
17a	mesa	x	
17b	butte	x	
18	inselberg	x	
19	volcanic cone		x
22	watergap		x
23	perennial river	x	x
23a	Humboldt River	x	x
23b	Quinn River	x	
50	fanhead trench	x	x

Table 2 - List of symbols for mountains and valleys

SKYLAB FRAME 2

Symbol	Name	Symbol	Name
AA	Kama Mountains	N	Winnemucca Mountain
A	Bilk Creek Mountains	O	Bloody Run Hills
B	Sonoma Range	P	Dev Hills
C	Humboldt Range	Q	Slumbering Hills
D	Jackson Mountains	R	Double Mountains
E	Maiuba Mountain	S	Junco Hills
F	Blue Mountain	T	Buena Vista Valley
G	Coyote Hills	U	Desert Valley
H	East Range	V	Grass Valley
I	Eugene Mountains	W	Paradise Valley
J	Hot Springs Range	X	Silver State Valley
K	Osgood Mountains	Y	Kings River Valley
L	Santa Rosa Range	Z	Lone Butte
M	Krum Hills		

SKYLAB FRAME 3

A	Shoshone Range	N	Reese River Valley
B	Battle Mountain	O	Crescent Valley
C	Fish Creek Mountains	R	Whirlwind Valley
D	Tobin Range	S	Boulder Valley
H	Sheep Creek Range	X	Buffalo Valley
M	Tuscarora Mountains	Z	Argenta Rim

of playa-born sand dunes, compound fans, railroad tracks, urban areas, and springs or seeps, are visible.

The Great Basin presently is an arid region, but during the Quaternary the climate was probably colder and more humid, and at times the valleys were occupied by pluvial lakes. Some of these lakes had outlets to the sea (or into sister lakes) but the majority did not rise high enough to find such an outlet. (Snyder and others, 1964). The history of the largest Quaternary lake, Lake Bonneville, has been described by Gilbert, (Gilbert, 1890). The second largest, Lake Lahontan, (Russell, 1885), located in northwestern Nevada, occupied much of the area covered by SKYLAB frame 2.

Russell recognized four "terrace" levels (hereafter called strandlines), at elevations of approximately 4,380, 4,350, 4,190, and 4,000 ft. Only small, laterally discontinuous portions of these strandlines still are evident around the periphery of many of the basins ~~because of~~ ~~because of~~ ~~because of~~ encroachment by alluvial fans, deflation, and complications from seasonal salina shoreline processes. All strandlines mapped on frame 2 can be correlated with the two highest elevations (4,380 and 4,350 ft.) as noted by Russell (1885) and Morrison (1964). Correlation is established by overlaying the proper 2⁰ topographic map with the frame (Figure 6). This correlation should be done with caution, because distinction between strandline, wave-cut benches, and curvilinear fault traces is locally difficult.

The most impressive landform shown on frame 2 is the band of sand dunes originating at the playa in Desert Valley and extending across two mountain ranges, the Slumbering Hills and the Santa Rosa Range, and into Paradise Valley. Resolution on the SKYLAB photography permits identi-

fication of these as crescent dunes. The deflation effect of the prevailing wind direction in this area is obvious. Dune structures can be traced for 30 miles from their source.

Compound fan development is distinguished by tonal variations of alluvial fan material. This variation probably results from differences in the amount of desert varnish accumulated on exposed surfaces of alluvial material in the fans. It is inferred, therefore, that the darker materials are older than, and underlie, the lighter materials. This is the same assumption that Hooke et al (1969) tacitly made in their electron microprobe study of desert varnish on a California compound fan. At least two and possibly three stages of fan development can be ascertained by recognition of as many different photo tones. Caution should be exercised because tonal changes may also represent lithological differences of the fan material. Fanhead trenches, also present on frame 2, are discussed subsequently.

Numerous springs occur in the area of frame 2, and those discernable as such were mapped. A rather large area of hot spring activity (Leach Hot Springs), as indicated on the Winnemucca topographic map, is visible in southern Grass Valley (labeled "V") just south of Winnemucca.

SKYLAB Frame 3

Figure 8 shows Battle Mountain and a prominent playa in Buffalo Valley. Note the short lineation (labeled "7a") just to the west of Battle Mountain. This appeared to be a fault scarp, but its hummocky appearance and limited areal extent indicated the possibility that it was the toe of some type of mass movement, possibly an earthflow, (Thornbury, 1969). Stereoscopic inspection of the same area on the scale of 1:120,000 (Figure 9) reinforced the fault interpretation. The hummocky

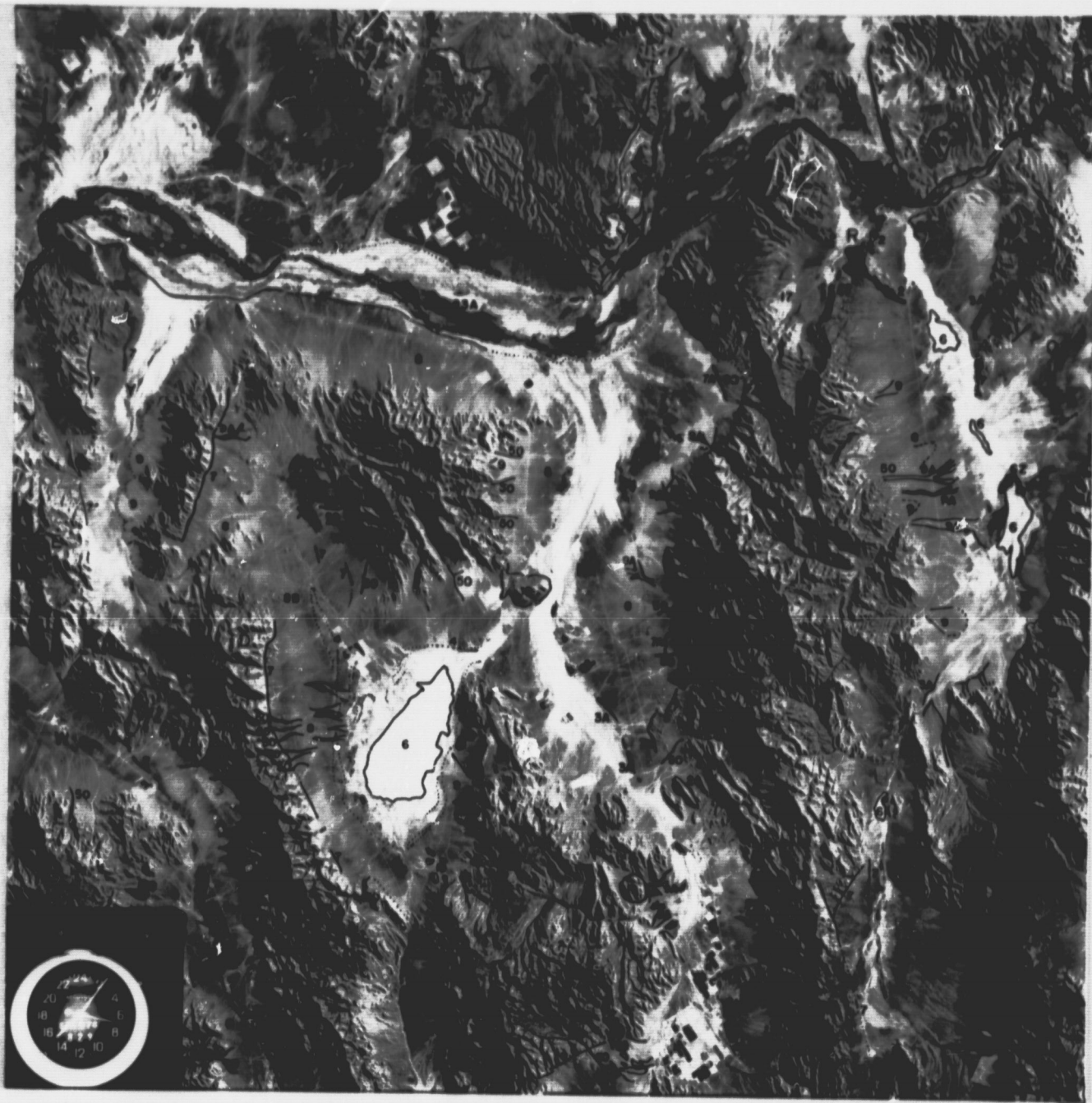


Figure 8. SKYLAB S-190B, frame 3, roll 85, scale 1:602,000. Overlay provides geomorphic interpretation. Numbers and letters identified in tables 1 and 2.

REPRODUCIBILITY OF THE
ORIGINAL PAGE IS POOR

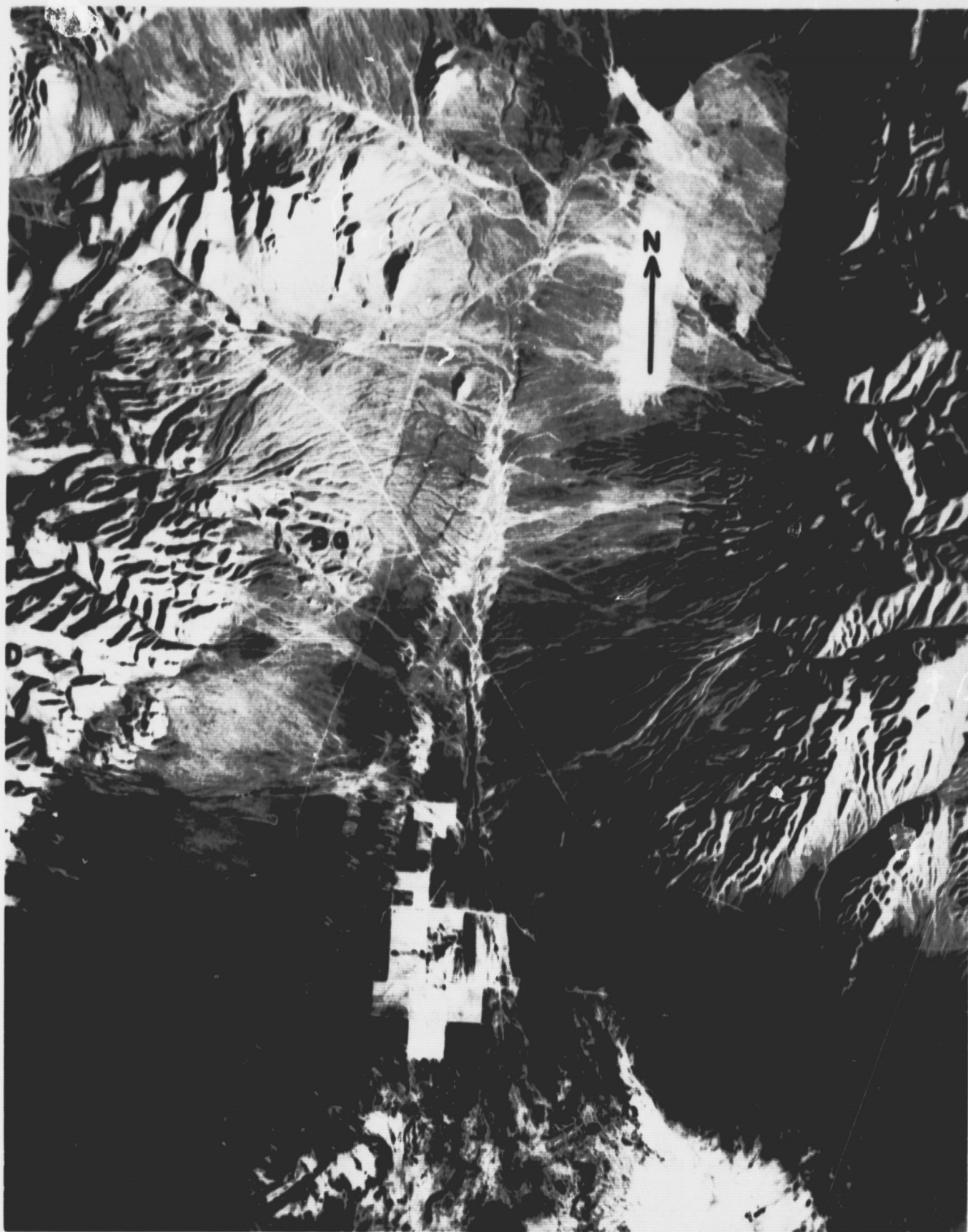


Figure 9. U-2 underflight photography showing west side of Battle Mountain (B) and adjacent Tobin Range (D). Notice small escarpment (7a), just west of Battle Mountain and similar, more highly dissected area (8a) on the east side of The Tobin Range. Original scale 1:120,000.

REPRODUCIBILITY OF THE
ORIGINAL PAGE IS POOR

texture perceived on the SKYLAB frame can instead be seen on the under-flight photography as a dissected area. Four additional observations preclude the possibility that this is some type of flow. First, with stereoscopic inspection, another scarp is discerned (at the mountain front) that continues through the suggested "flow" area. If this area is flow material this scarp would have been obliterated, unless faulting occurred after flowage. Secondly, there are no scalloped indentations of the mountain front to indicate where the flow material originated. Furthermore, owing to the extreme vertical exaggeration of the short focal length camera that recorded the 1:120,000 scale photography (Figure 9), and in viewing a stereo pair through a mirror stereoscope (or any stereoscope with a large field of view), it can be seen that this area is a topographic high. This can be inferred without use of stereoscopic equipment by observing the drainage pattern. The stream courses bend away from this topographic high on both the north and south sides. Finally, a slightly lower order of dissection can be discerned in the mountainous area adjacent to the area under consideration. A logical explanation is that this area is a bedrock high with alluvial fans covering it on both sides. This interpretation is supported by the presence of a similar structure (labeled "8b") across Buffalo Valley on the east side of the Tobin Range (Figure 9). If this is the case, the small linear escarpment on the west side of Battle Mountain is a fault, the area just to the east is a dissected pediment (labeled "8b"), and the straight mountain front is a fault-line scarp. Note the small alluvial fan developed over the pediment on the south side (Figure 9).

Identification of such exhumed or only thinly veneered pediments are significant because of their potential as mineralized areas. The

dissected pediment on the west side of Battle Mountain, described in the preceding paragraph, has been extensively prospected by pits and adits adjacent to the fault, and a small amount of gold has been produced. It is reasonable to assume that other favorable prospect areas are present 1) northward along the west side of Battle Mountain, 2) along the east side of the Tobin Range ("8a" on Fig. 4), and possibly 3) in the sag or saddle connecting these two areas. The rock-floored pediment, from analysis of the SKYLAB photography, is probably quite thinly veneered with alluvial or fan material in these areas and thus is a feasible target for shallow exploration.

Fanhead trenches, a common and obvious feature on frame 3 (Figure 8), are channels which either 1) cut into an alluvial fan at its apex and subsequently grow downfan or 2) are initially cut into the toe of the fan and then migrate upfan. In case 1) they have been interpreted as a normal evolutionary stage ^{of} an alluvial fan as mountain streams continue downcutting, (Gilbert, 1890). They may also represent the lowering of base level of the streams or basins in the valleys to which they are tributary, as in case 2). More recently they have been interpreted as representing response to changes in rainfall intensity, (Bull, 1964) reestablishing a gradient in accord with existing discharge and load conditions, (Denny, 1965). They have also been described in connection with the relationship of mudflows to fan and fanhead development, (Beaty, 1963 and Lustig, 1965).

Strandlines marking former lake levels, such as those in the southern end of Buffalo Valley, are easily discernible on the SKYLAB photography (Figure 8), except where masked by other aggradational forms.

With the aid of a magnifying lens they can be mapped with less difficulty. Much more detail is recognized on the large-scale underflight photography (Figure 10), including the complex relationships between strandlines and alluvial fans. In some places strandlines seem to truncate fans, whereas elsewhere a fan continues across the strandlines, indicating that fan development has occurred after the high stand of the lake. On the SKYLAB frame some strandlines ~~are~~ ^{have the same} ~~are~~ ^{as} the fans. Even with magnification, delineation of strandlines through alluvial material is difficult.

A different scalar problem is exemplified by the Sheep Creek Range. Preliminary analysis of the SKYLAB frame revealed three distinct volcanic cone forms (Figure 11). Another roughly circular area of a photo tone similar to the obvious cones also appeared to be a remnant cone (a dashed line on Figure 11). When the underflight photography of this area was examined, there seemed to be no sign of this volcanic cone (Figure 12). However, to erase the landform identified on the SKYLAB frame overlay would be self-defeating. The underflight photography was intended as a data enhancement tool, not a primary reference. The fact that this form did not show clearly on large-scale photography is merely a scalar problem. Each integral element seen on the large-scale photography was not enough clue in itself to depict the entire landform. On the small-scale SKYLAB photography (Figure 11) the combination of photo tone, geometrical pattern, and landform associations in the area led to the correct conclusion.

The importance of stereoscopic vision cannot be overestimated. An excellent example occurs on the east side of the Sheep Creek Range (Figure 11). This area was not recognized as a huge landslide block until

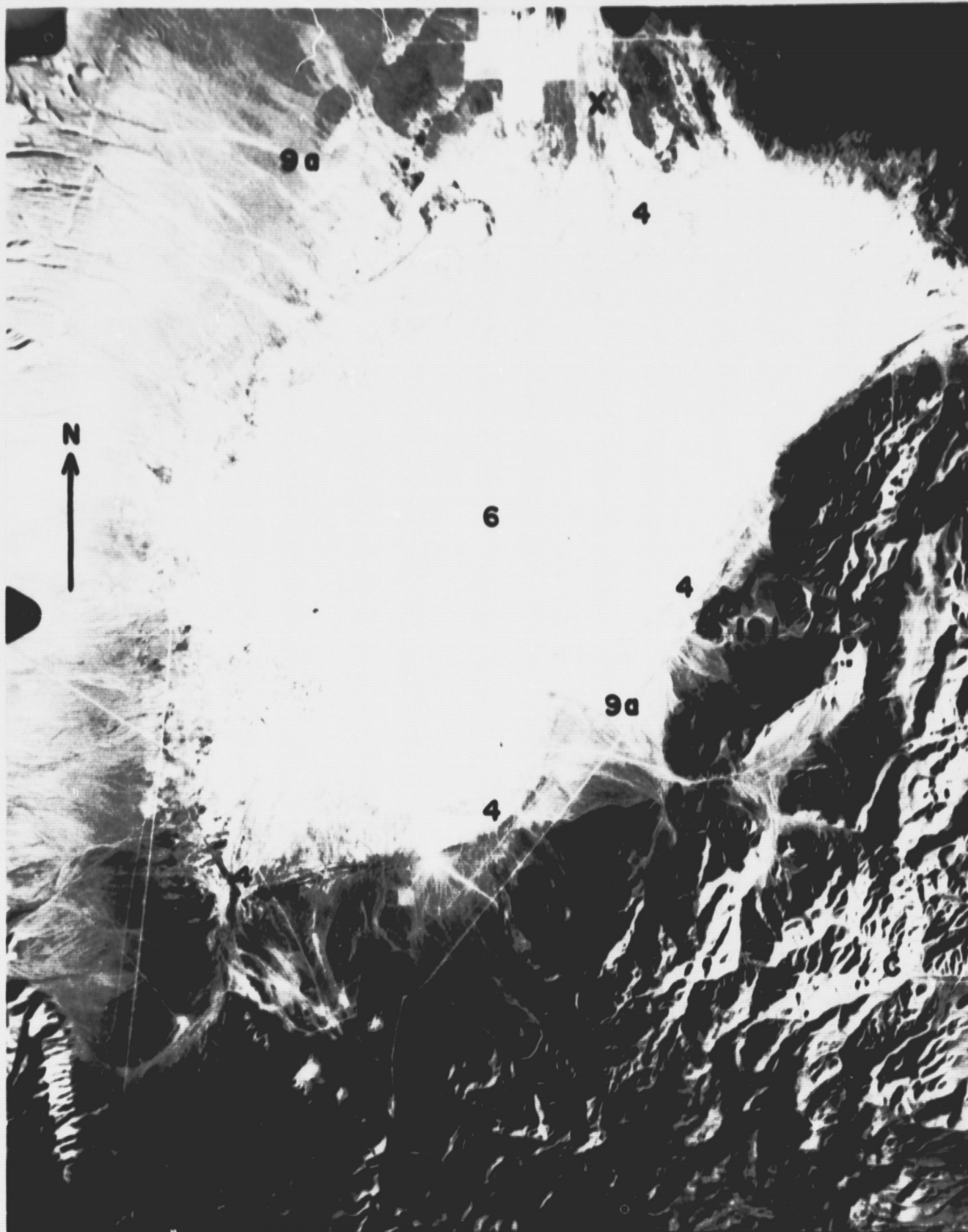


Figure 10. U-2 underflight photography showing well developed playa in Buffalo Valley (X). Note strandlines (4) possibly formed by glacial Lake Lahontan, volcanic cones (19) and compound alluvial fan formation (9a) as interpreted by three gray tones. Original scale 1:120,000.



Figure 11. Portion of SKYLAB frame 3 showing Sheep Creek Range (H), Humboldt River (23a), and Argenta Rim (Z). For identification key refer to Tables 1 and 2. Original scale 1:250,000

examined stereoscopically on the underflight photography (Figure 12). This landslide area is at different elevations and that the intervening light areas are scarps along which movement has occurred. This area was therefore mapped on the SKYLAB frame as a landslide.

There are several different drainage patterns on the Sheep Creek Range (Figure 11). Attempts to explain this apparent anomaly using only SKYLAB photography were speculative. Knowing that volcanics occur on the east side of the range, it was postulated that intense dissection of the western portion starts at the perimeter of the basalt that caps the range (Willden, 1963). With larger-scale underflight photography it is noted that this caprock exists over the entire range (Figure 12), but it has been dissected on the west side and only remnants remain on the tops of interstream divides ("c" on Figure 12). It is reasonable to assume that this caprock is thinnest this far removed from the volcanic cones, explaining the apparent greater degree of dissection. The prominent straight gully may represent a fracture along which dissection has been maximized.

An antiformal flexure is indicated by the Sheep Creek Range, which dips almost north, and Argenta Rim, which dips south. The axis of this structure lies somewhere between the Sheep Creek Range and Argenta Rim and appears to parallel the Humboldt River valley. The Humboldt may have followed the path of least resistance by flowing along a fracture zone that developed along the crest of this antiform.

Argenta Rim appears to be capped by a large plate of basalt (Figure 11), and was so mapped by Willden (1963). Although the whole area may be mostly basaltic, Argenta Rim is not completely covered by a resistant basalt layer. It appears on the underflight data to be capped by

louderbacks or, more precisely, louderback lava flows (Figure 13). A louderback is defined by the A.G.I. glossary as "a remnant of a lava flow appearing in a tilted fault block and bounded by a dip slope. It is named after George D. Louderback, a North American geologist, who used it as evidence of block faulting in basin and range topography". Fairbridge (1968) states that "where base level has been lowered, the louderback stands out as a special type of lava capped mesa, coulee or abutment". This definition is applicable to Argenta Rim and the Sheep Creek Range.

Conclusion

SKYLAB's synoptic view of the Earth's surface provides insight into geomorphological interpretation never before available. This photography in its original scale of 1:936,000 and the enlarged scale of 1:250,000 is excellent for reconnaissance interpretation. However, with these scales and no stereoscopic coverage, there is a decrease in detail and interpretative capability.

Conversely, through observation, experience, and intuitive insight, large magnitude landforms can be perceived for the first time in their entirety. Previous missions involving low altitude large-scale photography allowed viewing only of smaller components of these landforms. With SKYLAB's synoptic view these "macro landforms" become visible and can be related to other geomorphic elements.

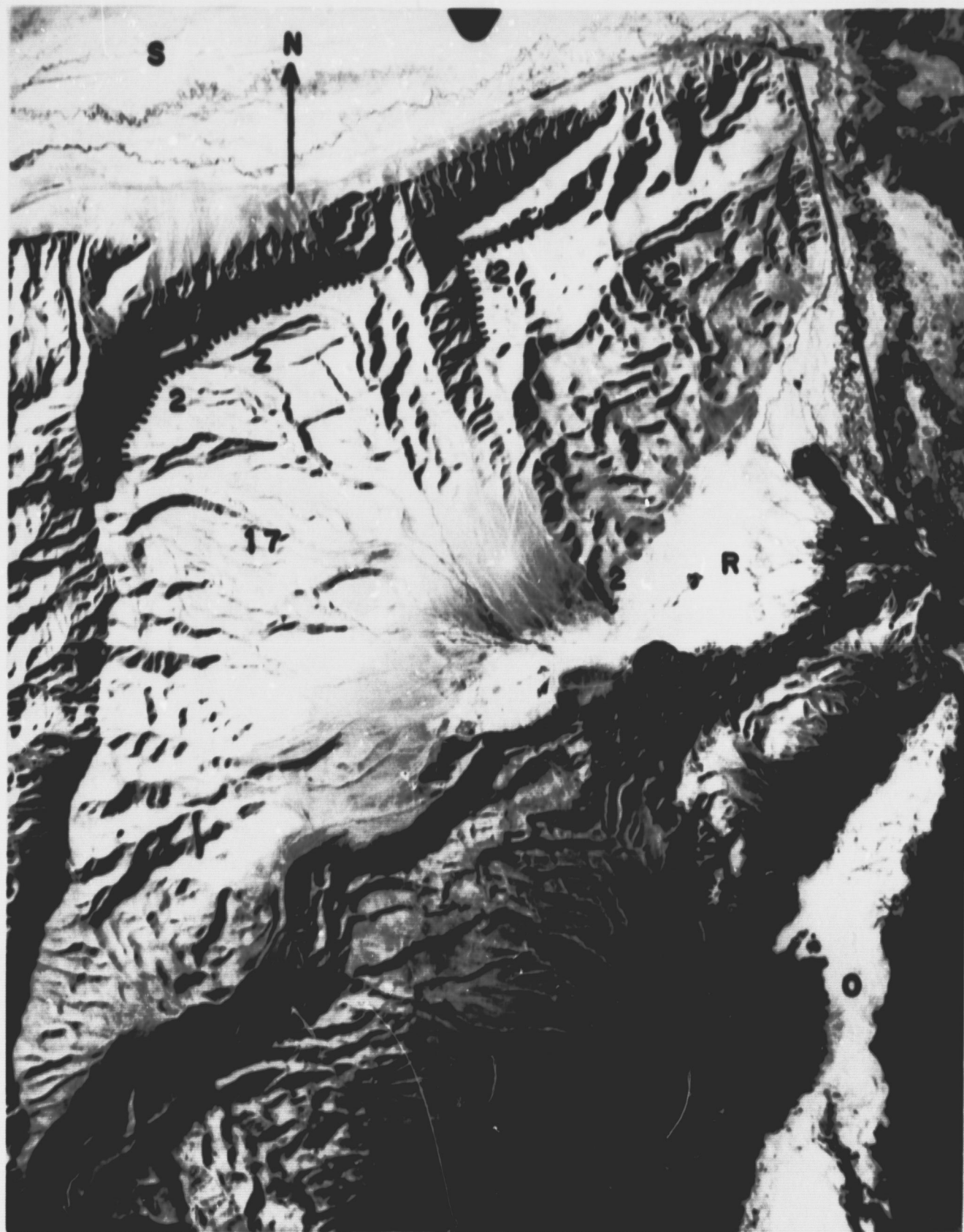


Figure 13. U-2 underflight photography showing Argenta Rim (Z) and Whirlwind Valley (R). Louderbacks (2) form resistant "caps" of Argenta Rim and associated areas. Note landslide (1) in Whirlwind Valley. Original Scale 1:120,000.

Geomorphic Reconnaissance Using S-190B Frames 1 and 4

In addition to the previous detailed geomorphic analysis of S-190B frames 3 and 4, roll 85 a reconnaissance type analysis of frames 1 and 4 are presented subsequently.

S-190B frame 1 (Figure 14) covers a portion of the Great Basin's western boundary. The northwestern portion of the frame is predominantly a volcanic plateau, whereas the southeastern portion, the Black Rock Desert, is primarily Quaternary alluvium (Nevada Bureau of Mines, Bull. 59, Geologic Map of Humboldt Co., Nevada). Identification key is presented in table 3.

Mesa forms as Gooch Table, Rock Spring Table, and Big Spring Table are readily identified as basalt-capped mesas. The ladderback ridges at the southeast end of the Calico Mountains as seen on the SKYLAB frame, have been geologically mapped as undifferentiated Tertiary volcanics.

Numerous landslides and/or mudflows can be identified. Of particular interest is the landslide that appears to have formed Summit Lake. It appears that the slide first moved downslope in a westward direction, and then was diverted southward, blocking the valley of Mud Meadow Creek. Such mass movements are detected on the geologic map only if the material of which they are composed slides or flows over different geologic materials. If this is the case (e.g. along the west side of Craine Creek), the lobe of slide material is geologically differentiated and also is identified by hummocky, irregular terrain with a blotchy tonal pattern.

The volcanics are clearly thrown into a series of fold ridges in the area northwest of the head of High Rock Canyon ("19" on map) appears

Table 3

IDENTIFICATION KEY FOR FRAME 1SKYLAB frame 1

- A Bilk Creek Mountains
- B Black Rock Range
- C Calico Mountains
- D Jackson Mountains
- E Pine Forest Range
- F Charles Sheldon Antelope Range
- G Coyote Hills
- H Black Rock Desert



Figure 14. S-190B frame 1, roll 85: scale 1:602,000. Overlay provides geomorphic interpretation number and letters identified in tables 3 and 5.

REPRODUCIBILITY OF THE
ORIGINAL PAGE IS POOR

to be a volcanic center and may be the source of the louderback flows south of High Rock Lake.

The whitish tonal patterns along the creeks leading south and west of Continental Lake (6g on map) result from erosional dissection of the volcanic cover and exposure of the fossil-bearing Tertiary lake sediments beneath the volcanics.

Evidence of former lake levels is sporadically present around the periphery of Black Rock Desert. This area periodically was part of Lake Lahontan during its higher stands (Russell, U.S.G.S. Monograph 11). Russell's maximum lake elevations roughly coincide with strandlines that can be identified on the SKYLAB frame. These strandlines can also be correlated with topographic data shown on the Vya, Nevada 2⁰ topographic sheet. A large wave-cut cliff (13 on map), terminated by a double-pronged spit formed at the end of the Black Rock Range "peninsula" is a compound form also believed to have been formed by Lake Lahontan waters. On the north side of ~~Black~~ ^{Black} Rock Point, a bay mouth bar encloses a perched "side-hill" playa.

Elsewhere around the margins of Black Rock Desert, particularly on the southwest side of the Jackson Range and north of Quinn River Crossing, are a complex series of strandlines or wave-planed benches. Clearly, more stands of Lake Lahontan are shown than the major episodes described by Russell and Morrison. The central part of the basin seems to be occupied by clay dunes (5 on map).

S-190B frame #4 (Figure 15) covers the southeastern portion of the study area. This frame is unusual for the region because it contains two through-flow valleys that are not closed intermontane basins. These

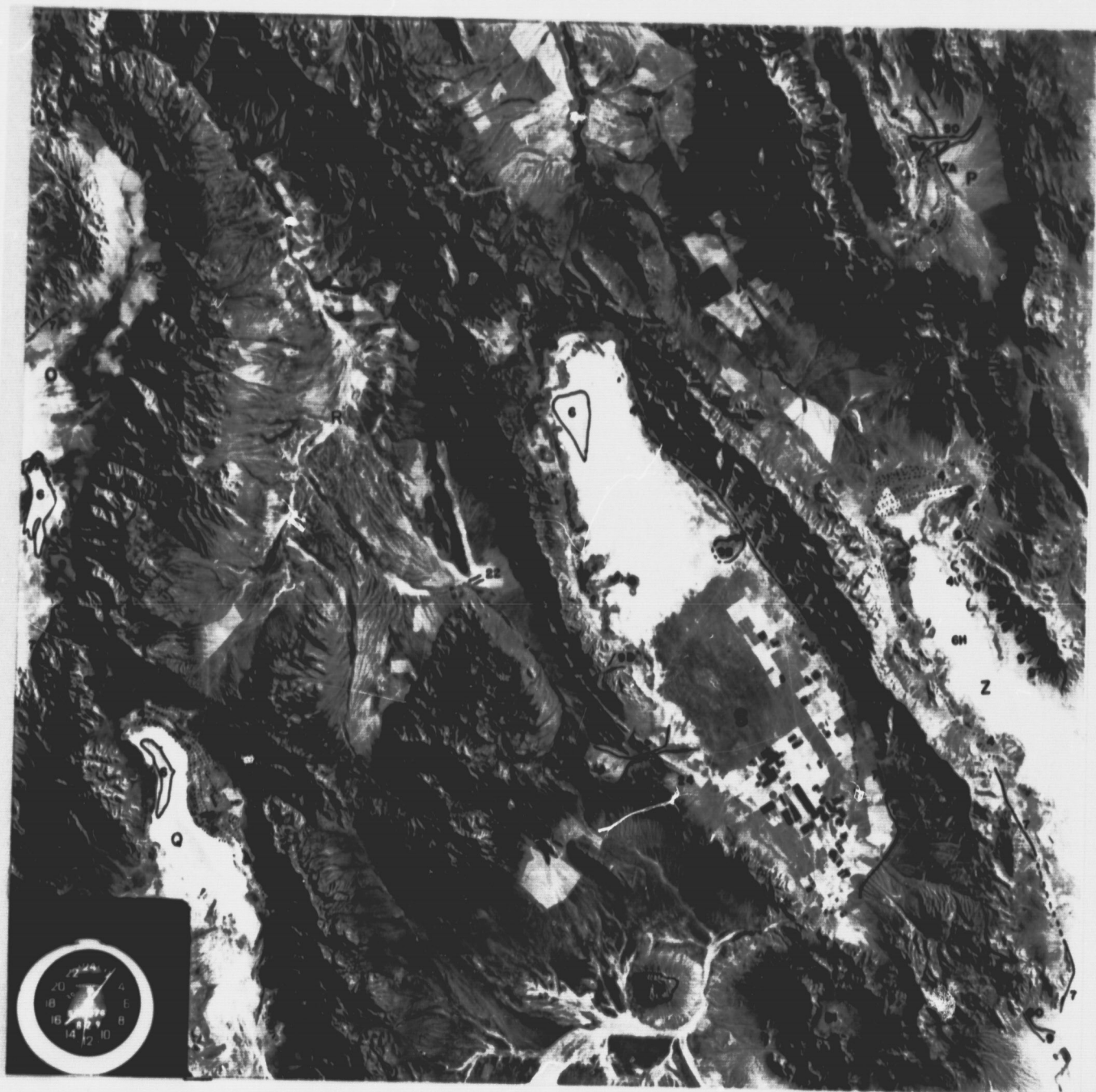


Figure 15. S-190B frame 4, roll 85: scale 1:602,000 . Overlay provides geomorphic interpretation. Numbers and letters identified on table 4 and 5.

drainages, Pine Valley ("R" on the map) and Huntington Valley ("N" on map) flow northward into Humboldt River. Most other valleys have the typical closed basin centripetal drainage of the Basin and Range Province, including rather extensively developed playas. Relict strand lines, indicating former high stands of Quarternary playa lakes, intermittently ring each of these basins. Identification key for frame 4 is presented in table 4.

The playas in Newark, Grass, and Diamond valleys are all located near the extreme northern ends of their respective basins, and each is bounded by extensive alkali flats on the south. Decrease in natural alkalinity southward results in limited agricultural and grazing development on leached nonalkaline soils. We suggest gentle epierogenic tilting northward of these basins over a long period of time and corresponding migration of water table intersection with a sloping ground surface results in a leaching-deposition interface, or precipitation threshold.

Two of the basins have interesting geodynamic aspects. Drainage from the northern end of Grass Valley has recently been diverted by the process of basin capture, and now discharges to a base level almost 1,100 ft. lower in Crescent Valley. Information from water table elevations in wells drilled in the Cortez area suggests that the groundwater divide has not shifted to the position occupied by the surface drainage divide. This indicates that basin capture and drainage reversal is a fairly recent geomorphic event.

A somewhat similar situation pertains in the Kobeh Valley-Diamond Valley section ("T" and "S" on map) on the bottom part of the SKYLAB

Table 4

IDENTIFICATION KEY FOR FRAME 4

SKYLAB frame 4

AA	Long Valley
BB	Diamond Valley
CC	Buck Mountain
A	Cortez Mountains
B	Ruby Mountains
C	Diamond Hills
D	Pinon Range
E	Dry Hills
F	Simpson Park Mountains
G	Table Mountain
H	Sulphur Springs Range
I	Toiyabe Range
J	Maverick Springs Range
K	Lone Mountain
L	Dry Hills
M	Tuscarora Mountains
N	Huntington Valley
O	Crescent Valley
P	Ruby Valley
Q	Grass Valley
R	Pine Valley
S	Diamond Valley
T	Kobeh Valley
U	Mahogany Hills
V	Fish Creek Range
W	Roberts Mountains
X	Whistler Mountain
Y	Mountain Boy Range
Z	Newark Valley

Table 5

Numerical key for all S-190B frames

1)	landslide	18)	inselberg
1a)	mudflow	18a)	Alpha Mountain
2)	louderback	19)	volcanic cone
3)	wave cut bench	20)	lava tongue
3a)	terrace	21)	caldera
4)	strandlines	22)	windgap or watergap
5)	dunes	23)	perennial river
6)	playa	23a)	Humboldt River
6a)	Massacre Lake	23b)	Quinn River
6b)	Middle Lake	24)	hogback
6c)	West Lake		
6d)	Fatty Martin Lake	49)	trench (headward migrating)
6e)	Gridley Lake	50)	fanhead trench
6f)	Gooch Lake		
6g)	Continental Lake		
6h)	Newark Lake		
6z)	playa lake		
7)	fault-line trace		
7a)	fault trace		
8)	bajada		
8a)	pediment		
9)	fan		
9a)	compound fan		
9b)	delta		
10)	spring or seepage area		
11)	lake		
11a)	Summit Lake		
11b)	Alkali Reservoir		
11c)	Swan Lake Reservoir		
11d)	Swan Lake		
11e)	Bilk Creek Reservoir		
11f)	Rock Spring Table Reservoir		
11g)	Rye Patch Reservoir		
12)	intermittant lake		
12a)	Onion Lake		
12b)	Pitt-Taylor Reservoir		
13)	spit		
14)	mountain (hill of circumalluviation)		
15)	urban area		
15a)	Winnemucca		
15b)	Battle Mountain		
16)	folds (?) (anticline and/or syncline)		
17)	plateau		
17a)	Rock Spring Table		
17b)	Gooch Table		
17c)	Big Spring Table		
17d)	Railroad Point		
17x)	mesa		
17z)	butte		

frame. Kobeh Valley historically has integrated the drainage basins of northern Monitor Valley and Antelope Valley (off map) into a single drainage net. At some point in time, it appears that basin capture has occurred and the Kobeh drainage has been diverted through the Devil's Gate into Diamond Valley. It is possible that this interbasin transfer occurred at the time of pluvial lakes, and the connection established to drain the northern Monitor Valley Lake was maintained after these lakes disappeared.

It is not clear from analysis of the SKYLAB photograph whether the Diamond Valley Lake drained in turn into Huntington Valley and the Humboldt River, though this connection is implied by Snyder, et al.

Diamond Valley ^{occupies} an asymmetric syncline. The dip slope and crest slope of an inward dipping hogback are clearly seen on the west side of the valley. Table Mountain (G on map) is also a hogback ridge of resistant rock standing above the surrounding terrain.

REFERENCES CITED

- Beaty, C. B., 1963, "Origin of alluvial fans, White Mountains, California and Nevada": *Ann. Assoc. Am. Geographers*, 53, p. 516-535.
- Bull, W. G., 1964, "Geomorphology of segmented alluvial fans in western Fresno County, California": *W.S. Geol. Surv. Profess. Paper* 352-E, p. 89-129.
- Denny, C. S., 1965, "Alluvial fans in the Death Valley region, California and Nevada": *U.S. Geol. Surv. Profess. Paper* 466, 62p.
- Eckis, Rollin, 1928, "Alluvial fans in the Cucamonga district, southern California": *J. Geol.*, 36, p. 224-247.
- Fairbridge, Rhodes W., (Ed.), 1968, Encyclopedia of Geomorphology: Reinhold, New York, Publishers, 1295p.
- Gilbert, Grove C., 1890, "Lake Bonneville": *U.S. Geol. Surv. Monograph* 1, 438p.
- Hooke, Roger LeB., Yang-H-Y, and Weiblen, P. W., 1969, "Desert varnish: an electron probe study": *J. Geol.*, 77, 275-88.
- Lustig, L. K., 1965, "Clastic sedimentation in Deep Springs Valley, California": *U.S. Geol. Surv. Profess. Paper* 352-F, p. 131-192.
- Morrison, R. B., 1964, "Lake Lahontan: Geology of Southern Carson Desert, Nevada": *U.S. Geol. Surv. Profess. Paper* 401, p.
- Snyder, C. T., George Hardman, and F. F. Zdenek, 1964, "Pleistocene Lakes in the Great Basin": *U.S. Geol. Surv. Misc. Geological Invest.*, Map I-416.
- Sheldon, John S., 1966, Geology Illustrated: W. H. Freeman and Co., San Francisco, California, 434p.
- Thornbury, William D., 1969, Principles of Geomorphology, 2nd edition: John Wiley & Sons, Inc., publishers, 594p.
- Way, Douglas S., 1973, Terrain Analysis - A Guide to Site Selection Using Aerial Photographic Interpretation: Dowden, Hutchison & Ross, Ind., Stroudsburg, Pennsylvania, 392p.
- Willden, Ronald, 1963, *Geology and Mineral Resources of Humboldt County, Nevada*: Nevada Bureau of Mines, Bull. 59, 154p.

FAULT STUDIES NORTH-CENTRAL NEVADA

The fault studies were conducted in the Battle Mountain area of northcentral Nevada, (Figure 16). The physical description of the area, the geological setting, vegetation, climate and land use have been described in the previous section on geomorphology.

The same basic data products were used for both studies having been taken from Skylab during SL-3, along track #20, on August 12, 1973. Although the S-190A data was used in comparison with the S-190B black-and-white photography, the studies were conducted primarily using the longer focal length S-190B photos. The choice was predicated entirely on the need for and the capability of the S-190B system to produce higher resolution photography. The data from Skylab were taken at 7:45 in the morning local time providing excellent low sun angle photography under completely cloud free conditions. The horizontal visibility from the ground at the time of the overflight was some 65 miles. The sun's azimuth was approximately due east and the sun's angle was near 28 degrees.

The Skylab data were analyzed in conjunction with black-and-white photography acquired during two U-2 underflights on September 18, 1974 and October 17, 1974. The first U-2 Sept. mission covered the entire Winnemucca 1:250,000 2 degree topographic map which included all of Frame #3, as seen from the August 12th, Skylab overflight. The U-2 missions required four east-west flight lines to provide complete photo coverage at 60% forelap and 20% sidelap using the 6" focal length RC-10 camera, thus producing a format of approximately 1:120,000 scale, assuming an average surface elevation of 5,000 ft. A second 24" focal



Figure 16. This is a 1.5x enlargement of a frame taken by the S-190B sensor on board SL-3 on Track 20, August 12, 1973. Approximate time, 0745 (local). Major structural features are mapped. General outlines of areas of concentrated studies, including underflight photography and ground truth data, are shown as areas 1, 2, and 3.

REPRODUCIBILITY OF THE
ORIGINAL PAGE IS POOR

length camera was operated simultaneously providing partial coverage at a scale of 1:30,000. The 1:30,000 photos were in stereo but covered only four miles on either side of nadir. This first mission was begun when the sun angle was at 20 degrees and during the one hour required to fly all four lines the sun angle had increased to 30 degrees. The second U-2 mission Oct. flew the same lines with the same cameras and film, from the same elevation but began the mission when the sun angle was 10 degrees and finished when the sun angle was 20 degrees.

These three sets of data at approximately the same azimuth but at three different sun angles gave us a unique opportunity to study structures using shadow enhancement and to make comparative judgements using varying sun angles, separate scales and different analysis techniques.

The state geologic maps covered by Frame #3 from Skylab and the U-2 underflights included parts of Eureka and Humboldt Counties in a published form and Lander and Pershing Counties in a preliminary form. All four maps are at a scale of 1:250,000.

The initial 5" x 5" transparent positives acquired from the S-190B system were utilized to make a set of contact negatives from which 3.77 enlargements were made. These enlargements closely approximate the 1:250,000, state topographic and county geologic maps.

Analytical Procedure

Since stereo coverage was not available from Skylab on August 12th, a secondary procedure was adopted that took advantage of the low sun angle enhancement. A number of mechanical and photo-interpretive techniques were experimented with before it was determined that the best method of observing the greatest detail was by using the 5" x 5"

positive transparencies on a light table from which the data could be scanned using a binocular microscope. When viewed in this manner the low sun-angle photography has a distinct three dimensional characteristic that is maintained thru all levels of magnification and a wide range of illumination. Using the binocular technique the structural information was transferred to a mylar overlay on the 1:250,000 photo. This was accomplished by two different interpreters and a consensus of their interpretations was then reproduced and is presented as the overlay for Figure 16. Where coverage occurred, these data were then compared to the existing geologic maps at the same scale.

A brief qualifying statement about how the county geologic maps are compiled is necessary to avoid any false impressions that may arise from comparing the maps with interpretations made from the Skylab photography. Firstly, the county maps are extremely variable partly because they are the product of many different authors who have had a great deal of freedom in interpreting what appears as a final product. These maps are often compiled from existing geological maps done on a smaller scale by a number of different geologists with widely varying backgrounds and often quite divergent interest. As a result a number of quadrangles, from which a county map is composed, have been mapped in greater detail while those quadrangles immediately adjacent to them may have been mapped on a reconnaissance basis only. Secondly, an area which has had a great deal of mining activity may have been mapped by a number of geologists who have had the benefit of information derived from drilling, trenching, and drifting as the exploration progressed.

The resulting county maps, therefore; are not uniform within a given county nor are they uniform from county to county.

Frenchie Creek Quadrangle Area #3

A good example of the dilemma in trying to compare and evaluate the data can be demonstrated in the Frenchie Creek Quadrangle which is included in the Eureka County Geologic Map, and is shown as Area #3 on figure 16. Excluding the areas of highest relief in the upper left and lower righthand corners of Area #3, it can be seen that a number of actual and probable faults have been mapped in the alluvium. These features which were mapped as actual or probable faults on the Skylab transparencies do not appear on the county map. However, some of the features do appear on the Frenchie Creek Quadrangle geologic map (detailed geologic mapping by L. J. Patrick Muffler, 1964). The features we showed as faults are included on Mr. Mufflers map of the area, but his interpretation was that they are beach lines of prehistoric lakes. A second interpretation is given by Robert Willson, a geologist on the Southern Pacific Mineral Survey, 1960, for the same area, where he refers to the features as probable or doubtful faults.

The authors of the Eureka County map (1963) choose not to include Mr. Willsons data but did include Mr. Mufflers work. However; in compiling the final county map, the authors excluded Mr. Mufflers interpretation of the features as beach lines and, instead, choose to leave the area blank. Part of the reasons why these interpretations are excluded, although there is seldom any explanation, is that authors edited out information they believe to be questionable or of limited value, or they simply decided not to include specific information.

Field examinations of the northeast trending features mapped by Messers, Muffler and Willson indicate that some of the features could be

relict stream channels that have been enhanced by vegetation as well as shadowing effects, although some of the features have a single scarp and are not enhanced by vegetation and are more likely to be actual faults.

The most prominent fault feature (Fault A, Figure 17) which has a scarp of over 9 feet in places and extends for a distance of approximately four miles, is outside of the area mapped by Willson and only the most southern portion is included within the Frenchie Creek quadrangle as mapped by Muffler. In this case, however, the fault does not appear on any of the maps. A reason for this is that the quadrangle to the west, where the fault is most prominent, is not mapped in detail.

For these reasons a direct comparison of Skylab photography with the existing geologic data is a highly speculative venture and should be approached with caution, as it is easy to make personal interpretations look good for the wrong reasons.

While there is considerable disagreement about the origin of the features at Frenchie Creek, no one who examined the Skylab photos had any trouble seeing them. What makes the identification problem intriguing is that the features were located and mapped from photography taken 270 miles above. Perhaps even more intriguing is the fact that field collected data revealed some of the features to be no more than 3 feet high. Granted, some of them were enhanced by shadows or in some cases by vegetation, but the fact remains that they were seen and mapped from Skylab photography.

Battle Mountain Airport Area #1

From Skylab a series of topographic features were mapped as northeast-trending faults or fault-traces cutting alluvium and fan material. The



Figure 17. Structural mapping from SL-3 and U-2 under-flight data on the western edge of The Frenchie Creek Quad and on the eastern edge of the Crescent Valley Quad (1:62,500). These structures have been called probable or doubtful faults on some maps, strandlines on other & completely omitted on still others. Fault A is relatively oblique to the topography and has a scarp of nearly 9 feet.

location is south and east of the Battle Mountain as shown in Area #1, figure 16. The same topographic features are shown as faults on the preliminary county geologic map for Lander County. Since the faults were mapped a comparison of how well we were able to map the same features was possible. We were encouraged to find that nearly ninety percent of the structures we had mapped from Skylab were comparable to those shown on the 1:250,000 scale county map.

~~U-2 missions overflew the same area with both a short and long focal length photo system, providing us with 1:110,000 and 1:30,000 scale photographic coverage at the same sun angle comparable to the Skylab photography with only a modest change in azimuth, approximately 10°.~~ The two U-2 missions overflew the same area with both a short and long focal length photo system, ~~providing us with 1:110,000 and 1:30,000 scale photographic coverage at the same sun angle comparable to the Skylab photography with only a modest change in azimuth, approximately 10°.~~

All of the U-2 ~~photographs~~ ^{photographs} were analyzed using different enlargement scales and photo-interpretive techniques from which comparisons were made with the geologic map of the county and with Skylab photography. Again, the best detail and greatest resolving power was achieved using the positive transparencies, ~~illuminations~~ ^{illuminations}, and a binocular microscope. Both sets of photographs from the U-2 flights were analyzed by different interpreters and a consensus of their analysis was used to produce the overlays for Figure 18 and Figure 19.

Although the ~~interpretation~~ ^{interpretation} presented here ~~were derived~~ ^{were derived} from the October overflight when the sun angle was nearer to twenty degrees, it was not significantly different from the ~~interpretation~~ ^{interpretation} of the September flight when the sun angle was closer to 30 degrees. Both sets of ~~interpretations~~ ^{interpretations} were comparable for the Area #1 which is one of very low relief.

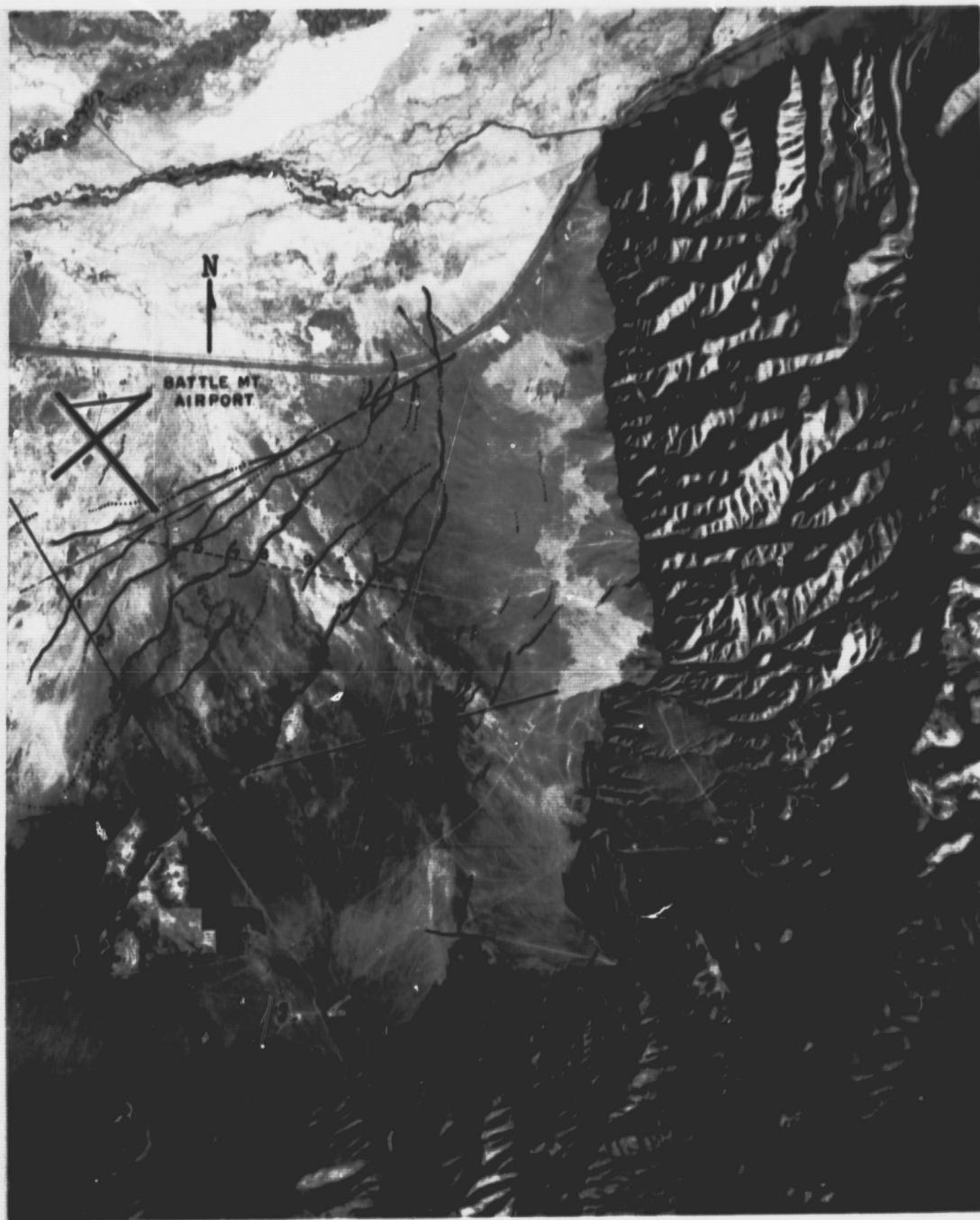


Figure 18. Area 1. A portion of a contact print taken by the U-2 aircraft underflight mission, October 1974. Scale is approximately 1:110,000 (6" focal length camera). Sun angle approximates that which was present during the SL-3 imaging. Structural features mapped include the prominent basin and range fault outlining the Northern Shoshone Mountains and the extensively faulted alluvium.



Figure 19. Area 1. A portion of a contact print taken by the U-2 aircraft underflight mission, October, 1974. The approximate scale is 1:30,000 (24" focal length camera), and the sun angle approximates that which existed at the time of SL-3 imaging. Structural features mapped are recent faults in the alluvial deposits at the northern flank of the Northern Shoshone Range near Battle Mountain, Nevada.

Field examinations were made of Area #1 to determine what we had mapped and how accurately we were mapping using the various techniques. Measurements were conducted along two lines which traversed most of the major topographic features. The following are comments taken from the field observations at specific locations which are numbered from 1 to 10 on both sets of aircraft photos.

Measurement site:

#1. This feature is enhanced by thick green foliage growing on the down dropped side of a scarp that has about 30 inches of relief.

#2. Not mapped from Skylab...the topographic relief is not more than two feet...the feature is discernable as a slight dip with a change to thicker vegetation on the lower side.

#3. Feature is not discernable as it crosses the road...it has about 3 feet of relief on the northwest side of the road enhanced by a change in vegetation.

#4. Not mapped from Skylab...seen only as a change in vegetation with a very slight dip...possibly a relict stream channel.

#5. Highest scarp on the fan complex...crosses road with about 14 feet of relief...some vegetation enhancement which may be associated with water which occurs from seepage along the scarp.

---Topographic feature 6-10 measured along second traverse---

#6. Steep fault scarp with vegetation enhancement...approximately 5 feet of relief.

#7. Not mapped from Skylab...very subtle topographic feature...no vegetation enhancement...about 3 feet of relief.

#8. Part of this fault mapped from Skylab, but north of the intersection with the road...approximately 3 feet of relief...no vegetation enhancement.

#9. Part of this fault was mapped from Skylab, but only that portion north of the intersection of the road...5 feet of relief and no vegetation enhancement.

10. Steep fault scarp with relief averaging 5 to 8 feet...slight vegetation enhancement..."Sag Pond" like structures along the scarp...water seepage...this feature is most likely a continuation of the fault seen at site #5.

The results of the ground-based analysis indicate that in each case the low sun-angle photography enhanced the small topographic variations or breaks in slope or intensity of the vegetation.

Most of the major structural features mapped from the aircraft photography were also mapped from Skylab data, and, although some of the features were not discernable, the principle differences were very subtle. Again, the problem was not so much a matter of seeing and mapping the features but rather, agreeing on their probable origin.

The authors of the preliminary geologic map for Lander County show the features in Area #1 as faults in very much the same manner as we have mapped them from the Skylab photography.

~~Earlier, Dr. William Melhorn~~ Dr. William Melhorn of Purdue University took strong issue with those of us who labeled the topographic features as "faults", *after he had completed his field investigation.* ~~Field~~ "Field examinations and study of the photography clearly suggest that the area is a complex of intersecting and anastomosing channel scars and meander scrolls which are relicts of past migrations of Reese or Humboldt rivers as they have progressively wandered back and forth across their floodplains. The features mapped as faults on the Lander County map are seen as sinuous,

braided channel segments of magnitude and form similiar to those of the present streams and therefore are no more than vegetationally enhanced relict channels no more than a few feet deep".

Jack Quade

From ~~an~~ point of view not all of the features can be shown to be faults using photography, but ^{he is} I am confident that the descriptions provided at sites #5 and #10 are excellent field criteria for faults and, to a lesser extent, so are parts of many of the others.

It seems opportune that channel scars and meander scrolls would survive in their present form and number in only one area, when one considers the size of the flood plains of the Reese and Humboldt rivers as seen from the area we have mapped Figure 1. The northeast orientation of the features approximates the basin-range structures and closely parallels the existing fault-trends. It is also difficult to explain how fluvial features can survive many thousands of years of erosion and deposition when they are nearly perpendicular to the existing drainage.

While it is difficult to arrive at an agreement as to the exact origin of the topographic features from what has been observed, it would be a relatively simple task to trench several of the features and make the appropriate sub-surface determinations of these and similar features at Frenchie Creek.

A high percentage of the faults mapped during this study were related to the northeast trending mountain ranges formed by basin-range tectonics. As a result the greater number of faults mapped trend parallel to the mountains and can be seen as very light or very dark colored scarps depending on their orientation to the eastern sun light.

Trout Creek Area #2

Those faults darkened by shadows were along western facing fans adjacent to the mountains; a good example of this can be seen in Area #2, figure 16.

The selection of Area #2 was made after numerous field examinations in other localities as a typical example of basin-range faults with slight changes in orientation, and with a wide range in elevations which could be viewed from several sun-angles at different scales. None of the faults in Area #2 showed any appreciable amounts of vegetation enhancement, and, in most cases there was none.

Initially the area was mapped from Skylab, and later from the photography acquired on the U-2 missions, the example shown here, being the 1:110,000 scale data from the October overflight. The photography (Figure 20) is annotated for the purposes of referencing the text, with numbers 1 thru 4 representing individual sites. The mapping on all photography was accomplished using positive transparencies, ~~illumination~~ ^{illumination} and a binocular microscope. Two interpreters did the work independently and a consensus of their work was used for the final interpretations.

Site #1, which is on the drainage west of Trout Creek, is the location of the highest fault scarp in Area #2. At this location the north-trending scarp was nearly 40 feet high with varying slope angles averaging slightly more than 6 degrees. Following the same fault scarp south from Site #1, the elevation decreases to less than 8 feet before turning nearly due west. At this point the fault orientation is less than 30 degrees from being parallel to the azimuth of the sun. At the time of the overflight the sun azimuth was estimated to be near 25 degrees south of east.



Figure 20. Area 2. A portion of a contact print taken by the U-2 aircraft underflight mission, October, 1974. The scale is approximately 1:110,000 (RC-10 camera with 6" focal length lens). The sun angle approximates that which was present during the SL-3 photography. Structured features mapped include discontinuous basin and range faults and more recent faulting in the alluvium.

This demonstrates, that while it is ideal to have the sun's azimuth perpendicular to the fault scarp, fault orientation need only be within 60 degrees of either side of the sun's azimuth to be enhanced by shadowing effects providing, of course, that the sun angle is low enough.

From mathematical models derived by Lee and Sawatzky (1974) it can be inferred that a fault scarp may still be enhanced when the sun azimuth is nearer 20 degrees of being parallel to the fault orientation.

Figure 21 is a photo taken from site #2 of the very straight north-east-trending fault whose scarp is in shadow. The photo was taken when the azimuth and sun angle were very similar to those seen on the Skylab photography. The scarp varies from 8-10 feet in height with an average slope of some 8 degrees. Both of the previous faults were mapped in detail using Skylab photography.

At sites #3 and #4, only the fault at site #4 was mapped with certainty from Skylab photography, while the fault at site #3 was inferred. A photograph of these two faults was taken from the ground looking SE from site #3 toward the mountains Figure 22. The photo was taken at a time when the azimuth of the sun and the sun angle were close to those seen on the Skylab photography. The fault at site #3 is delineated by the dashed line where it crosses the road. The fault scarp at site #4 can be seen in the background as a dark line parallel to the range front. The maximum height of the fault scarp at site #3 did not exceed 3 feet along its entire strike, while the fault scarp at site #4 exceeded 5 feet in some places.

The remaining aircraft photography did not add substantially to that which had already been interpreted. The comparisons made previously



Figure 21. Looking south in Area 2. Projecting from the left is one of the prominent fault scarps. It is shown here shadow enhanced with almost the same sun angle as was present for the SL-3 and U-2 photography.



Figure 22. Looking southeast toward the mouth of Mill Creek in Area 2. This photograph attempts to show the shadow enhancement of faults of very low relief. The sun angle is very closely approximated to that which was present during the SL-3 and U-2 flights.

between all three camera systems used during the study of Area #1 are a typical example of what is lost in terms of the overview and what is gained by better resolution.

More than ninety percent of the faults mapped in Area #2 using Skylab photography are shown as faults on the preliminary geologic map for Lander County, by John H. Stewart and Edwin H. McKee, 1970.

Conclusions

The Skylab photography provided an excellent format on which to map faults at a reconnaissance scale that compared favorably to that which was mapped ^{previously} at 1:250,000 scale. In the case of the more recent faulting, the detail mapping was better than that shown on a 1:250,000 scale.

There are many different land forms unique to arid lands, and the basin and range in particular, ^{all of which} we had to learn to cope with before we became proficient at ^{discriminating} faults from other features. For instance, ~~many basin-range faults trend~~ many basin-range faults trend ^{but so do} parallel to the mountain ranges, ~~the shore lines of the ancient lakes, vestiges of which can be seen in many of the basins along fans and margins of the mountains. On occasions the faults and the shore lines are parallel or subparallel to one another making positive identification difficult. When the ancient lakes retreated, however, they often left more than one shore line, and the parallel~~ ^{strand lines are} ~~helpful to the interpreter. Another feature of shore lines is that they tend to follow the same elevation and tend to curve around areas of higher relief which assists in their identification. There are examples where parts of~~

shore lines have survived along the long axis of basins making identification less certain even at ground level. There are shore lines which probably coincided with fault traces in the areas north and east of Walker Lake and along the eastern side of Pleasant Valley.

Shore lines are not the only linear or curvilinear feature that can be confused with fault traces when interpreting Skylab data. Many of the products of fluvial process such as relict streams, channels, drainage patterns, bars and spits may also be confused as faults at these scales.

In areas of higher relief changes in lithologies, color, patterns, dikes, and many different types of ~~erosional~~ ^{erosional} features are commonly suspected as faults. Vegetation, or the lack thereof, or ~~boundaries~~ ^{boundaries} created by it will be suspected as a fault trace at different times of the year. ~~Misinterpretations~~ ^{be attributed} can also ~~be attributed~~ to the effects of grazing and the routes taken by animals to grazing areas.

Many of these problems are not unique to mapping geology from air-photos, but the problems are compounded when viewed from Skylab where a single photographic frame can cover over 10,000 square miles. We have examples where a single frame covers five basins and four different mountain ranges.

Because we had the benefit of good aircraft and spacecraft photography over the same area, it seems appropriate that we should make some comments concerning the photography, the coverage, ~~and~~ ^{and} some of the operational constraints of the two systems.

There is ample evidence to show that the August 12, 1973, mission provided good low sun-angle photography from which we were able to extract

a great deal of useful geologic information. The black-and-white photography used was the best format for 7:45 in the morning, and it gave us the best resolution possible. The coverage, while not ⁱⁿ stereo, nor over our initial test sites, was none the less over a similar area and one where we could conduct most of the experiments we had originally planned.

The weather conditions were ideal, and the speed at which the orbitor flew resulted in the production of over 20,000 square miles of coverage as it crossed the state at what was essentially an unchanging sun angle.

However, when consideration is given to how many times Skylab flew over Nevada; how often it passed over a given site; at what times it passed over a given site; what the weather conditions were like at the time of each pass; what the priorities were along the flight track at the time of each pass; what the operational constraints may have been; it is evident that we were not planning for what we got, but rather took what we could get.

~~Some examples of the flexibility required to obtain ideal data.~~ The U-2 overflights at Battle Mountain are a good example. We selected the camera systems we needed, the film load, the camera settings, the flight elevation, the time of flight, the geography and direction of flight, and finally, working with the operations group the systems were launched under ideal weather conditions. When the September mission ran into operational problems and arrived over the target one hour late, and therefore could not provide data with the exact sun angle requested, the mission was reflown a month later.

During the one hour it took the U-2 to fly the mission, the 6" focal length camera expended 60 frames of 9" x 9" film which provided

complete coverage at 60% forelap and 20% sidelap of over 7,000 square miles. The 24" focal length camera required more than 10 times as much film for one half the coverage. The total cost ^{of photography} for each U-2 mission including film processing was about \$6,500.

A single frame of S-190A photography provides complete coverage of nearly 10,000 square miles on a single 70mm frame, while the S-190B camera produces nearly 4,500 square miles of coverage per 4.5" frame.

We have no idea of the cost of a single frame of ~~REP~~ ^{EREP} photography, nor are we sure than anyone else does, although logic tells us that a comparison would be lopsided.

There are many reasons to suspect that equating aircraft and space-craft photography on the basis of dollars per frame or miles per frame etc., are not realistic. They are probably sufficiently different to be unique unto themselves. ~~There are many reasons to suspect that equating aircraft and space-craft photography on the basis of dollars per frame or miles per frame etc., are not realistic. They are probably sufficiently different to be unique unto themselves.~~

References Cited

- Muffler, P. J. L., 1964, Geology of Frenchie Creek Quadrangle North-Central Nevada, U.S. Geol. Soc. America Bull., 1179. Plate 1.
- Roberts, R. J., Montgomery, K. M., Lehner, R. F., 1967, Geology and Mineral Resources of Eureka County, Nevada, Nevada Bureau of Mines, Bull. 64. Plate 3.
- Sawatzky, Don, L., Lee, Keehan, 1974, New Uses of Shadow Enhancement. Remote Sensing Report 74-5, Dept. of Geol., Colorado School of Mines.
- Stewart, J. H., McKee, E. H., 1970, Preliminary Geologic Map of Lander County, Nevada, Scale 1:250,000.
- Willden, Ronald, 1963, Geology and Mineral Resources of Humboldt County, Nevada, Nevada Bureau of Mines, Bull. 59.
- Willson, Robert, 1960, Geology of Frenchie Creek Quadrangle, Southern Pacific Mineral Survey, Eureka County, Nevada, Map.

RECONNAISSANCE FAULT MAPPING WEST-CENTRAL NEVADA

From what we had learned about mapping from Skylab in the Battle Mountain area, we now applied on a reconnaissance basis to other areas. Utilizing the same analytical techniques, we mapped approximately 20,000 square miles using S-190A and S-190B photography.

The area encompasses the west-central portion of Nevada, and parts of the basin-range, bordering eastern California.

The photography was taken at 8:30 a.m., on August 11, 1973, along track #6 and 12:30 p.m. on September 13, 1973, along track #59, both overflights occurring during the SL-3 mission. The track #6 photography that was used extends along a line from north of Walker Lake to south of Goldfield, Nevada, while the track #59 photography starts over the Sierra Nevada of California, passes over Mono Lake and terminates on a line south-east of Walker Lake.

The August overflight provided good low sun-angle photography at a time when there were no clouds and the horizontal visibility at ground level was more than 65 miles. The September overflight was at 12:30 p.m. when the sun was nearly vertical, and at the time there were some patchy cumulus clouds, although the horizontal visibility was nearly 50 miles.

Analytical Procedure

From track #6 we used both the S-190A and S-190B low sun-angle photography. From the S-190A system we mapped on 4x, black-and-white, positive transparencies using illumination and a binocular microscope.

S-190A Analysis

The S-190A photography used in the analysis is on a scale of 1:702,000 with each frame covering ten thousand square miles, only part of which are shown in Figures 23 and 24. The overlays for the figures were compiled from a consensus of two separate interpretations.

The northern half of Figure 23, shows a strong north and northwest fault trend which parallels the basin-range fault block mountains. A major northwest fault set exists east of Walker Lake in an area that is referred to as the Walker Lane. The Walker Lane has been described as a zone of faults with major right lateral slippage, although considerable disagreement about its origin, distinctive faulting, the amount of movement along the faults, and its geographic limits can be found throughout the literature. The time in which movement began along the Lane is also uncertain although very recent faulting has cut drainage patterns and alluvial fans within and parallel to the ^{"Lane"} ~~area~~.

A predominantly east-west pattern of fault traces can be seen on the south-west portion of Figure 23. This trend begins near Mina, Nevada and continues westward past the northern end of the White Mountains where it bends in a more southerly direction. This strong east-west alignment has been described by Speed and Others (1975) as a possible vestige of a former wide spread zone dominated by NE to E-striking basin-range faults. A number of hypotheses were proposed as to why the east-west trend has survived the dominant effects of north-south faulting which are still active.

Nearly all of the area west of the north-south line between Tonopah and Goldfield, see Figure 24, is included within Esmeralda County while



Figure 23. A portion of SL-3 S-190A frame 56, roll 30, showing the Walker Lake area of west-central Nevada. Overlays provide structural interpretation and epicenter locations.

REPRODUCIBILITY OF THE
ORIGINAL PAGE IS POOR

REPRODUCIBILITY OF THE
ORIGINAL PAGE IS POOR

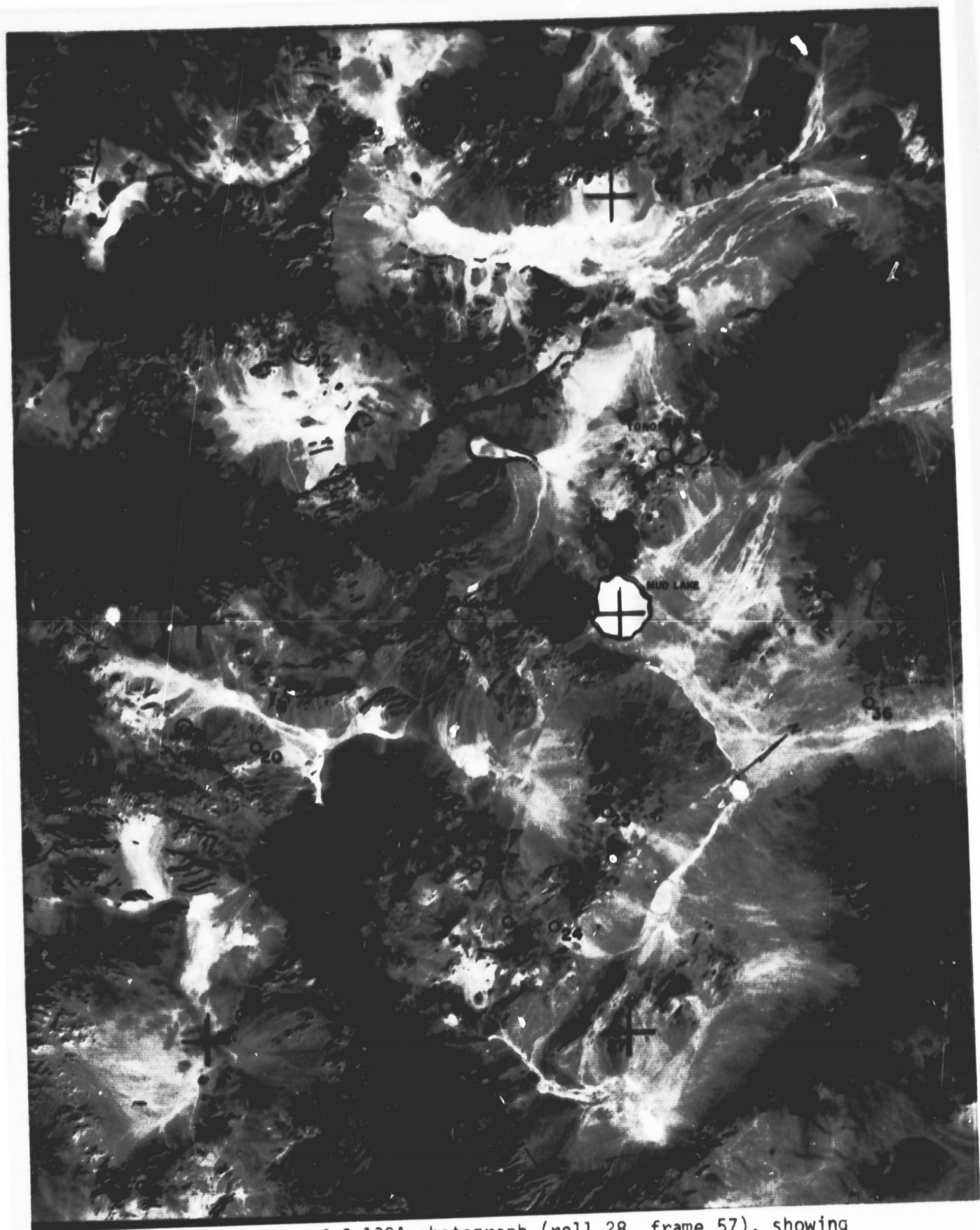


Figure 24. A portion of S-130A photograph (roll 28, frame 57), showing relationship of metal mining districts to faulting. Numbers refer to Table 6. The initial overlay displays the structural trends of South Central Nevada. The second overlay displays metal mining camp locations and their dollar production of precious metals.

the remaining area to the east is part of southern Nye County, both of which are in Nevada.

The eastern margin of the White Mountains can be seen in the upper left hand corner of Figure 24, and is the location of a very large ~~fault~~ ^{strike} slip fault. Displacement along this fault, according to Albers and Stewart, 1972, may be as much as eighteen miles. On the left side of Figure 24, along the south and western portion of Esmeralda County, are a series of arcuate fault sets. This pre-Tertiary bend in the topography has been referred to as the Silver Peak-Palmetto-Montezuma Oroflex by Albers, 1967, and is thought to be the result of tectonic bending of the crust.

Most of the faults associated with the arcuate features have a dip-slip movement with the down thrown side of the faults toward the valleys suggesting a very large area of subsidence.

The prevalent fault traces on the right side of Figure 24, are the result of north-northwest and northeast high angle faults associated with basin-range tectonics.

In the south-central portion of Figure 24 several circular features have been identified by Cornwall, 1972, as collapsed calderas that are related to a sequence of young ~~volcanic~~ ^{eruptive} at Black Mountain.

Summary

Working from the S-190A photography at a scale of 1:702,000 and comparing the results with existing geologic maps has suggested that the larger scale structural features can be mapped and related to regional trends which provides an overall view not available at lower altitudes.

S-190B ANALYSIS

S-1908 Anal - 1.

~~SECRET~~ The S-190B photographic coverage is about two thirds of that seen from the S-190A system. ~~XX~~

On the right hand side of Figure 26 is a long white playa that marks the center of the Big Smokey Valley, the southern limit of the S-190B photograph. ~~_____~~

~~Continued~~ The comparative analysis between the S-190A and S-190B photography was limited to the areas shown in ~~the following figures~~ Figures 25 and 26, because S-190B Coverage terminated with frame 13.

Where coverage was available from both systems it can be seen that more than twice as many faults were mapped using the S-190B photography. The major fault trends as seen from the S-190A photography have not changed significantly but have been accentuated in both density and detail. Faults associated with subtle changes in topography, particularly drainages and alluviated surfaces, were easily discernable.

Several fault trends not seen on the S-190A photographs were mapped from the S-190B photography. In the center of Figure 26, east of Mina.

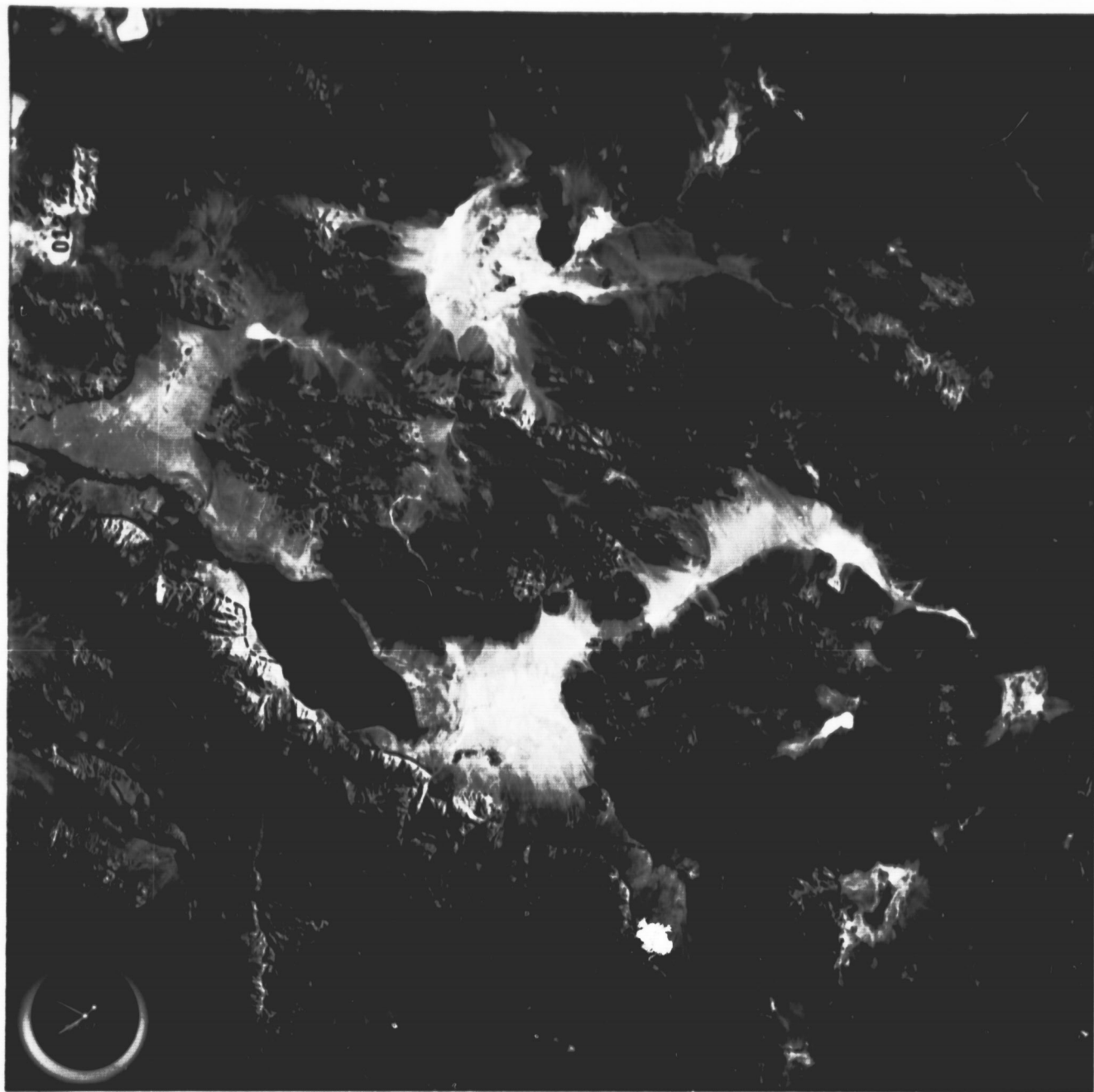


Figure 25. Frame 12 on track 6, S-190B. Major structural trends can be mapped directly on this quality data. The Walker Lane fault zone is depicted as the major north-west fault zone just east of Walker Lake. The Gabbs Anticline is at top center.

REPRODUCIBILITY OF THE
ORIGINAL PAGE IS POOR

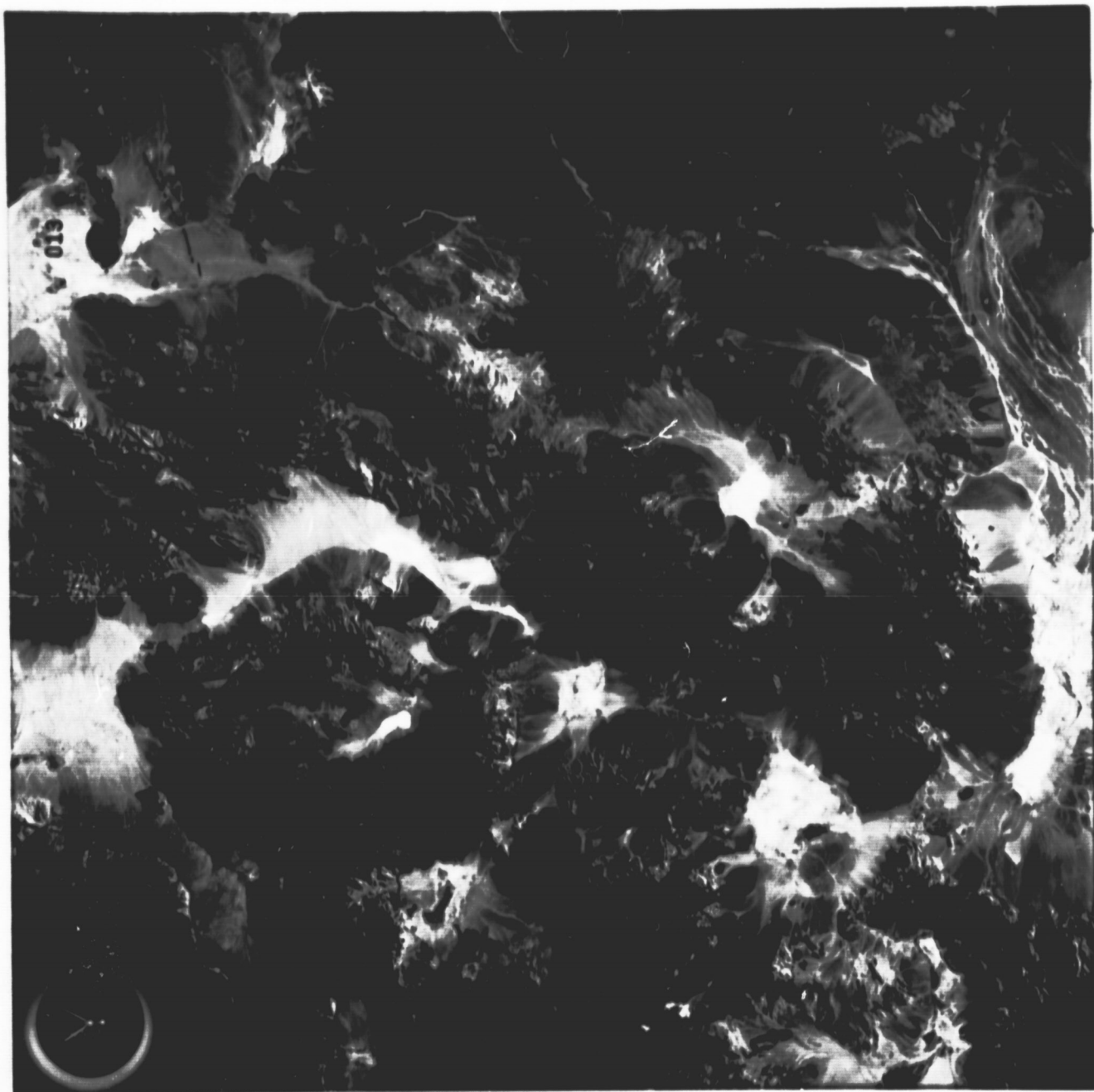


Figure 26. Frame 13 on track 6, S-190B, (Figures 25 and 26 are a stereo pair). Structural trends again show very clearly on the S-190B data. Detail mapping was accomplished using transparencies, and magnification from which the overlays were made.

in the northern part of the Pilot Mountains, a series of east-west fault traces were mapped in the pre-Tertiary rocks. Another series of east-west fault sets were mapped in the Ryan Canyon area east of Walker Lake in the center of Figure 25. The 1:250,000 scale Mineral County Geologic Map, by Ross, 1961, shows the area to be composed of granitic rocks but without any east-west faulting. The presence of granites suggest the trends may be dikes, but this was not confirmed by field observations.

Another very dominant set of faults which is slightly curvilinear were mapped west of the Big Smokey Valley as seen on the right side of Figure 26. These faults are more ~~northerly~~ ^{northwesterly} and were found from field observations to be related to youthful basin-range faulting as they ~~cut~~ ^{cut} ~~the~~ the uppermost volcanic sections which have been dated as late Tertiary.

The east-west fault traces mapped west of Mina can be seen in much greater detail on Figure 26 and on Figure 27, as this trend bends south around the northern end of the White Mountains. Much of the structural detail was lost in Figure 27, because the photography was taken near midday which tends to flatten out topographic enhancement.

The Gabbs Valley Anticline

Evidence of a large anticline was observed in the northwestern portion of Nye County, Nevada. The structure is some 12 miles long and five miles wide, and from the photos it appears to have been faulted (In which case, the structure, should probably be called a breached anticline) parallel to its north-south axis. The western half may be part of a down-dropped block which is now being exposed by erosion. The prominent eastern half is being ~~eroded~~ ^{eroded} along the ~~scarp~~ ^{fault-line} scarp, exposing the underlying beds. The remainder of the eastern half of the anticline is intact



Figure 27. S-190B photograph (role 88, frame 7), showing Mono Lake and the southern extension of the structural belt of the Walker Lane in the northern White Mountains and Fish Lake Valley. Numbers refer to targets used in interpretation of S-192 data.

and is crudely crescent-shaped with a stream drainage traversing north to south around its eastern margins. Except at the northern end of the structure, the beds strike slightly east of north and dip to the southeast, while the plunge of the anticline was also determined to be slightly east of north. At their highest point, the north striking beds form an escarpment about 700 ft. above the valleys on either side.

Photographic coverage of the anticline was obtained on two separate SL-3 passes. The first was along Track #6, on August 11th, (Figure 26), and the second was on Track #59 on September 13, 1973, (Figure 28). Coverage was obtained from NASA's RB-57 high altitude mission #248 (Figure 29), also flown on September 13th. The aircraft coverage was fortuitous as the mission was being flown in support of the S-191 Infrared Spectrometer aboard Skylab. The August 11th overflight, utilizing the S-190B camera, provided excellent color stereo photography of the anticline. The photographs were taken at 8:30 in the morning when the ^{solar} ~~azimuth~~ azimuth was nearly perpendicular to the strike of the structure; hence, there is considerable shadow enhancement along the north striking beds. Both the Skylab and aircraft missions of September 13th, were flown when the sun-angle was near 55 degrees; hence, there was no shadow enhancement.

Figures 25, 28, and 29 should be compared to the S-190A photography of the anticline, Figure 30, taken during the September overflight to see the advantages of resolution and sun-angle. As a result, the structural interpretations were best accomplished using the August 11th, low sun-angle imagery. The midday photography of September 13th provided the best radiometric data and was utilized in making lithologic determinations. The RB-57 employed two RC-8, 6" focal length cameras, one loaded with color

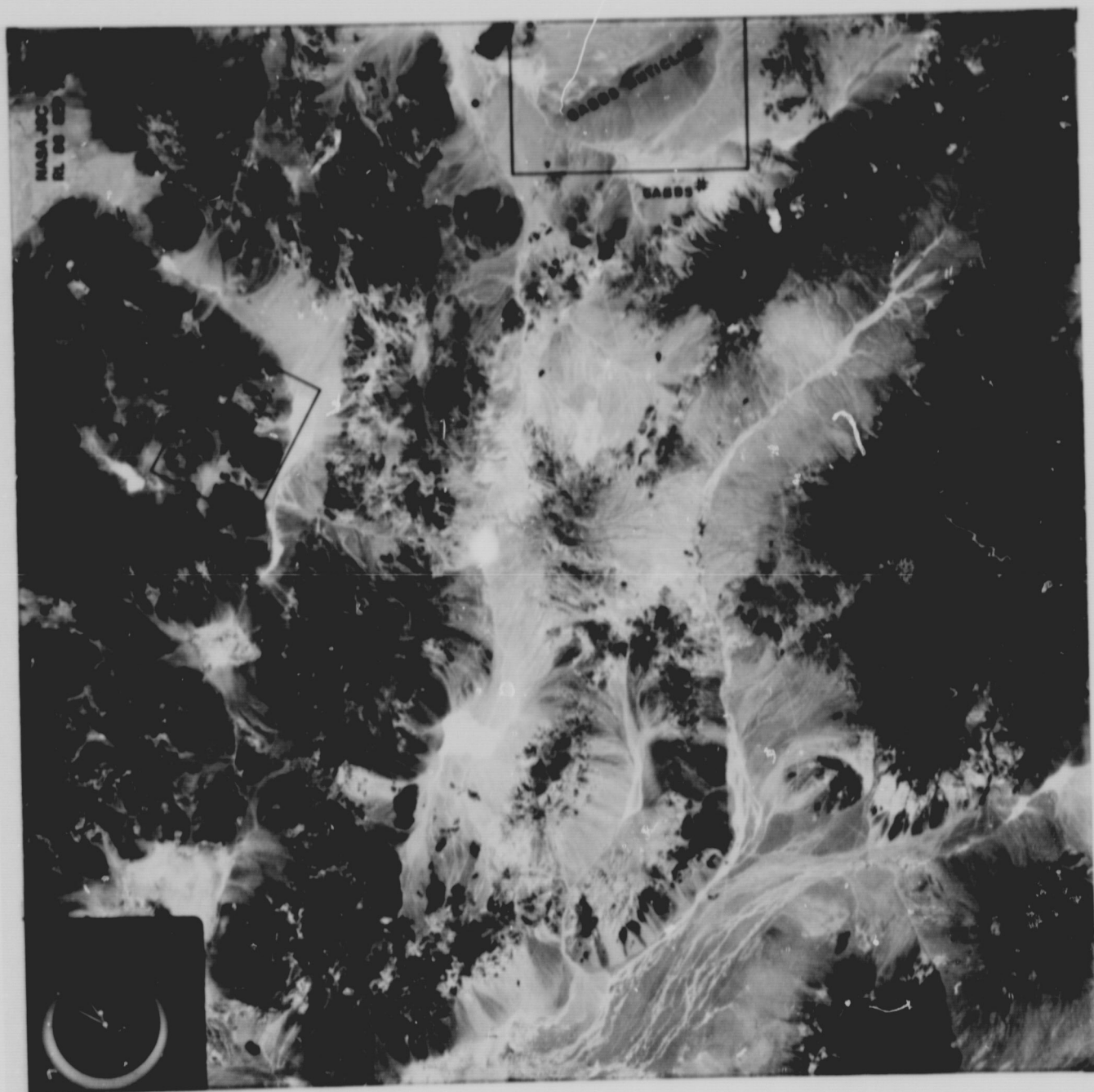


Figure 28. Photography from SL-3 with the S-190B sensor on tract 59, September 13, 1973. The Gabbs Anticline is noted at top center. Note the white ash bed along the breached axis of the anticline. Walker Lake is just out of view in the extreme upper left hand corner.

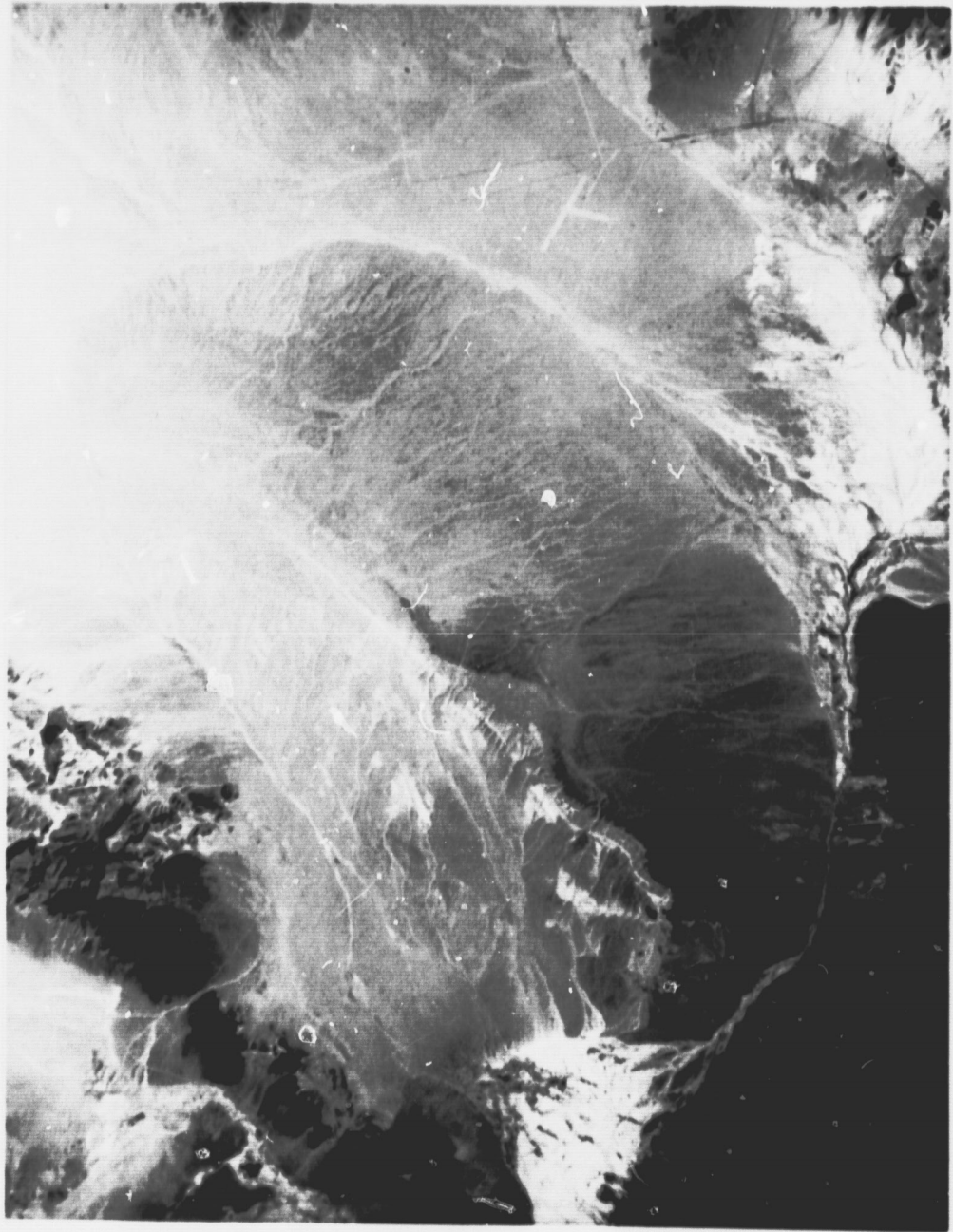


Figure 29. This photograph of the Gabbs Anticline was made by taking a picture of a color positive transparency. The original photograph was the product of an RB-57 high flight (mission 248), taken on Sept. 13, 1973. The Anticline is nearly 12 miles (22km) along its axis, and is aligned slightly east of north. Lack of structural enhancement is attributed to the sun being nearly vertical.

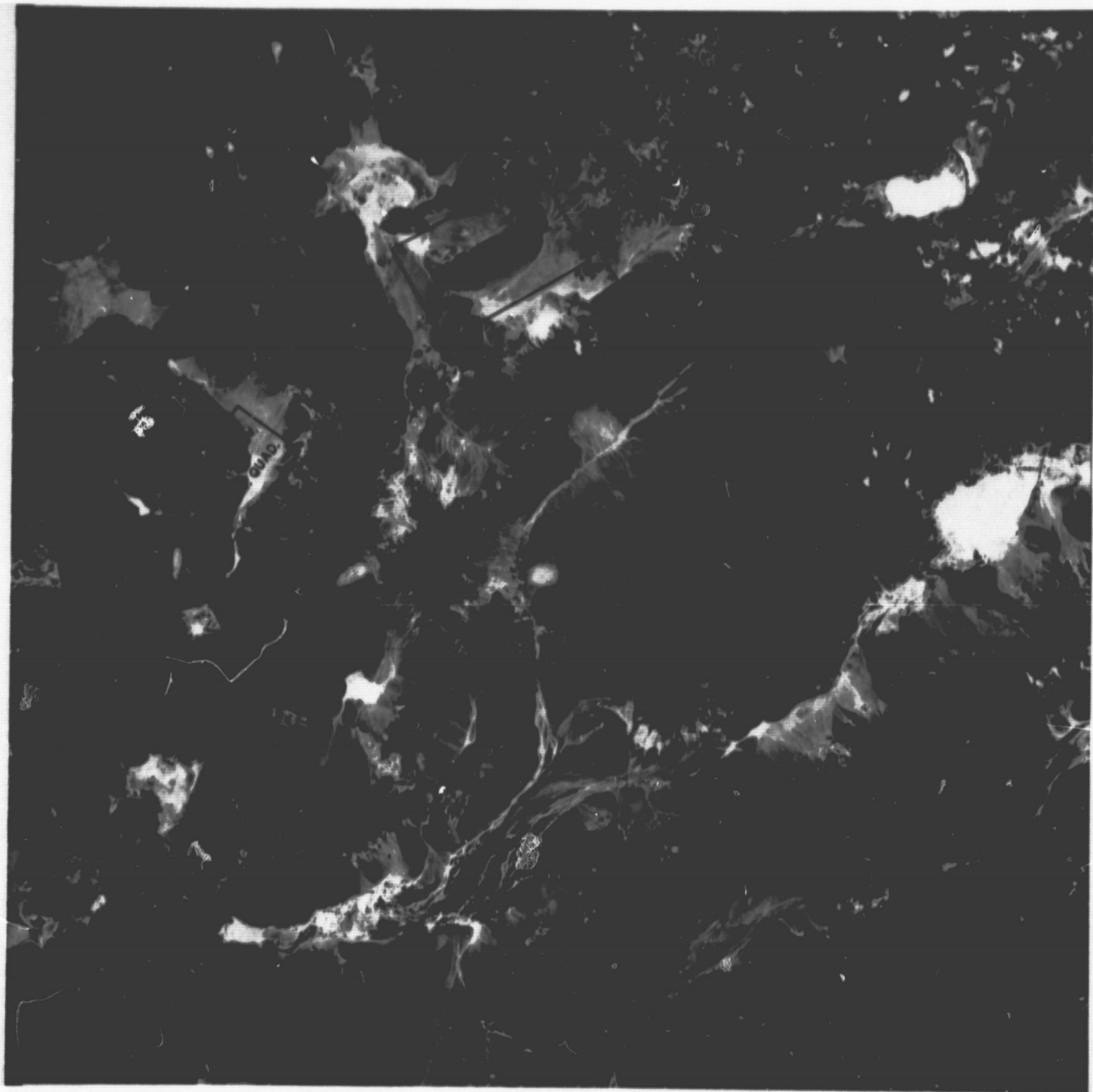


Figure 30. Photography acquired by the S-190A sensor on SL-3, track 59, September 13, 1973. Depicted are Walker Lake, The Gabbs Anticline and the Multi-spectral Test Site.

**REPRODUCIBILITY OF THE
ORIGINAL PAGE IS POOR**

infrared and the other with colored Ektachrome. The resulting 110:000 scale photos provided good large scale coverage.

The state geologic map for northern Nye County is a preliminary map by Frank J. Kleinhample and Joseph I. Ziony, (1967). The map does not indicate the presence of an anticline nor associated faults west of Gabbs Valley.

From field observations we were able to confirm what had been interpreted from Skylab photography -- that the uppermost beds were not continuous along the north-south escarpment, but had been removed in part by ^{erosion} ~~erosion~~. The best preserved section of the upper beds is at the northern end of the anticline. On the highest part of the anticline along the north-south escarpment a thin, dark-colored conglomerate caps the very light colored underlying beds. This conglomerate is not continuous along the entire escarpment and is completely missing on the southern end of the structure. The west dipping beds, which are only exposed at the northern end of the anticline, are being covered by alluvial fan deposition from the west. See Figure 31.

The underlying light colored beds are waterlaid ash fall tuffs, which can be traced continuously on the Skylab photos for about 10 miles along the north-south escarpment. From field measurements it was determined that these beds strike approximately N 20°E with an average dip of about 10° to the SE, (Figure 32).

While examining the contact between the conglomerate and the ash tuff, some silicified vertebrate fossils were found. Further examination along the contact revealed more fossils weathering from the uppermost portion of the tuff. Several bags of fossils were collected and returned



Figure 31. Looking north-northwest at the most prominently exposed beds and the nose of the Gabbs Anticline. These beds appear to be the youngest deposition of the stratigraphy of the Anticline and here exhibit an apparent dip to the northwest.



Figure 32. Looking east at the west facing outcrops of the breached Gabbs Anticline. The prominent white ash bed, which was first noticed in SL-3 photography and later in RB-57 photography, is dipping approximately 10° into the hill (East) and crops out nearly the entire length of the Anticline.

to the University for analysis. Dr. James Firby, a resident paleontologist at the Mackay School of Mines, was able to identify these specimens as belonging to two different animals, one a camel (camelidae), and the other an antelope (Antilocapridae). There was not enough fossil information collected to determine the exact species, but the ~~presence~~^{presence} of both animals was helpful in establishing a more precise geologic date for the deposition of the ash tuff. The beds immediately underlying the tuff are composed of a silicified, course grained, poorly sorted sandstone, grading to a pebble conglomerate. Frequent occurrences of opalized wood are found throughout the vertical and horizontal extent of these beds, particularly at the northern end of the anticline. The silica was probably carried downward from the overlying ash tuffs by descending ground water.

This information, along with other field observations on the stratigraphy, provided a type section which compared favorably with similar sections in a number of adjacent localities. This section, along with the fossil remains, has been identified as part of the Esmeralda Formation in locations to the south at Crow Springs, to the east at Ione, and to the west near the Cedar Mountains. Based on this information a date of 11 to 12 million years was established for the deposition of the ash tuff.

Although the ash tuff is not the youngest unit in the stratigraphic sequence, it is close to the top of the section, which suggests a date of not more than eleven million years for the age of the anticline.

The origin of the forces which caused the folding associated with the anticline are obscured by the fact that it is surrounded by areas of intense tectonic activities related to the Walker Lane and basin-range

faulting. The inception for both of these tectonic periods is greater than eleven million years. It is very likely, therefore, that the origin of the anticline can be traced to one of these two events.

One possible explanation for the origin of the folding associated with the anticline can be shown by using the Moody and Hill theoretical model for wrench faulting. From the model it can be demonstrated that the anticline may be a second order drag fold of the right lateral faulting of the Walker Lane. The Walker Lane, as discussed in the previous section, can be seen on the same Skylab frame #12 as a zone of intense northwest strike-slip faulting passing to the southwest of the anticline. The younger basin-range tectonics are probably responsible for the fault that bisects the anticline close to its north-south axis.

One of the unique characteristics of the anticline is the fact that much of it is still intact considering its age, size and its proximity to areas of intense deformation. This can best be observed with the fault studies overlay and frame #12, Figure 25. The anticline can be seen as one of the largest areas of positive relief with the least amount of deformation.

A number of questions concerning the structure of the anticline were not answered by our limited field examination, such as ^{structural} ~~unconformity~~ closure, ~~which~~ which can be determined by more detailed geological and geophysical field work.

In summary, the S-190B photography provided an excellent first look over-view of the anticline and its relationship to regional trends, ~~from~~ from which future studies can be applied.

Summary

S-190B

Although total coverage was not available along track #6, all in-house coverage was in stereo; stereo coverage was not acquired by the S-190A system during the same flight. The extra dimension of stereo viewing was used in the final data analysis along with the aforementioned techniques. The stereo capability was helpful in resolving problems relating to elevations and the attitude of bedding etc., but the greatest single contribution from the S-190B photography was the resolution capability.

Because of a unique operational coincidence, we were able to make an evaluation of the black-and-white photography as opposed to the color photography during low sun-angle conditions over an arid land region.

The S-190B system was operated over Nevada on two consecutive days. First over Battle Mountain using black-and-white film and the following day over Walker Lake using color film. Except for the locations the conditions were nearly identical with the same sun-angle, azimuth and atmospheric conditions. By selecting similar targets in both areas and by comparing the two kinds of photography, it was determined that the color photography was grainier and therefore had slightly less resolution; and with resolution capability a ^{key} ~~key~~ to geologic mapping, some of the detail is lost. We did not feel, however, that the loss of resolution significantly ^{affected} ~~affected~~ the reconnaissance mapping along track #6. Where the ^{of color photography} factors do seem relevant is in developing and processing, and in the questionable radiometric information that survives through to the final product. From the initial exposure to the processing to the color balancing and to the reproduction there are too many possible variables to produce

replicate data. We were never able to get color photography reproduced in the same colors or tones from one processing request to the next, which made differentiation by color a hazardous undertaking.

We strongly suggest, therefore, that future missions give a higher priority to black-and-white film during low sun-angle conditions over arid lands.

References Cited

Albers, J. P., Stewart, J. H., 1972, Geology and Mineral Deposits of Esmeralda County, Nevada, Nevada Bureau of Mines, Bull. 78, Plate 1.

Albers, J. P., 1967, Belt of Sigmoidal Bending and Right-Lateral Faulting in the Western Great Basin; Geol. Soc. America Bull., V. 78, No. 2, p. 143-155.

Cornwall, Henry, R., 1972, Geology and Mineral Deposits of Southern Nye County, Nevada, Nevada Bureau of Mines, Bull. 77, Plate 1.

Kistler, R. W., 1960, The Geology of the Mono Craters Quadrangle, California; California Univ. Berkeley, Ph.D. thesis.

Kistler, R. W., 1966, Structure and Metamorphism in the Mono Craters Quadrangle Sierra Nevada, California, Bull. 1221-E.

Kleinham, F. J., Ziony, J., 1967, Preliminary Geologic Map of Northern Nye County, Nevada. Scale 1:200,000.

Moody, J. D., and Hill, M. J., Bull. Geol. Soc. America; Vol. 67, 1956, pp. 1207-46.

Moore, James, G., 1969, Geology and Mineral Deposits of Lyon, Douglas, and Ormsby Counties, Nevada, Nevada Bureau of Mines, Bull. 75, Plate 1.

Ross, Donald C., 1961, Geology and Mineral Deposits of Mineral County, Nevada, Nevada Bureau of Mines, Bull. 58, Plate 2.

Speed, R. C., 1975, Tectonics of Nevada Seismic Zone, Report to U. S. Geological Survey, Technical Report 1 under contract 14-08-0001-G.

COMPARISON OF EARTHQUAKE EPICENTERS TO FAULTS AS MAPPED FROM S-190A DATA

Regional Seismic Patterns

Distribution of earthquake epicenters in Nevada shows a north^{-south} trend in the western Great Basin. This concentration of seismic activity has been termed the Nevada Seismic Zone (Gumper and Scholz, 1971) and trends generally north over a 500 km length between ^{Owens Valley on the south to} Pleasant Valley on the north. ~~the north.~~ In the area of Mono Lake and Mina, Nevada the Nevada Seismic Zone makes an easterly to northeasterly jog. This region of change in orientation of the zone ^{termed as} ~~the Mina~~ segment (Speed and Others, 1975).

The northern segment of the Nevada Seismic Zone occupies the Pleasant-Dixie Valley-Fairview-Cedar Mountain zone of modern faulting. These modern seismic events ^{were caused by} ~~are~~ a predominantly dip-slip ^{faults.} ~~movements.~~ Dip-slip displacements were associated with the Pleasant Valley earthquake of 1915 (Page, 1935), the Rainbow Mountain earthquake of 1954 (Siemmons, 1957). Although predominantly dip-slip displacement occurred on large magnitude events which caused ground breakage, interpretation of first motion and composite fault plane solution show of the Fairview Peak earthquake of 1954 (Romney, 1957) indicated that right-lateral oblique-slip motion occurred on generally north striking faults. Subsequent composite fault plane solutions on microearthquakes in the area of Figure 23 by Stauder and Ryall (1967) found dip-slip movement to be predominant.

The area of Figure 23 was selected for analysis of epicenter location and structural interpretation from S-190A data because the area is presently

under study by the U. S. Geological Survey as a potential site for controlled earthquake experiments. In addition accurate seismic data on epicenter location is available from the Nevada Seismological Laboratory which has been actively participating in the U. S. Geological Survey's program.

Faulting and Seismic Activity in the Mina Area

The Mina region of the Nevada Seismic Zone differs from adjacent tracks of the Great Basin in that it is topographically anomalous when compared to regions northwest and southeast where north-northwest ^{or} north-northeast trending fault block mountains and parallel alluviated valleys are dominant features. Figure 23 shows a characteristic change in the pattern of faulting. The area east of Walker Lake has a predominantly northwest trend of fault features while near the town of Mina this northwest trend abruptly ceases. The fault trends south of Walker Lake and west of Mina show a striking east-northeast orientation, which is opposed at approximately 90° to the normal trend of the Walker Lane. The southerly continuation of the western limb of the structural bend is shown in the lower left hand corner of Figure 23, and on Figure 27, which encompasses Mono Lake and the northern end of the White Mountains and Fish Lake Valley.

Earthquake epicenters for 1971-1973 are plotted on the overlay of Figure 23 to show the correspondence of epicenter location with faults mapped from S-190A photographic products. This particular photograph (Frame 56, Roll 30) was ~~amenable~~ ^{amenable} to structural interpretation since it was obtained at approximately 0827 local time on August 11, 1973 which produced a sun-angle of approximately 28° .

Accuracy of epicentral location of the Nevada Seismological Laboratories computer generated listing of seismic events for the area of Figure 23, is ± 1 km (Ryall, personnel communication). At the scale of Figure 23, (1:702,000) 1 km is equal to 1.4 mm. The small circles representing magnitudes less than 3 are 2 mm in diameter and the larger circles representing magnitudes greater than 3 are 3 mm in diameter. Therefore the diameter of the larger circles correspond to the accuracy of the location of the epicenters on the earth's surface. To maintain the accuracy during plotting the epicentral location of each event was plotted on an AMS Sheet (1:250,000 scale) which was optically reduced to match the scale of Figure 23.

Striking correspondence of epicentral locations of the 1971-1973 seismic data with faults of the east-northeast trend can be seen west and southwest of Mina. There is also good correlation of epicenter locations along the northwest trending faults east of Walker Lake. The correspondence of epicenters for both fault trends and the concentration of seismic activity near the town of Mina indicates an area of intense activity although the magnitudes were not large, that is not exceeding 6.0 magnitude Richter.

Several epicenters are located south of Mina in the Candelaria Hills area where only a few faults of relatively short lengths (a few kilometer) occur. The anomalously low density of faults in this area as interpreted from the S-190A data is probably due to the Tertiary and Quaternary extrusive volcanic rocks that comprise the Candelaria Hills. In reality, numerous faults, some with lengths on the order 10 km have been mapped by Speed and Other (1975). In fact the density of faulting in the Candelaria

Hills equals or exceeds the density of faulting associated in other adjacent ranges when mapped by conventional geologic mapping.

The concentration of seismic activity in the Mina area and the divergent trends in fault orientation have been inferred to be the result of a kinematic change in basin and range faulting within the last 6 ($\frac{1}{2}$) m.y. A hypothesis proposed by Speed and Other (1975) suggests a shifting of the axis of extension from possibly a northwest direction to a more westerly trend. This trend can be seen in Figure 23 as the fault traces along the lower left side of the figure trend northwest and then appears to coalesce with fault more easterly trend. Then passing through the Mina area the trend of faults ^{again} ~~again~~ assumes a northwesterly orientation from Mina towards Walker Lake.

References

- Byerly, Perry; Slemmons, D. B.; Tocher, Don; Steinbrugge, D. V.;
Moran, D. F., and Cloud, W. K., 1956, The Fallon-Stillwater
Earthquakes of July 6, 1954: Seis. Soc. America Bull., v. 46,
p. 1-40.
- Gumper, F. J. and Scholz, Christopher, 1971, Microseismicity and Tectonics
of the Nevada Seismic Zone: Seis. Soc. America Bull., v. 61,
p. 1413-1432.
- Page, B. M., 1935, Basin-Range Faulting of 1915 in Pleasant Valley,
Nevada: Jour. Geology, v. 43, p. 690-707.
- Romney, Carl, 1957, Seismic Waves from the Dixie Valley-Fairview Peak
Earthquakes: Seis. Soc. America Bull., v. 50, p. 187-196.
- Slemmons, D. B., 1957, Geological Effects of the Dixie Valley-Fairview
Peak, Nevada, Earthquakes of December 16, 1954: Seis. Soc. America
Bull., v. 47, p. 251-265.
- Speed, R. C., 1975, Tectonics of Nevada Seismic Zone, Report to U. S.
Geological Survey, Technical Report 1 under contract 14-08-0001-G.
- Stauder, William and Ryall, Alan, 1967, Spatial Distribution and Source
Mechanism of Microearthquakes in Central Nevada: Seis. Soc. America
Bull., v. 57, p. 1317-1345.

RELATIONSHIP OF METAL MINING DISTRICTS
TO STRUCTURAL INTERPRETATION OF S-190A

The relationship of metal mining districts of central Nevada to the structural interpretation of S-190A, frame 57, roll 28 obtained on August 11, 1973 is shown in Figure 24. The metal mining districts represent various metallic ore deposits including, contact (skarn type), replacement, fissure and placer. Table 6 shows the mining district name, type of deposit and principal products.

Cursory observation of Figure 24 does not reveal any distinct relationship between mining districts and structural analysis provided from interpretation of S-190A data. However, two of the most productive districts, Goldfield and Tonopah, numbers 1 and 2 respectively do appear to be associated with some structural control. Other districts which are associated with faults or regional lineaments as mapped on frame 57 are the Divide (3), Lone Mountain (5), Weepah (6), Fish Lake Valley (11), Dyer (14), Gold Crater (26), Bullfrog (30), Eden (33), and Hanapah (37) districts. One thing that is apparent is that vein or fissure type deposits in Tertiary volcanic rocks can be related to the S-190A structural interpretation. Whereas replacement type deposits or those as vein types in older rocks do not show a correspondence to the structural interpretation.

It therefore appears that structural interpretations of small scale lineaments can be useful in locating structurally related ore deposits in Tertiary rocks. Larger scale, more pervasive structural zones could be associated with deposits located in older pre-Tertiary rocks.

22

RELATIONSHIP OF METAL MINING DISTRICTS TO STRUCTURAL INTERPRETATION OF S-190A

The relationship of metal mining districts of central Nevada to the structural interpretation of S-190A, frame 57, roll 28 obtained on August 11, 1973 is shown in Figure 24. The metal mining districts represent various metallic ore deposits including, contact (skarn type), replacement, fissure and placer. Table 6 shows the mining district name, type of deposit and principal products.

Cursory observation of Figure 24 does not reveal any distinct relationship between mining districts and structural analysis provided from interpretation of S-190A data. However, two of the most productive districts, Goldfield and Tonopah, numbers 1 and 2 respectively do appear to be associated with some structural control. Other districts which are associated with faults or regional lineaments as mapped on frame 57 are the Divide (3), Lone Mountain (5), Weepah (6), Fish Lake Valley (11), Dyer (14), Gold Crater (26), Bullfrog (30), Eden (33), and Hanapah (37) districts. One thing that is apparent is that vein or fissure type deposits in Tertiary volcanic rocks can be related to the S-190A structural interpretation. Whereas replacement type deposits or those as vein types in older rocks do not show a correspondence to the structural interpretation.

It therefore appears that structural interpretations of small scale lineaments can be useful in locating structurally related ore deposits in Tertiary rocks. Larger scale, more pervasive structural zones could be associated with deposits located in older pre-Tertiary rocks.

TABLE 6
METAL MINING DISTRICTS

<u>District</u>	<u>Type of Deposit</u>	<u>Principle Metals (in decreasing importance)</u>
1. Goldfield	Veinlike irregular bodies in Tertiary dacite flows that were warped into a dome and faulted.	Au, Cu, Ag
2. Tonopah	Replacement veins in Tertiary rhyolitic rocks and altered andesite.	Ag, Au, Pb
3. Divide	Veins along shear zones in upper Tertiary pyroclastic.	Ag, Au, Pb
4. Klondyke	Replacement bodies in Cambrian sedimentary rocks.	Ag, Au, Pb, Cu
5. Lone Mountain	Replacement bodies in Cambrian limestone along contact with porphyry dike or with granite intrusive	Pb, Cu, Zn
6. Weepah		Au, Ag
7. Crow Springs		
8. Gilbert		Au, Ag, Cu, Hg
9. Rock Hill	Scheelite placers.	W, Fe
10. Black Horse		W, Fe
11. Fish Lake Valley	Silicification of rhyolite tuff	Hg
12. Silver Peak	Gold-bearing quartz lenses in Paleozoic limestone beds.	Au, Ag, Pb, Cu
13. Argentite		Ag
14. Dyer		Ag, Pb
15. Good Hope		Ag
16. Palmetto		Pb, Au, Ag, Cu
17. Railroad Springs		Cu, Au, Ag

<u>District</u>	<u>Type of Deposit</u>	<u>Principle Metals (in decreasing importance)</u>
18. Lida	Veins and replacement bodies in Cambrian rocks.	Ag, Au, Pb, Cu
19. Sylvania	Contact deposits of scheelite in tuffite	W, Au, Pb, Ag
20. Gold Point	Veins in calcareous shale near granitic intrusive.	Au, Ag, Cu
21. Tule Canyon		Au, Ag
22. Stonewall		Au, Ag, Cu
23. Cactus Springs		Au, Ag
24. Antelope Springs		Ag, Pb, Au
25. Wellington		Au, Ag
26. Gold Crater		Au, Ag, Pb
27. Wilsons		Ag, Au
28. Kawich		Ag, Au
29. Tolicha		Au, Ag
30. Bullfrog	Crustified gold-bearing quartz- pyrite veins in Tertiary rhyolite.	Au, Hg, Ag
31. Fluorine		
32. Bellehelen	Fissure veins in rhyolite ashflows.	Ag, Au, Cu
33. Eden		Au, Ag
34. Silver Bow	Veins in altered Tertiary rhyolite welded and non-welded tuffs.	Ag, Au, Pb
35. Golden Arrow		Ag, Au
36. Ellendale		Au, Ag, Cu
37. Hannapah		Ag, Au
38. San Antone	Veins in Permian rocks and Ordovician limestone.	Ag, Pb, Cu

Mention has been made by Horton (1966) who statistically analyzed the distribution of mining districts in Nevada that two northwesterly mineral belts may be valid; the Broad Walker Lane, and a narrower belt in the north-central part of the state which coincides with Robert's (1966) Battle Mountain-Eureka belt. The southwestern (left side) of Figure 24 includes a portion of the Broad Tectonic environment known as the Walker Lane. It appears that there is no preferred orientation to coincide with the northwest trend of the Walker Lane. This may be related to the uniform extension hypothesis proposed by Speed (1975) and described in detail in other sections of this report.

The usefulness of Skylab S-190A data for reconnaissance structural mapping should be apparent. The synoptic view provided aids the interpreter in viewing large areas which would not be possible from conventional aerial photography, where mosaicing and splicing many times interfere with the mapping of regional structural lineaments.

A Possible Ore Deposit

A report of a possible large "Mineral Deposit" being discovered in White Pine County, Nevada, using Skylab Photography, was made by Dr. Mead L. Jensen of Utah University in September, 1973. The location for the discovery was reported as north of the Kennecott Copper Pit at Ely, in the Robinson Mining District.

The statements made in the numerous press releases that generally relate this discovery to Skylab data are: "The light colored areas amid the dark colored volcanics are suggestive of limestone" and "obviously, therefore the volcanics are very thin in these areas" and as a result "the magnetic anomaly that surrounds this area isn't due to the volcanics

but is due to the fact that something from below has given rise to mineralization in the limestone rocks".

The discovery area was overflown by an RB-57 during mission #239 flown on our behalf on June 5, 1973, and by Skylab on SL-2 along track #20 on May 30, 1973. The aircraft photography was good quality color at a scale of 1:110,000, while the Skylab photography was color and black-and-white from the S-190A system. In an attempt to clarify the newspaper statements, the aircraft photography was compared with existing gravity maps, aeromagnetic maps and the preliminary geologic map of White Pine County by Richard K. Hose and Clarke Blake, Jr. (1970).

The analysis technique used was to make a mylar overlay of the aeromagnetic map by J. E. Carlson and D. R. Mabey (1963) at a scale of 1:150,000 so as to conform to the geologic map of White Pine County. From these data it was determined that the magnetic highs were associated with the Tertiary, older volcanics, while the magnetic lows occurred over the Quaternary Sedimentary rocks and Tertiary younger sedimentary and volcanic rocks. The magnetic anomalies were not associated with the light colored limestone.

A field trip revealed that approximately half of the light colored rocks amid the darker volcanics were not limestone, but Quaternary and Tertiary younger sedimentary and volcanic rocks, very similar in color to the limestone. Because of the similarities in color and tone, individual light-colored rock types could not be discriminated using Skylab photography. Some bedding and preferred vegetation made identification of the limestone possible on the color IR and color Ektachrome taken during mission #239. However, nothing new could be said about these individual geologic units or their time and space relationships that had not already been mapped.

During the field trip all of the contacts were traversed with special emphasis on the limestone without revealing any evidence of alteration or mineralization that might be related to an ore deposit.

It was determined therefore, that in the absence of surface mineral indications or any subsurface exploration information, that any references to mineral types or economic evaluations were pure conjecture.

REPRODUCIBILITY OF THE
ORIGINAL PAGE IS POOR

References

- Horton, R. C., 1966, Statistical Studies of the Distribution of Mining Districts in Nevada, in Papers presented at the AIME Pacific Southwest Mineral Industry Conference, Sparks, Nevada, May 5-7, 1965: Nevada Bur. Mines, Report 13, Part A.
- Roberts, R. J., 1966, Metallogenic Provinces and Mineral Belts in Nevada, in Papers presented at AIME Pacific Southwest Mineral Industry Conference, Sparks, Nevada, May 5-7, 1965: Nevada Bur. Mines Report 13, Part A.
- Speed, R. C., 1975, Tectonics of Nevada Seismic Zone, Report to U. S. Geological Survey, Technical Report 1, under contract 14-08-0001-G.

LITHOLOGIC MAPPING

Multispectral Test Site Description

An area southwest of Coaldale Junction, Nevada in T. 1 N., R. 35 and 36 E., T. 2 N., R. 35 and 36 E. was selected for detailed photomapping and spectroradiometric measurements. The purpose of the spectroradiometric measurements was to provide data for selection of optimum film-filter combinations for the S-190A and aircraft AMPS camera systems for lithologic mapping in arid-semiarid regions of the world. Spectral data collected at this site and methodology of data acquisition are presented in Appendix A. Figure 30 outlines the area of the multispectral test site.

The test site ^{contains} a complex of Late Tertiary volcanics consisting of welded and non-welded ash flows which disconformably overlie shale with locally abundant chert, limestone and quartzite of Lower Paleozoic age. These units have been faulted and ^{tilted} ~~eroded~~ to the northeast. The Lower Paleozoic rocks are dominantly black or dark green while the overlying volcanics range from black to white with numerous shades of red, orange, tan and brown. Figure 33 is a photograph looking northeast across a small valley which dissects the volcanics. The figure shows to some extent the complexity of the area and the wide range of diverse colors available for spectral measurements within a small area. The selection of this area was based on: 1) accessibility, 2) variability of colors available in a small area, and 3) the ^{opportunity to make} spectral measurements ~~on the site~~ almost continuously on lithologies with vastly different spectral reflectances.

Photographic Data Products

Some problems arose in obtaining both aircraft and Skylab photographic data over the test site. Aircraft mission 239 did not overfly the site



Figure 33. Ground photograph of the Multispectral test site looking northeast across Gap Spring.

REPRODUCIBILITY OF THE
ORIGINAL PAGE IS POOR

because prior permission to fly over the northern portion of the Nevada Test Site was not obtained from the Atomic Energy Commission. Mission 249 photography did cover the test site, but only the RC-8 cameras provided stereo overlap. The AMPS system intervalometer was set to provide only 10% forelap because of limited magazine capacity. S-190B system was not operating over the test site during the SL-2 mission. On the SL-3 mission (track 6) the S-190B camera was shut-off. ~~On SL-3 track 59 the test site would have been visible if the 60% forelap mode of operation had been in effect, but it was not and the test site is covered by the clock inset.~~ On SL-3 track 59 the test site would have been visible if the 60% forelap mode of operation had been in effect, but it was not and the test site is covered by the clock inset.

Track 59 on SL-3 would have provided the best data for geologic mapping since the time of the overflight was midday. The photographic products derived from the camera systems on SL-3 track 6 were marginal for lithologic mapping because of the early morning time of fly-by which precluded a sun angle of approximately 28 degrees.

Geologic Photomapping

Geologic photomapping was performed with 1) the RC-8 9" x 9" Ektachrome at a scale of approximately 1:120,000, 2) the AMPS Ektachrome 70 mm at a scale of 1:120,000, ~~transferring the interpretation~~ to 9" x 9" black-and-white enlargements from the same camera, ~~system at a~~ scale of 1:30,000, and 3) S-190B Ektachrome ~~positive~~ ^{transparencies} enlarged to a scale of 1:250,000.

Figure 34 is the geologic interpretation ~~prepared~~ ^{transparencies} prepared from the 1:250,000 ~~enlargement~~ of S-190B frame 013 roll 84. It can be seen that only the gross features can be mapped at this scale. Comparison with a portion



Figure 34. Geologic interpretation of the Multispectral Test Site.
Prepared from 1:250,000 scale diapositive of frame 13, roll
84.

REPRODUCIBILITY OF THE
ORIGINAL PAGE IS POOR

of the Esmeralda County map (Figure 35) which has a scale of 1:250,000 shows only a minor correspondence between reconnaissance geologic mapping and the interpretation of S-1908 data at a scale of 1:250,000. The S-1908 photography was obtained at approximately 0830 local time and therefore has shadows on the west facing slopes.

At this scale the best correspondence with mapped units of the Esmeralda County Geologic map are the Q1b units Figure 35 and the gray areas of S-1908 interpretation Figure 34. The correlation is due to the distinctive pattern and dark black tone of the basalt flows. Discrimination between the lower sedimentary unit (Tsl) and the upper and lower non-welded ash flow (Taft and Tafu) and the welded ash flows (Taw) is difficult at this scale. On the geologic map (Figure 35) the ash flow units each contain ~~many~~ ^{multi-colored} members ~~of various~~ colors which are sometimes confused during photointerpretation at this scale as to the genetic affiliation.

In one area (number 4 on Figure 27) there is no difficulty in mapping the extent of the quarry area (white) and the surrounding volcanics. The quarry ~~is~~ diatomaceous earth (diatomite) ~~is~~ owned by Grefco, Inc. The lateral extent of the yet unmined diatomite cannot be discerned on the S-1908 photography, ~~the~~ ^{the} outcrop ~~is~~ of the diatomite ~~is~~ generally covered by colluvium from the surrounding volcanic rocks.

Geologic mapping from the RC-8 photographs is presented in Figure 36. The complexity of the multispectral test site is exemplified in this interpretation from stereo pairs of 1:120,000 scale color Ektachrome transparencies which has been plotted on 1:24,000 scale preliminary topo-

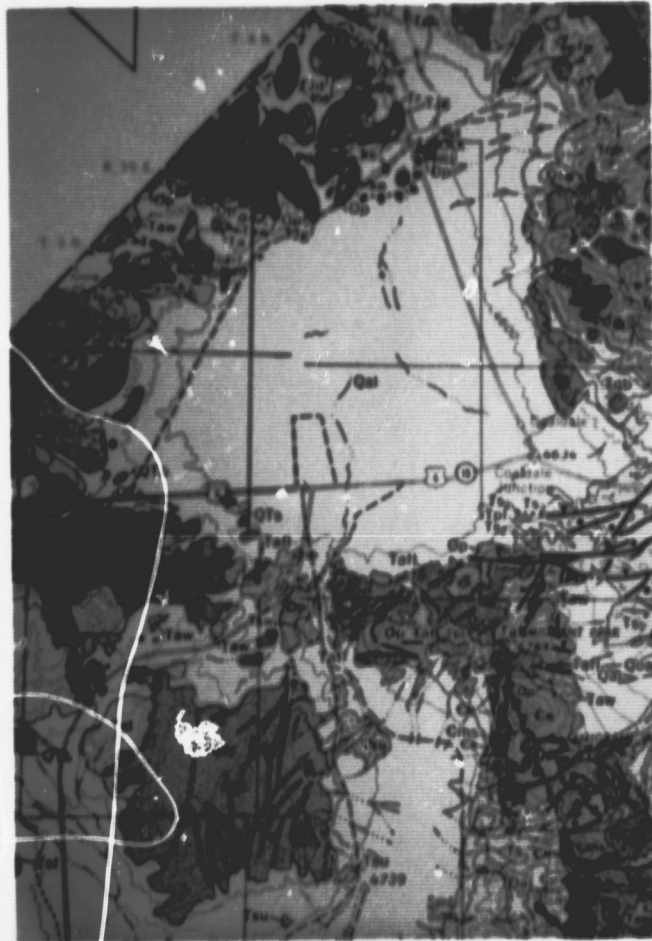


Figure 35. A portion of the geologic map of Esmeralda County, Nevada. Original scale 1:250,000, by John P. Albers and John H. Stewart.

REPRODUCIBILITY OF THE
ORIGINAL PAGE IS POOR



Figure 36. Geologic map of the multispectral test site from RC-8 color ektachrome photography with a scale of approximately 1:120,000. Original scale of the map is 1:24,000.

graphic maps. Figure 37 (roll 27, frame 26, mission 249) shows the area of multispectral test site at a scale of approximately 1:154,000. In this figure the numerous members of the upper and lower ash tuff units can be differentiated (compare with Figure 35, a portion of the Esmeralda County Geologic map). The individual members of the ash flow units have a complex outcrop pattern developed from differential erosion and structural modification due to faulting. The purple color on the interpretive map is the lowest unit stratigraphically, but due to its resistant nature it crops out in an area as large as the less resistant non-welded ash flows and welded ash.

The geologic interpretation of the AMPS camera system which employed the same film-filter combinations as the S-190A camera shows the detailed complexity of the multispectral test site, Figure 38. Geologic interpretation was performed without the aid of stereographic pairs which limited the detail that could be mapped at a scale of 1:24,000.

Usefulness of S-190B Photographs for Geologic Mapping in Areas of Complex Lithologies.

The foregoing discussion and comparison of S-190B photographic products and aircraft photography shows the limitations of S-190B products for geologic mapping in areas of small outcrop pattern, even though diverse color and tonal qualities are present. Comparison of Figures 36 and 38 will show that the complexity of the multispectral test site, which is amenable for the rapid collection of spectral data, is an area which exceeds the resolution capabilities of the S-190B data products. The subsequent section on the Mina NW 7.5-minute quadrangle will provide an example of the capabilities of geologic mapping with S-190B data.

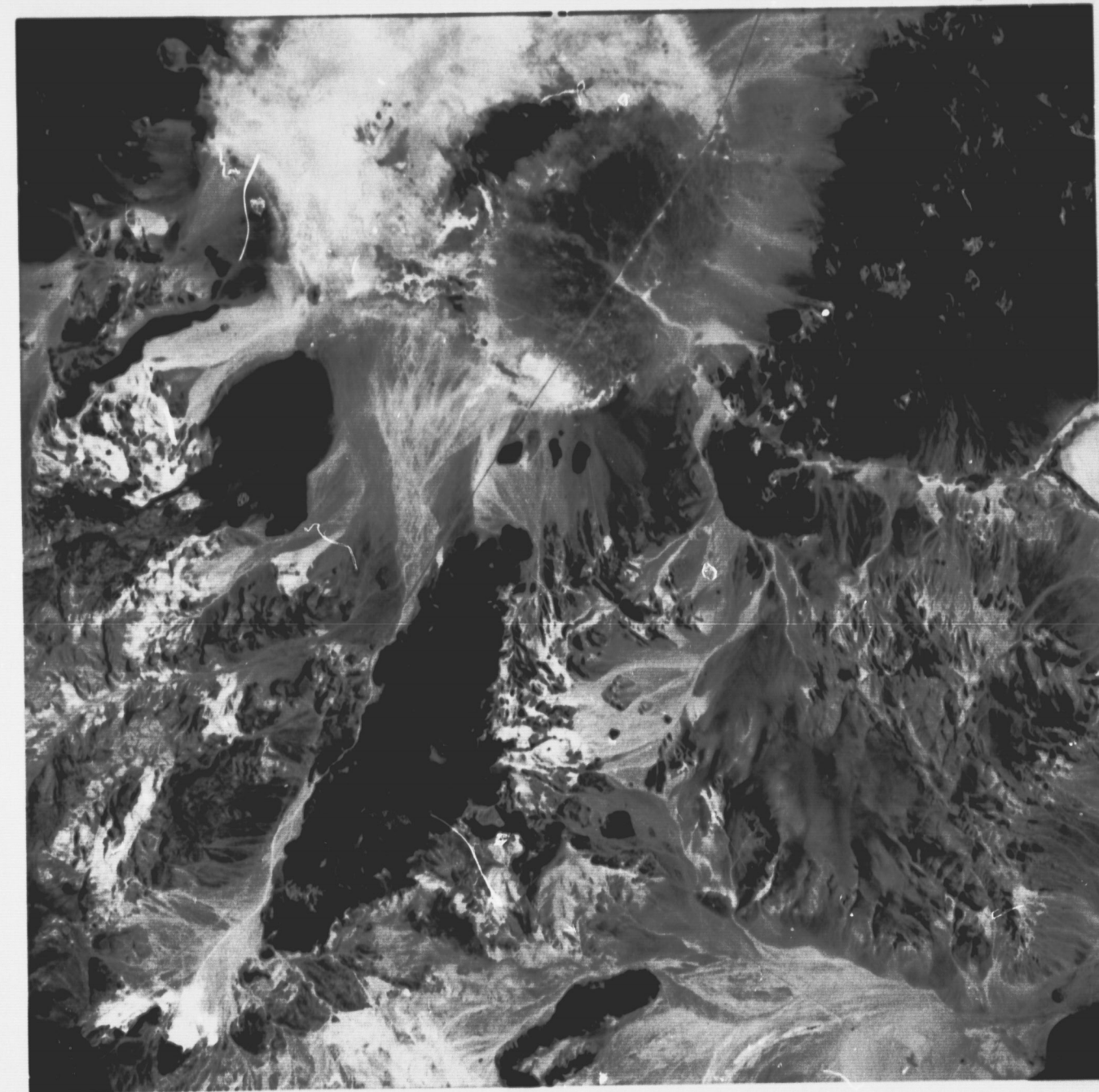


Figure 37. RC-8 photograph of Multi-spectral Test Site (mission 249, roll 27, frame 26). The complexity of the test site, right center, can be seen.

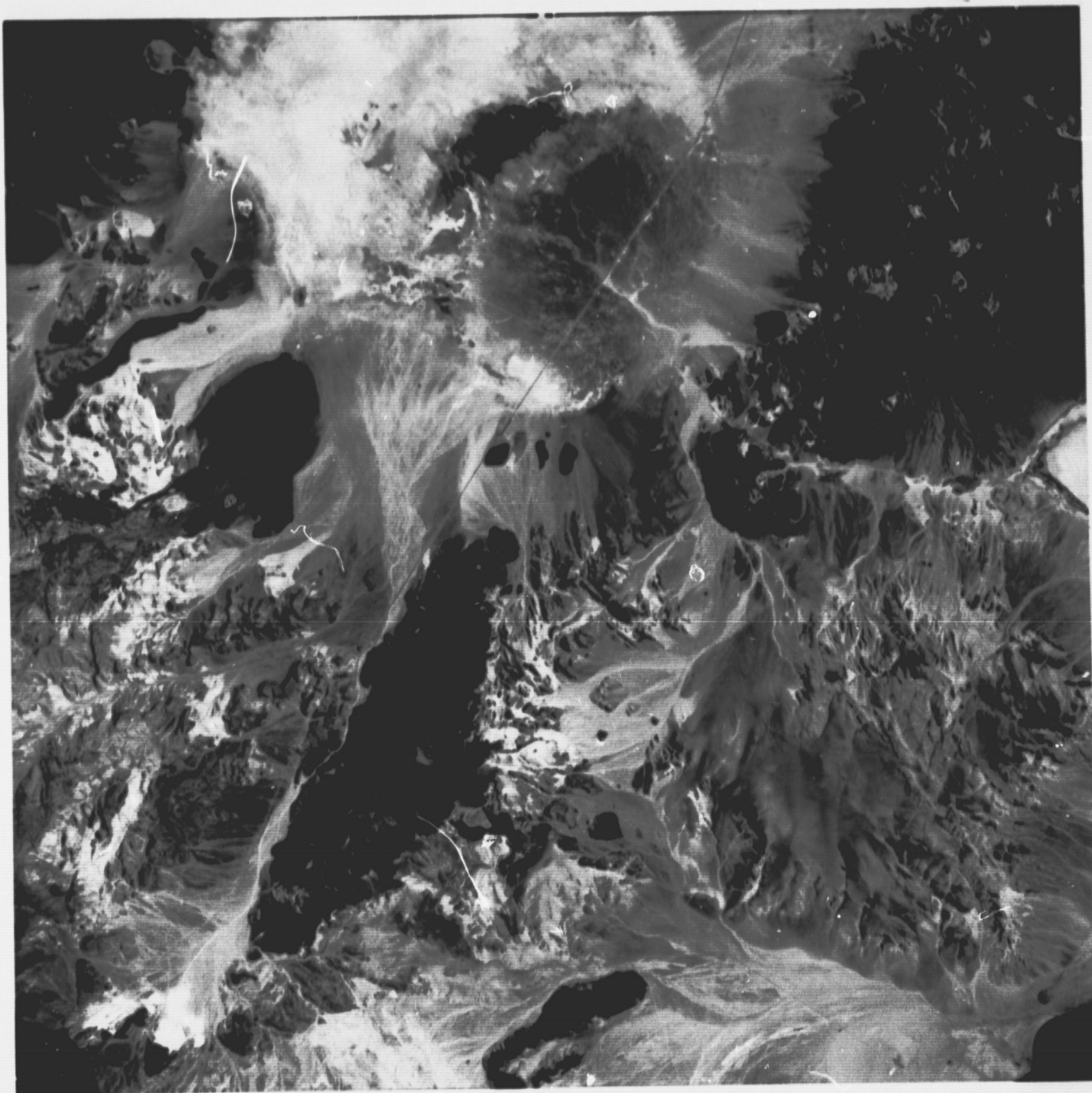


Figure 37. RC-8 photograph of Multi-spectral Test Site (mission 249, roll 27, frame 26). The complexity of the test site, right center, can be seen.

REPRODUCIBILITY OF THE
ORIGINAL PAGE IS POOR



Figure 38. Geologic map of the multispectral test site prepared from AMPS color ektachrome at a scale of approximately 1:120,000. Original scale of the map is 1:24,000.

Mina NW, 7.5-minute Quadrangle, Nevada

The Mina NW 7.5-minute quadrangle was selected to determine to what extent S-190B photography could be used in geologic mapping. The area has sparse vegetation consisting mainly of sagebrush. Geologically the Mina NW quadrangle consists of intrusive and extrusive igneous rocks and sedimentary rocks. The sedimentary rocks have been folded and are cut by numerous high angle normal faults. The area of the Mina NW quadrangle is outlined on Figure 30.

The photo interpretation was performed with a Wild stereoscope with 8X oculars. Two-X enlargements of color Ektachrome, Figures 25 and 26, roll 84, covered the area stereoscopically. Scale of the photography is approximately 1:460,000

Comparison of Figures 39 and 40 shows that gross lithologic discrimination is possible with Skylab imagery. Discrepancies occur in distinguishing ~~between~~ ^{difference between} in the sedimentary units, especially the Luning and Dunlap formations. The map (Figure 40) used for comparison was prepared from U.S.G.S. Map GQ-45 Geologic map of the Mina quadrangle, Nevada, by H. G. Ferguson, S. W. Muller and S. H. Cathcart, 1954, scale 1:125,000.

Figure 41 provides an explanation of Figure 40.

The most ~~discrepancies~~ ^{widespread} discrepancies between the map prepared from S-190B photography and that prepared from reconnaissance geologic mapping, occur in the northern portion of the map. This area ~~include~~ ^{include} the outcrop pattern of the Luning and Dunlap formations. The Luning formation consists of ^{recrystallized} limestone, slate with a little conglomerate within the upper limestone unit and slate with varying proportions of conglomerate in the

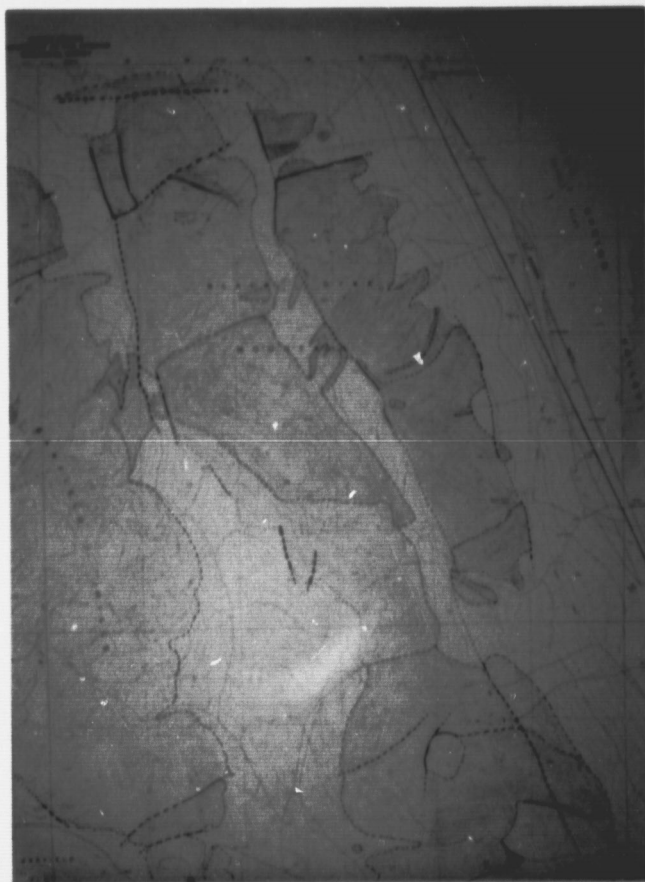


Figure 39. Geologic interpretation of S-190B. Frames 12 and 13, roll 84, using a Wild stereoscope with 8X magnification. Compare with Figure 40.

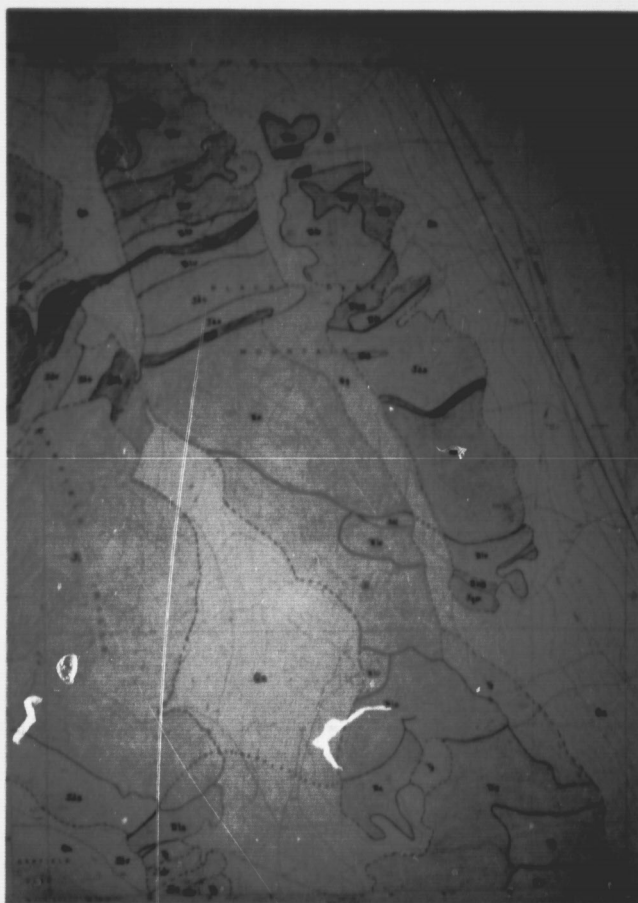


Figure 40. Map prepared from U. S. Geological Survey Map. GQ-45, geologic map of the Mina quadrangle, Nevada, by H. G. Ferguson, S. W. Miller and S. H. Cathcart, 1954, scale 1:125,000. Figure 41 provide explanation of mapped units.

EXPLANATION	
<input type="checkbox"/>	DESERT OUTWASH AND ALLUVIUM
<input type="checkbox"/>	OLDER GRAVELS AND LAKE BEDS
<input type="checkbox"/>	GILBERT ANDESITE
<input type="checkbox"/>	RHYOLITE AND RHYOLITE TUFF
<input type="checkbox"/>	INTRUSIVE ROCKS UNDIFFERENTIATED
DUNLAP FORMATION	
<input type="checkbox"/>	conglomerate with interbedded sandstone
<input type="checkbox"/>	conglomerate "thrust conglomerate"
<input type="checkbox"/>	greenstone and greenstone breccia
<input type="checkbox"/>	interbedded sandstone and conglomerate
LUNING FORMATION	
<input type="checkbox"/>	thick massive limestone
<input type="checkbox"/>	slate with minor conglomerate
<input type="checkbox"/>	slate and conglomerate
<input type="checkbox"/>	EXCELSIOR FORMATION

Figure 41. Explanation of units on Figure 39.

lower unit. Sedimentary rocks of the overlying Dunlap formation consist of conglomerates with interbedded sandstones, greenstones and greenstone breccias with varying amounts of sandstone and conglomerate.

The highly folded nature of the rocks of Jurassic age and their similarity in composition make the delineation from one another difficult. Similarities in weathering characteristics of both formations form areas of moderate relief which topographically have very little resemblance to the folded nature of the materials. Differentiation between units within the Dunlap formation along the western margin of the mapped area which are conglomerates and greenstone breccias with interbedded sandstones was not possible because of the similar composition and weathering characteristics.

Of the sedimentary rocks exposed in the Mina quadrangle the thick massive limestones of the upper part of the Luning formation (T1u, Figure 40) were most easily differentiated and mapped with fair degree of accuracy. Errors in mapping the extent of the massive limestones from other formations was approximately 10%; however, the ~~amount of error~~ ^{degree of accuracy} in differentiating the limestones from other sedimentary units was on the order of 35%.

The discrimination of intrusive and extrusive igneous rocks is the easiest in this particular area. Intrusive rocks are irregular masses and dikes of Jurassic age related to the Sierra Nevada batholith. The granitic rocks are light colored and have a characteristic subdued weathering characteristics. ~~The~~ ^{Pre-}dominant jointing was not observed and therefore could not be used in identifying granitic rocks. Extrusive rocks

are the Excelsior formation (T_e) and the Gilbert andesite (T_g). The Excelsior formation is dominantly dark pyroclastics and altered lava with some minor dark siliceous slate and dark tuffaceous sandstone. This unit is characteristically dark on the photography and forms broad rolling summits on the ranges. The Gilbert andesite consists of andesite flows grading to basalt, with much andesite breccia and agglomerate. It forms areas of low relief with little dissection.

Few ^{range} frontal faults were mapped on the reconnaissance geologic map; many are inferred from the S-190B photography. Faults between ~~formations~~ ^{Jurassic} were harder to discern and were interpreted as normal contacts from the photography. Inter-formational faults were easier to identify based on linearity of stream channels and alignment of saddles.

Comparison of geologic mapping from Skylab S-190B photographic products and reconnaissance mapping at 1:125,000 scale shows a good correlation for the three basic rock types. Differentiation between sedimentary units which have been highly folded is difficult. Differentiation between sedimentary-igneous intrusive, sedimentary-igneous extrusive and intrusive-extrusive rocks is readily apparent. This technique shows benefit for reconnaissance geologic mapping of gross lithological units. In areas not previously mapped the general relationship between igneous and sedimentary rocks can be made. Determination of these relationships would provide a basis for further geologic exploration based on the commodity of interest, such as more detailed mapping in igneous units and contacts for metallic minerals.

INTERPRETATION OF S-192 DATA PRODUCTS

Interpretation of S-192 data consisted of visual analysis of ^{positive film images of} the 13 sands in the conical scan, calibrated format. ~~Quaternary~~ ^{selected for} Areas of diverse lithology, alteration and vegetation were ~~used~~ in the analysis of 3 sections of data obtained on August 11, 1973 and September 13, 1973. Data from the August 11 mission were obtained at approximately 0830 local time and therefore do not provide the optimum illumination for comparison of multispectral differentiation of lithologic units, since west facing slopes were in shadow.

The targets selected for evaluation of the September 13, 1973 (GMT 19 32' 45") segment of imagery are enumerated on Figure 27. Target 1 is an older alluvial fan and volcanic flow, target 2 is a cultivated-uncultivated field complex, and target 3 is the Bodie Mining District, California. Table 7 lists all sites used for comparison of effectiveness of detection of S-192 imagery.

Table 7
Selected targets for S-192 interpretation

<u>Date</u>	<u>Time (GMT)</u>	<u>Target</u>
August 11, 1973	15 27' 20"	1) Red cinder in black cinder cone. 2) Alteration in Goldfield area. 3) Green alluvial fan material.
September 13, 1973	19 32' 45"	1) Basalt flow and older alluvial fan. 2) Cultivated and uncultivated fields. 3) Bodie mining district.
September 13, 1973	19 33' 10"	1) Natural vegetation. 2) Volcanics in Pilot Mountains.

Complete detailed comparisons of the usefulness of the individual bands in delineating the various selected targets is presented in Table 8. A comparison of which bands were most useful in distinguishing the various lithologies during the August 11, 1973 mission is presented in Table 9.

Table 8

August 11, 1973 GMT 15 27' 20"

<u>Channel</u>	<u>Microns</u>	<u>Remarks</u>
1	.41- .46	Appears noisy, of no value.
13-1	10.2 -12.5	Playas and ephemeral streams appear colder than alluvial fans. Playas with vegetation show mottled appearance such as Rhodes salt marsh, Columbus salt marsh and Big Smokey Valley.
9	1.09- 1.19	1) Red in cinder cone NE of Silver Peak shows lighter as compared to black cinder. 2) Caldera at Goldfield accentuated by light tones of the grays and lt. tans. 3) Green alluvial fan on eastside of Paymaster Ridge appears darker than rest of fan.
8	.98- 1.08	1) Red in cinder cone not apparent. 2) Same as 9. 3) Same as 9.
2	.46- .51	1) Red in cinder cone not apparent cinder cone is darker than in any previous band. 2) Circular light tones near Goldfield apparent. Basalt not as dark as other bands.

<u>Channel</u>	<u>Microns</u>	<u>Remarks</u>
10	1.2- 1.3	1) Red in cinder cone apparent. 2) Green on alluvial fan east of Paymaster Ridge is apparent, i.e., darker than rest of fan. 3) More variation in tone at the Goldfield alteration.
12	2.1 -2.35	1) Red in cone shows best of all as compared with previous bands. 2) Green on alluvial fan eastside of Paymaster Ridge apparent. 3) Alteration near Goldfield does not appear as well as other bands.
11	1.55-1.75	1) Red in cinder cone is best displayed in this band. 2) Green on fan eastside Paymaster Ridge shows only slight variation from rest of fan. 3) Halo around Goldfield shown by light tone of lighter colored rocks.
7	.78- .88	1) Basalts around Goldfield have better contrast, alteration zone not readily apparent. 2) Red of cinder cone in Clayton Valley not apparent. 3) Green on fan shows up but not as good as other bands.
6	.68- .76	Same as 7.
5	.62- .67	Similar to 6 except tonal contrast is less, overall resolution is also less.

Table 8 (Continued)

September 13, 1973 GMT 19 32' 45"

<u>Channel</u>	<u>Microns</u>	<u>Remarks</u>
1	.41- .46	Noise of no use in interpretation.
13	10.2 -12.5	Of marginal quality for geologic interpretation. 1) Not apparent on imagery. 2) Cultivated field apparent. Uncultivated field not apparent. 3) Bodie mining district faintly apparent, not distinctive.
9	1.09- 1.19	1) Basalt flow and older alluvial fan appear the same. 2) Cultivated field not apparent while uncultivated is. 3) Bodie mining district not readily apparent.
8	.98- 1.08	1) Basalt flow slightly darker than fan. 2) Uncultivated field barely apparent due to drop outs in data. 3) Same as 9.
2	.46- .51	1) Flow and fan distinctly different contrast. 2) Both cultivated and uncultivated fields apparent. 3) Bodie mining district apparent.
10	1.2 - 1.3	1) Basalt flow and fan distinction possible, not markedly good. 2) Cultivated field not apparent while uncultivated is. 3) Bodie mining district not readily apparent.

<u>Channel</u>	<u>Microns</u>	<u>Remarks</u>
12	2.1 -2.35	1) Same as 10. 2) Cultivated field apparent. Uncultivated difficult to distinguish from Bajada. 3) Same as 10.
11	1.55-1.75	1) Basalt flow and older fan distinguishable. 2) Same as 12. 3) Same as 10.
7	.78- .88	1) Same as 11. 2) Cultivated field not apparent. Uncultivated field apparent. 3) Same as 10.
6	.68- .76	1) Basalt flow and fan distinctly different. 2) Same as 7. 3) Bodie mining district marginally apparent.
5	.62- .67	1) Contrast between fan and basalt flow marginal. 2) Both cultivated and uncultivated field apparent. 3) Bodie mining district not apparent.
4	.56- .61	1) Basalt flow distinctly darker than fan. 2) Both cultivated and uncultivated fields apparent. 3) Bodie mining district not readily apparent.
3	.46- .51	1) Same as 4. 2) Same as 4. 3) Same as 4.

Table 8 (Continued)

September 13, 1973 GMT 19 33' 10"

<u>Channel</u>	<u>Microns</u>	<u>Remarks</u>
1	.41- .46	Noisey, of no value.
13	10.2 -12.5	Only gross features recognized, playas void or vegetation appear colder than adjoining alluvial fans. Cloud shadows are cold.
9	1.09- 1.19	1) Vegetation not apparent. 2) Volcanics better defined than in photo.
8	.98- 1.08	1) Same as 9, noise. 2) Same as 9, noise.
2	.46- .51	1) Vegetation defined. 2) Volcanics not as well defined as photo.
10	1.2 - 1.3	1) Vegetation not apparent. 2) Volcanics well defined.
12	2.1 - 2.35	1) Vegetation apparent. 2) Volcanic defined as well as photo.
11	1.55- 1.75	1) Vegetation marginal. 2) Volcanics well defined.
7	.78- .88	1) Vegetation not apparent. 2) Volcanics defined as well as photo.
6	.68- .76	1) Same as 7. 2) Volcanics not as well defined as photo.

<u>Channel</u>	<u>Microns</u>	<u>Remarks</u>
5	.63- .67	1) Vegetation well defined. 2) Same as 6.
4	.56- .61	1) Vegetation well defined. 2) Volcanics defined as well as photo.
3	.52- .56	1) Vegetation well defined. 2) Volcanics not well defined.

Table 9

Degree of usefulness of S-192 bands
August 11, 1973

	<u>Least useful</u>	<u>Moderately useful</u>	<u>Most useful</u>
Red in cindercone	2,5,6,7,8	9,10	11,12
Goldfield Alteration	5,6,7,12	2,8,9	10,11
Alluvial material of Harkless fm.	5,6,7,11	12	8,9,10

As seen in the above tabulation the longer wavelength bands, as a whole, are more useful in the differentiation of these lithologic types. In only one case, the alluvial material of the Harkless formation are the longest wavelengths in the near infrared not the most useful. This is undoubtedly due to the green color of the material.

To ascertain the resolution capabilities of the various bands in the S-192 system the detection of drainage patterns on alluvial forms was used since there is little contrast between the drainage channels and the alluvial fan material. Table 10 presents a comparison of the usefulness of the various bands in discerning drainage patterns.

Table 10

Usefulness of S-192 bands in the delineation
of drainage patterns on alluvial fans

<u>Least useful</u>	<u>Moderately useful</u>	<u>Most useful</u>
1,2,8,9 and 13	6,7,10	3,4,5,11,12

It can be seen that longer wavelength (.46-.88 microns) in the visible portion of the spectrum and bands 11 and 12 are the best for differentiation of low contrast objects. The usefulness of the .46 to

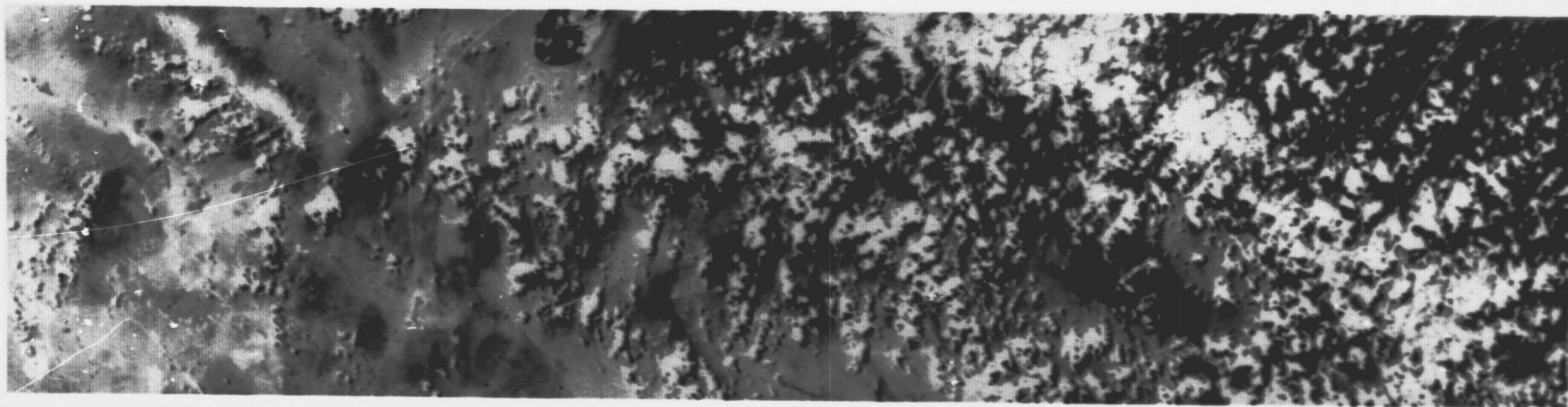
.88 micron range is not surprising. The surprising fact is that the 1.55 to 2.35 micron range is equally useful. The reason for this phenomena is not readily apparent.

Another interesting fact that was noted during the visual analysis of the September 13 mission (GMT 19 32'45") was the ability of certain bands to detect and discriminate between cultivated and uncultivated fields. Bands 2-5 (.46-.67 microns) showed both cultivated and uncultivated fields, (Target 2 on Figure 27). Uncultivated areas were discernable in bands 6-10 (.68-1.30 microns) while the cultivated field was not discernable. Conversely the cultivated field was detected in the near infrared portion of the spectrum, bands 11 and 12 and also in the thermal infrared portion band 13, while the uncultivated field was not detected. Figure 42 shows an example of the ability of certain bands to detect cultivated and uncultivated fields. It would appear that proper band selection could be used to rapidly identify total area of land cleared for agricultural purposes and which areas were under cultivation at the time of the overflight.

Another useful benefit derived from the S-192 multispectral scanner is the ability to differentiate between snow and clouds. Uncalibrated quick look data from channels 2 and 11 are presented in Figure 43. These data were derived on June 3, 1973. Track 6 traversed the western edge of Nevada from north of Lake Tahoe to south of Mono Lake. Band 2 shows the extent of snow cover along the eastern slope of the Sierra Nevada Mountains and at high elevations in the White Mountains south and east of Mono Lake. Snow reflectance in band 11 (1.55-1.75 microns)



Figure 42. Upper image (Band 9, 1.09-1.19 microns) shows uncultivated field while lower image (Band 12, 2.0-2.35 microns) shows only the portion of the field with vegetation.



BAND 2

BAND 11



Figure 43. S-192 imagery obtained on 3 June, 1973. Comparison of band 11 (1.55-1.75 microns) and band 2 (0.46-0.51 microns). Note distinct reversal of snow reflectance while cloud reflectance remains the same in both bands.

is very low and appears darker than surrounding terrain which is barren of snow. By selecting the appropriate bands, S-192 data can be used to automatically distinguish between snow and clouds because of their relative difference in reflectance.

APPENDIX

- A -

Field Spectral Studies

Field spectral data were collected at selected sites in support of the S-190A multispectral camera system.

The principle objectives of these studies was to acquire spectral signatures from geologic targets and to use these data in making determinations on film-filter combinations for discrimination purposes using multispectral photography.

The field measurements were conducted using a ISCO model SR spectrometer. Basically, the instrument consists of a light chopper, monochromator, measuring photo cell, amplifier, coherent detector and indicating meter. The spectrometer incorporates two wavelength ranges, the visible 380-750 milli micron, and the near infrared, 750-1550 milli micron. The instrument operates in the second interference order of the visible ranges and the first order on the near infrared range. The visible range detector is a silicon junction photo cell. The near infrared detector is a germanium junction photo cell.

The ISCO instrument is capable of recording the gross aspects of spectra in the wavelength range of .38 to 1.55 micron. It is possible to estimate the features in the spectrum to .005 micron in the range .38 to .75 micron and .01 micron in the range .75 to 1.55 micron.

Fiberfrax type 970JH, a ceramic fiber material, was used as a reflectance standard during all of the field measurements. The Fiberfrax was attached to a cardboard surface to offer resistance against tearing and to provide a perfectly smooth surface while taking field measurements.

Data Collection and Site Selection

During all of the spectral measurements, a standard field operating procedure was followed. The ISCO was always operated from a 110v, 60 cycle portable power supply, and batteries were checked and changed periodically. The ISCO was always operated utilizing the portable optic head from which the diffuser disk had been removed. The diffuser disk had been replaced by a metal washer with a 0.25 in. hole, which accepted only those rays which came from the field of view, and not 2π , as is necessary with global illuminance. The ISCO was operated from a tripod from which a metal extension held the portable head at the same vertical height during all of the studies, Figure 44. The measurements were always taken with the portable head looking downward normal to the target, with the instrument looking toward the sun. At such time as the sun was vertical to the target, the metal extension would cause a shadow but the total area involved was less than 1% of the field of view.

A typical set of measurements involved taking vertical reflectance readings from both the target and the fiberfrax standard at each site. This particular type of measurement is called "bidirectional reflectance".

Site selection was based on acquiring enough spectra from a given geologic target so that an average reflectance for any given unit could be generated. Geologic units were selected on the basis of their size, homogeneity and tonal (color) differences between formations. The criteria was based on the fact that targets had to be big enough to be seen from space, with enough tonal differences between formations to create a good contrast, and with sufficient homogeneity that an average spectra would be meaningful.



Figure 44. ISCO mounted on tripod and probe on metal extension, with white Fiberfrax standard mounted on flat board.

REPRODUCIBILITY OF THE
ORIGINAL PAGE IS POOR

Figure 45 shows the locations of sites used during the field spectral reflectance studies which has been annotated for the purposes of referencing the text to selected spectral reflectance curves shown in appendix A.

Figure 46 demonstrates how selected portions of the visible light and infrared bands might be selected from actual spectral curves taken in the field. Any attempts to discriminate individual geologic targets requires the selection of some portion of their curves which has a different reflectivity at a given wavelength. It can be seen from Figure 46 that any portion of the spectra will discriminate the White Ash Tuff, while discrimination of the Quartz Monzonite below .60 microns is in direct conflict with four other units.

The last five sets of curves in Appendix A are sky radiation curves taken during Skylab and aircraft overflights. During overflights, the diffusing screen was placed in the portable head and operated in a vertical mode while monitoring across the spectral bands as a function of time.

Conclusion

The original intent was to use these data in photographic multiband experiments, first from aircraft systems and later from space. Operational constraints made such plans impossible and our multiband evaluations were conducted using a standard film-filter configuration.

Collecting large numbers of spectra during the field studies is a very time consuming process. A single site requires more than thirty minutes to read and record the data from both the standard and the target.

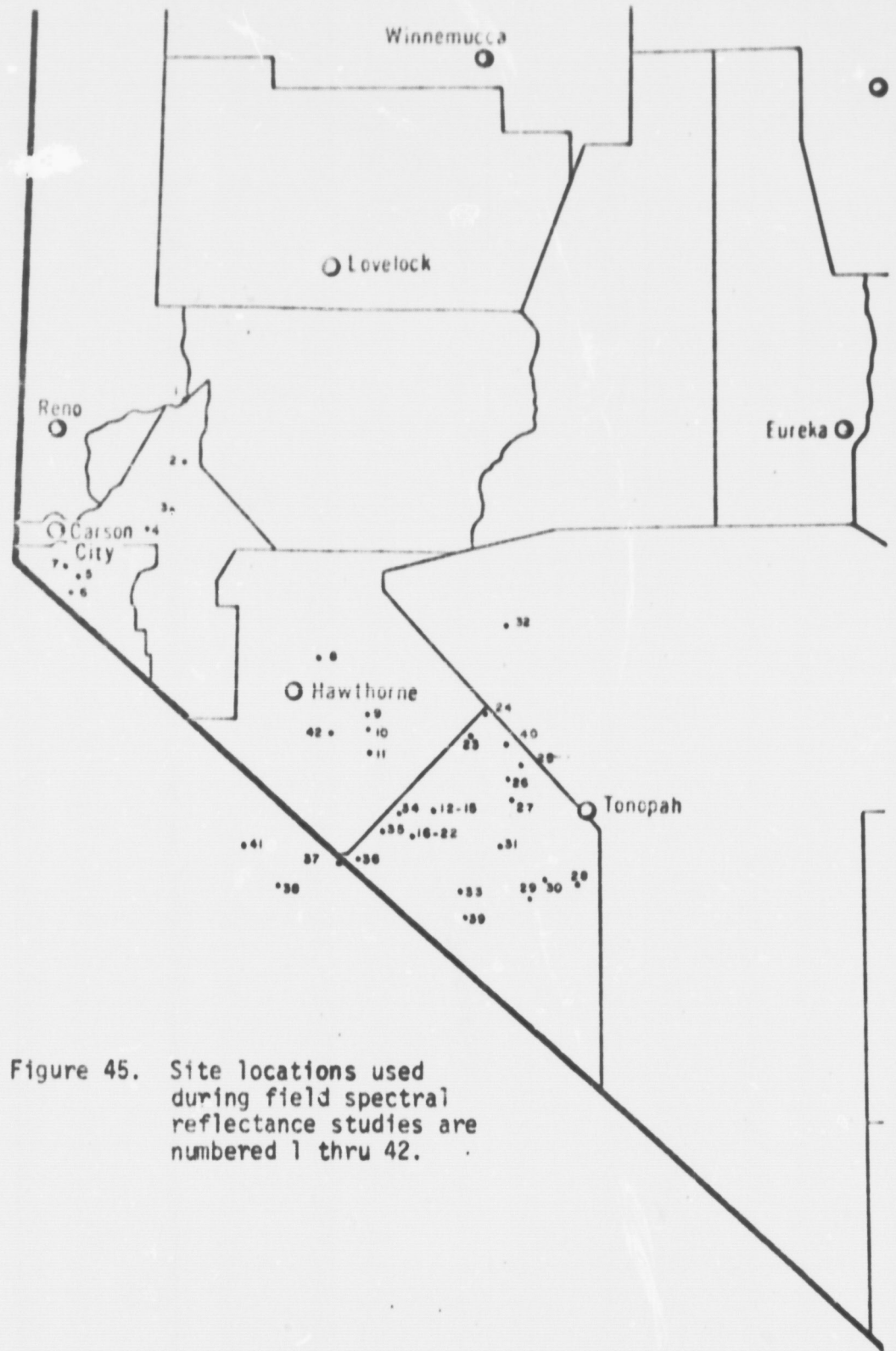


Figure 45. Site locations used during field spectral reflectance studies are numbered 1 thru 42.

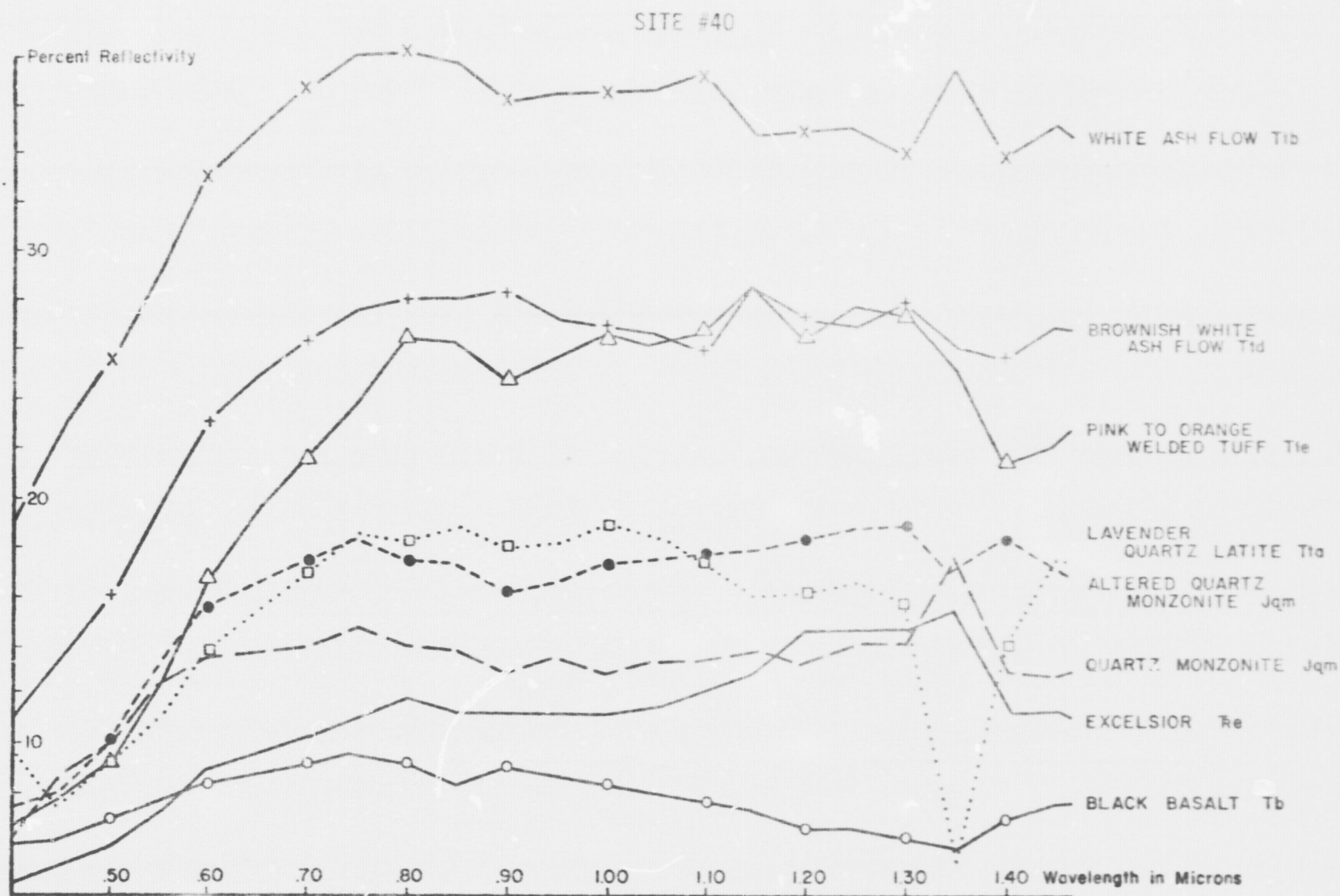


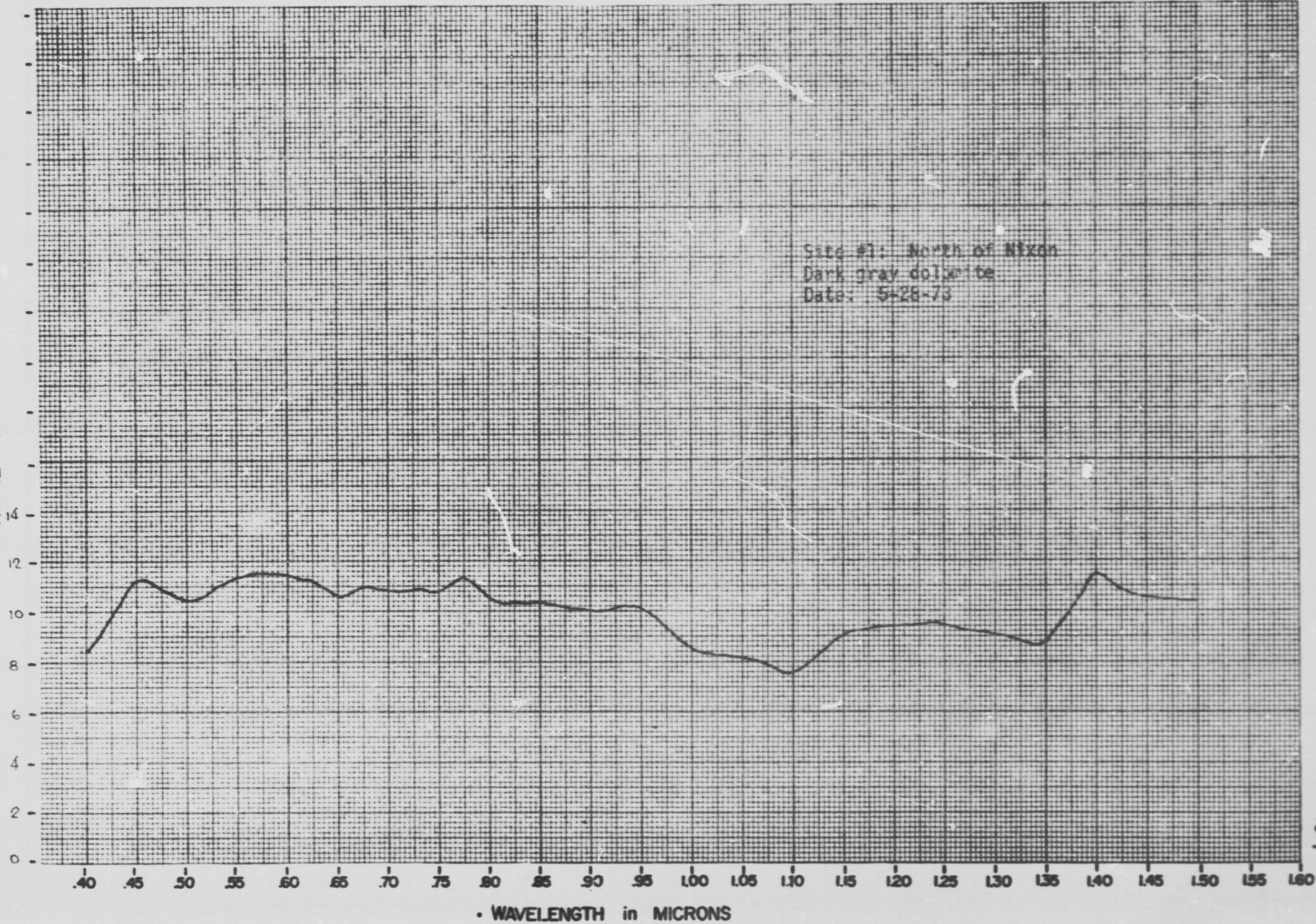
Figure 46. Spectral reflectance curves from the Crow Springs Mining District.

Further, the delicate equipment must be stored, moved and unpacked for each set of measurement. Driving time between targets is often time consuming. Cloud free conditions are mandatory, and only those hours between 9:30 and 3:30 can be used because the sun-angle changes are too radical before and after.

The question of how many spectra should be taken from each unit, what size sampling grid should be used and where to make the measurements is time consuming. The size of the target area from which the spectra are taken, or the field of view, with respect to the homogeneity of the unit are also a factor.

Our measurements program accomplished its objectives but required a great deal more time than we had originally envisioned. If such a field program were to be undertaken again, we would strongly recommend the use of a spectrometer and a data system that would allow for rapid data acquisition and storage. Under ideal conditions a helicopter would provide a variable field of view, hovering capability, and the means to acquire data in relatively inaccessible areas.

PERCENT REFLECTIVITY



PERCENT REFLECTIVITY

40

30

20

10

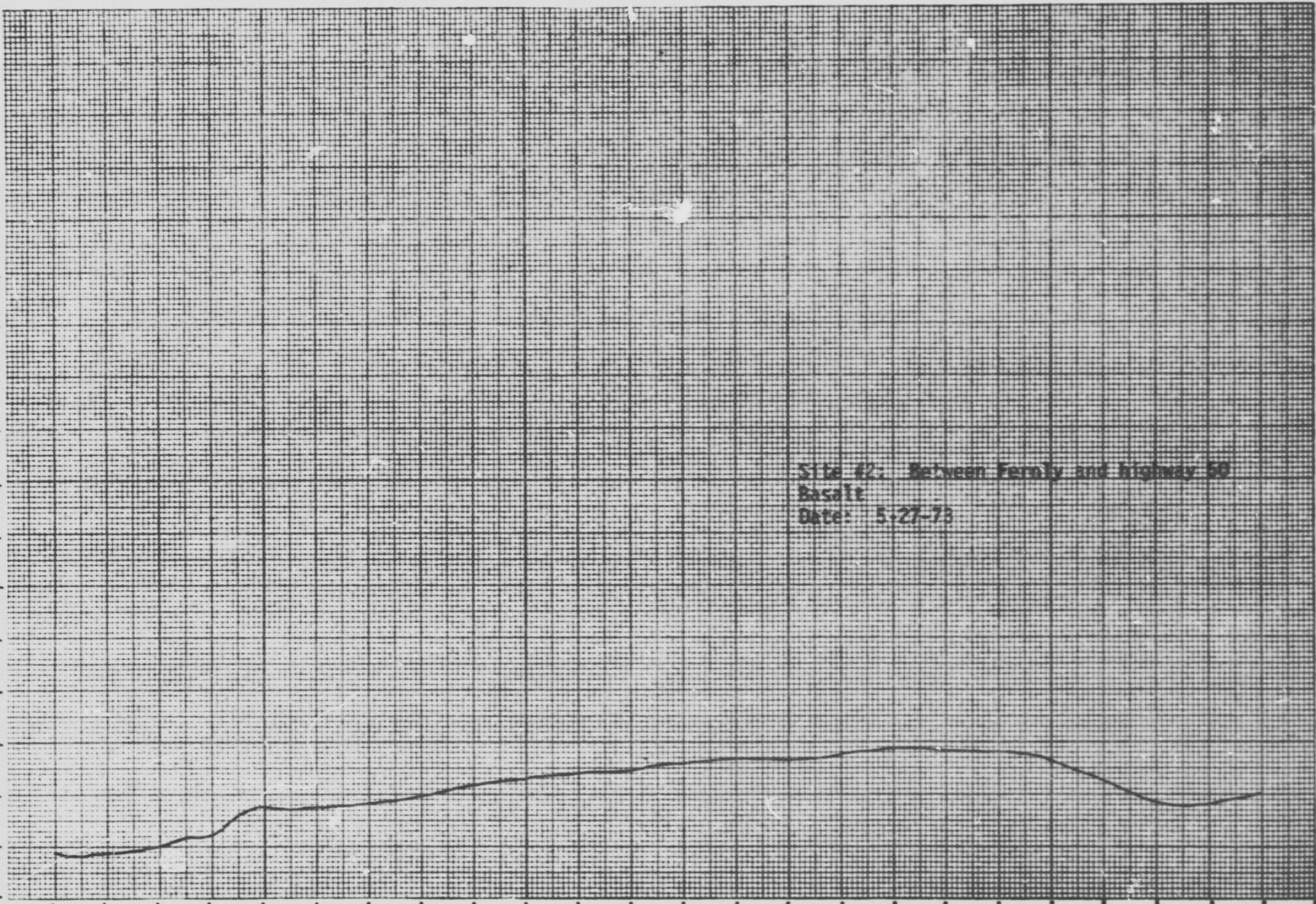
0

Site #2: Between Fernly and Highway 50
Basalt
Date: 5-27-78

.40 .45 .50 .55 .60 .65 .70 .75 .80 .85 .90 .95 1.00 1.05 1.10 1.15 1.20 1.25 1.30 1.35 1.40 1.45 1.50 1.55 1.60

WAVELENGTH in MICRONS

765



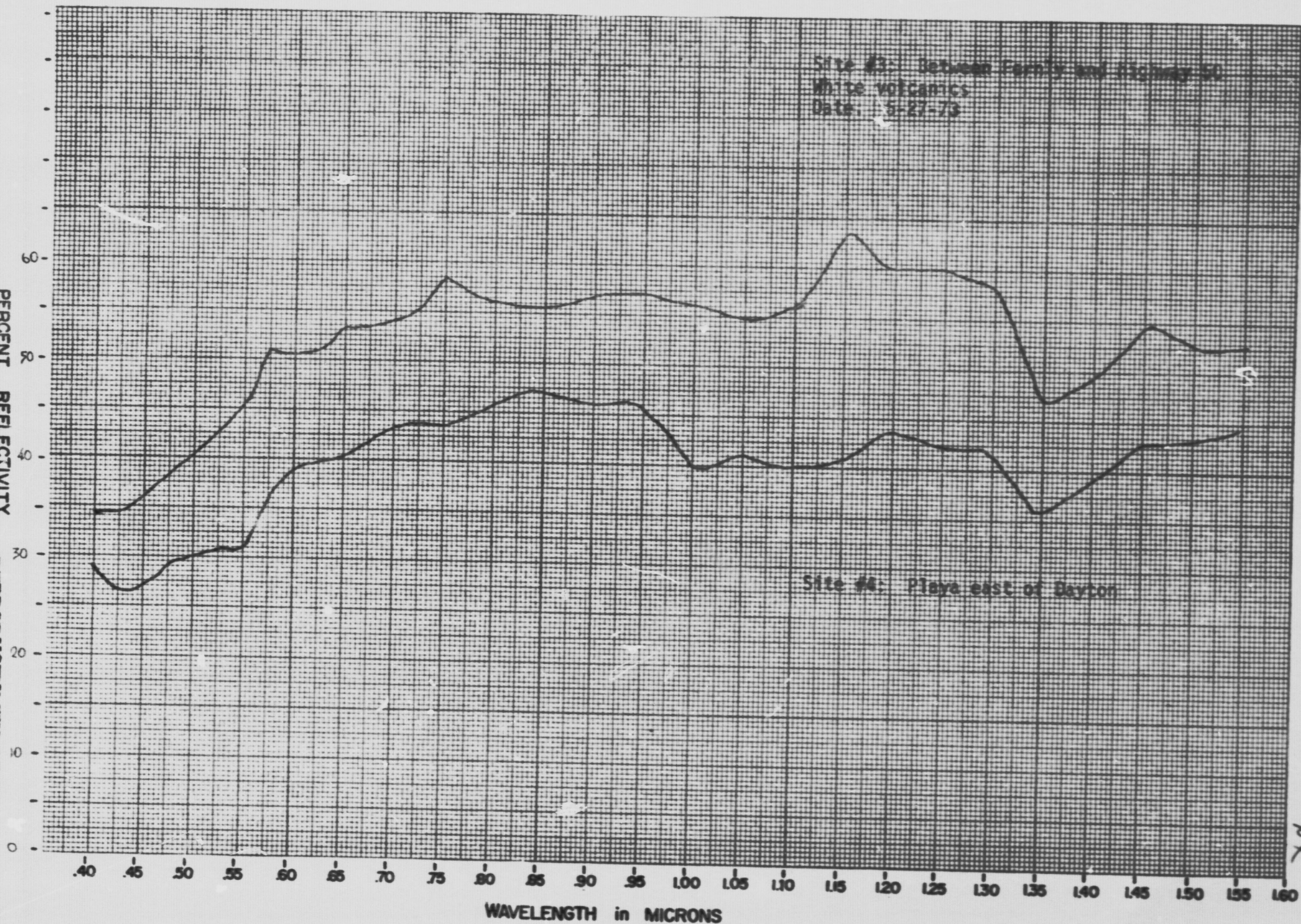
Site #3: Between Farmly and Highway 50
White volcanics
Date: 5-27-73

PERCENT REFLECTIVITY

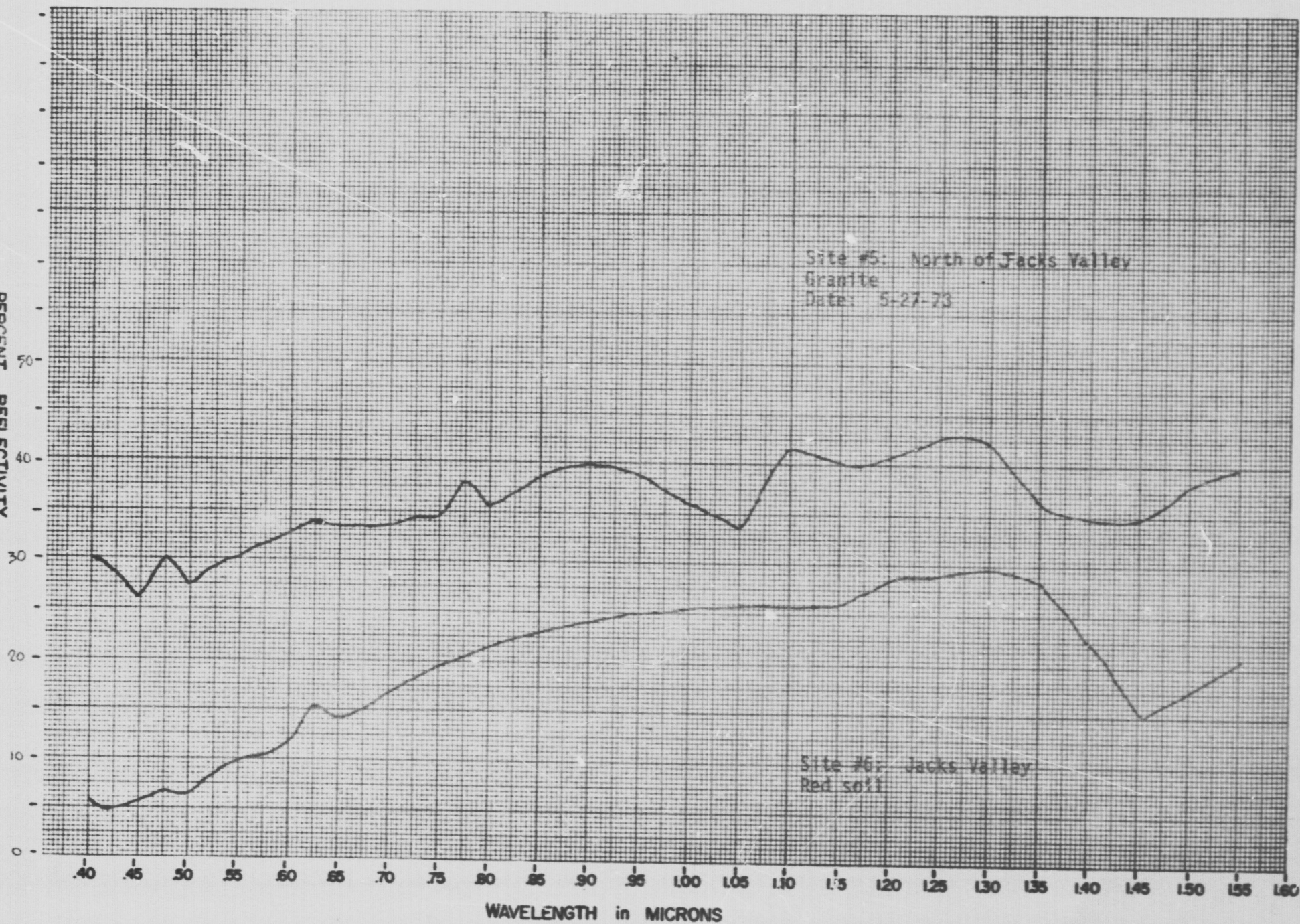
REPRODUCIBILITY OF THE
ORIGINAL PAGE IS POOR.

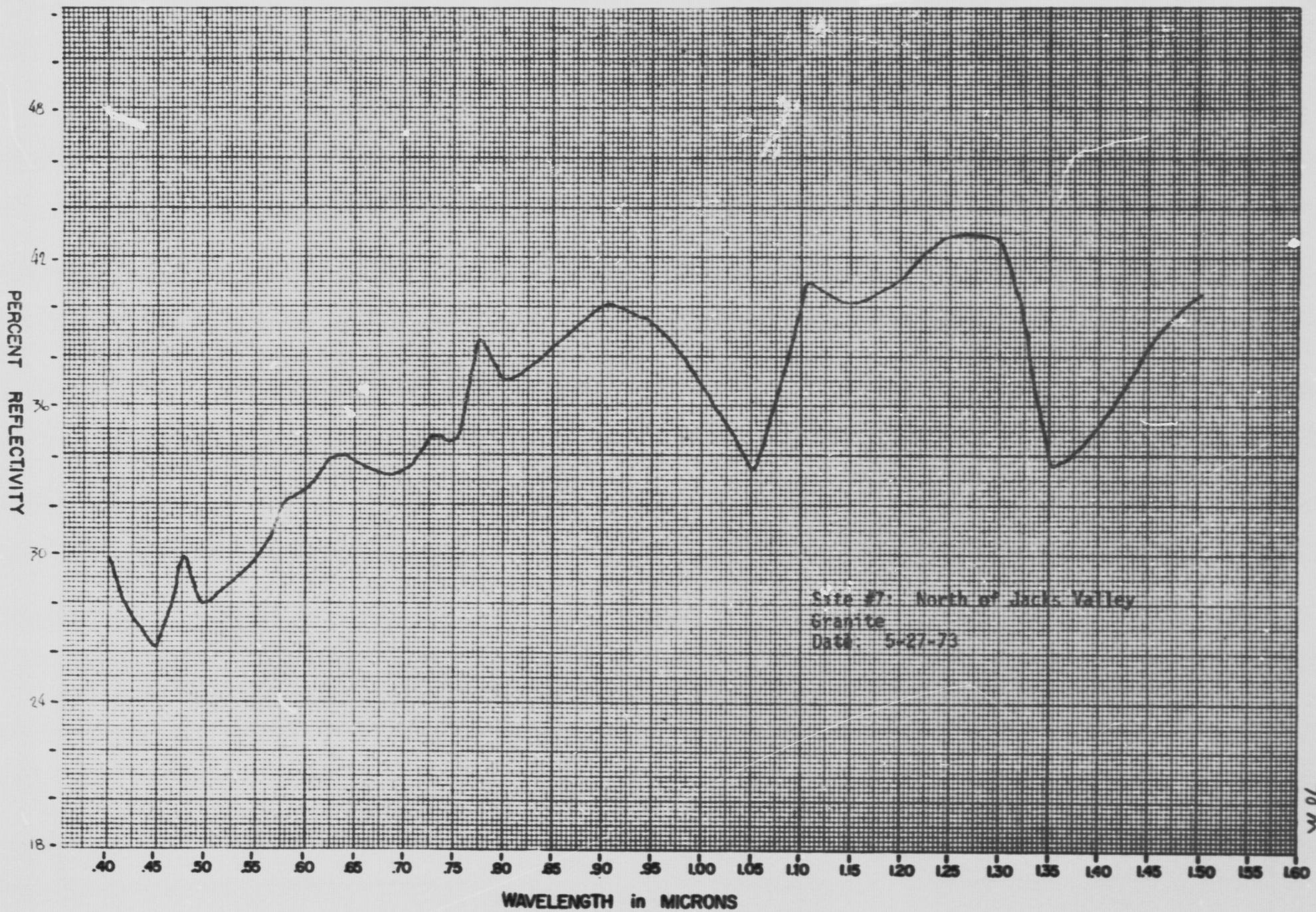
Site #4: Playa east of Dayton

WAVELENGTH in MICRONS



PERCENT REFLECTIVITY





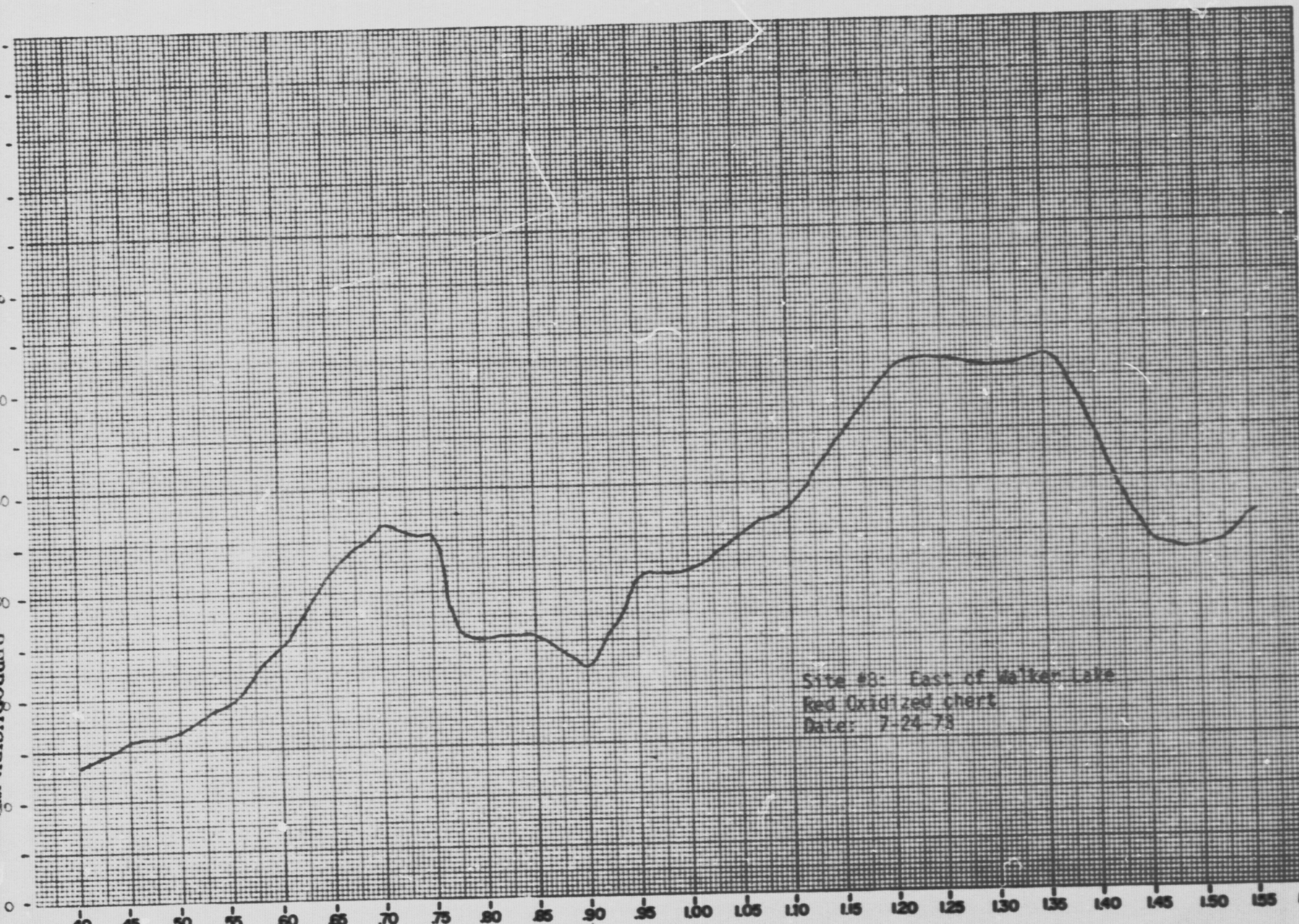
PERCENT REFLECTIVITY

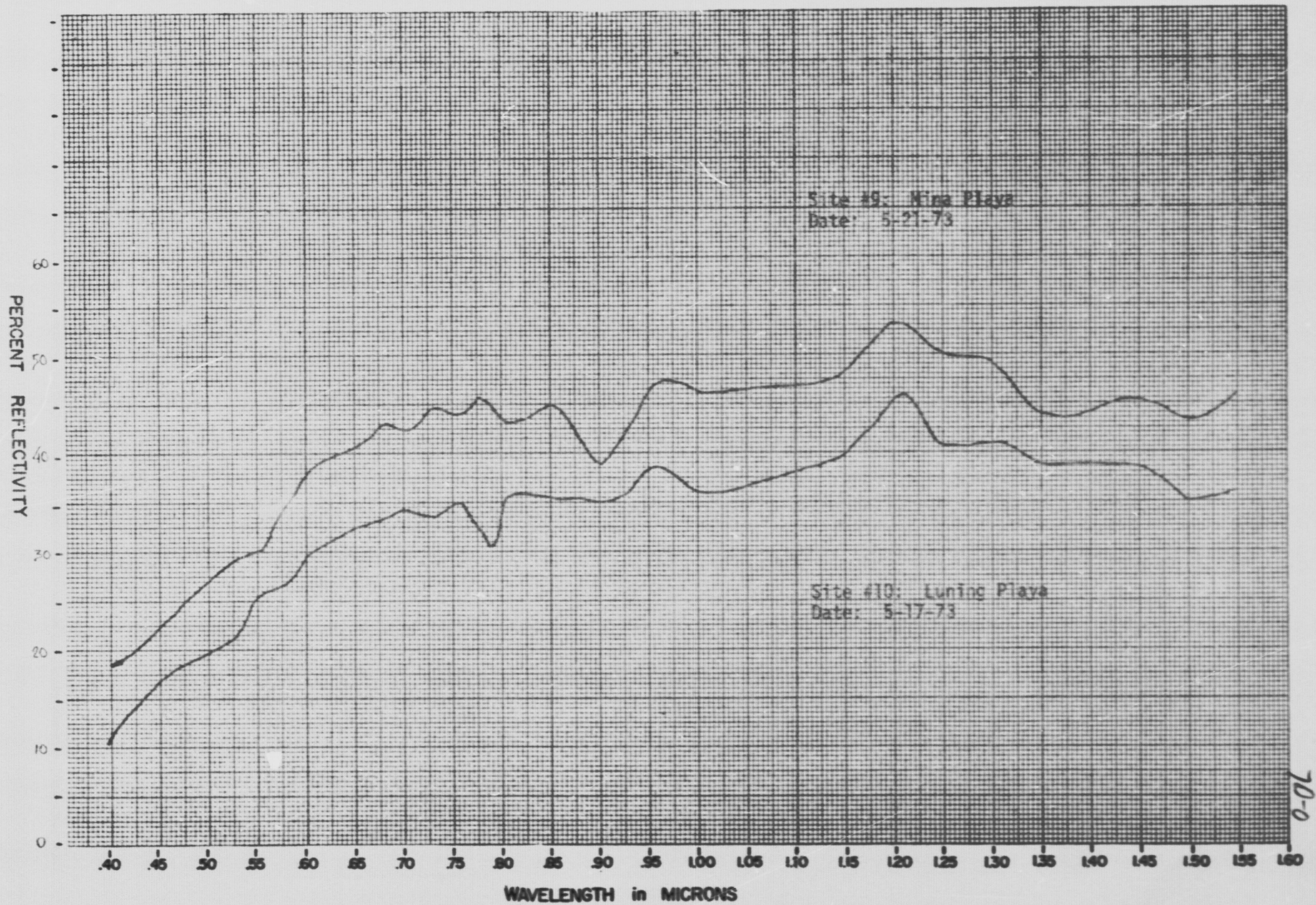
REPRODUCIBILITY OF THE
ORIGINAL PAGE IS POOR

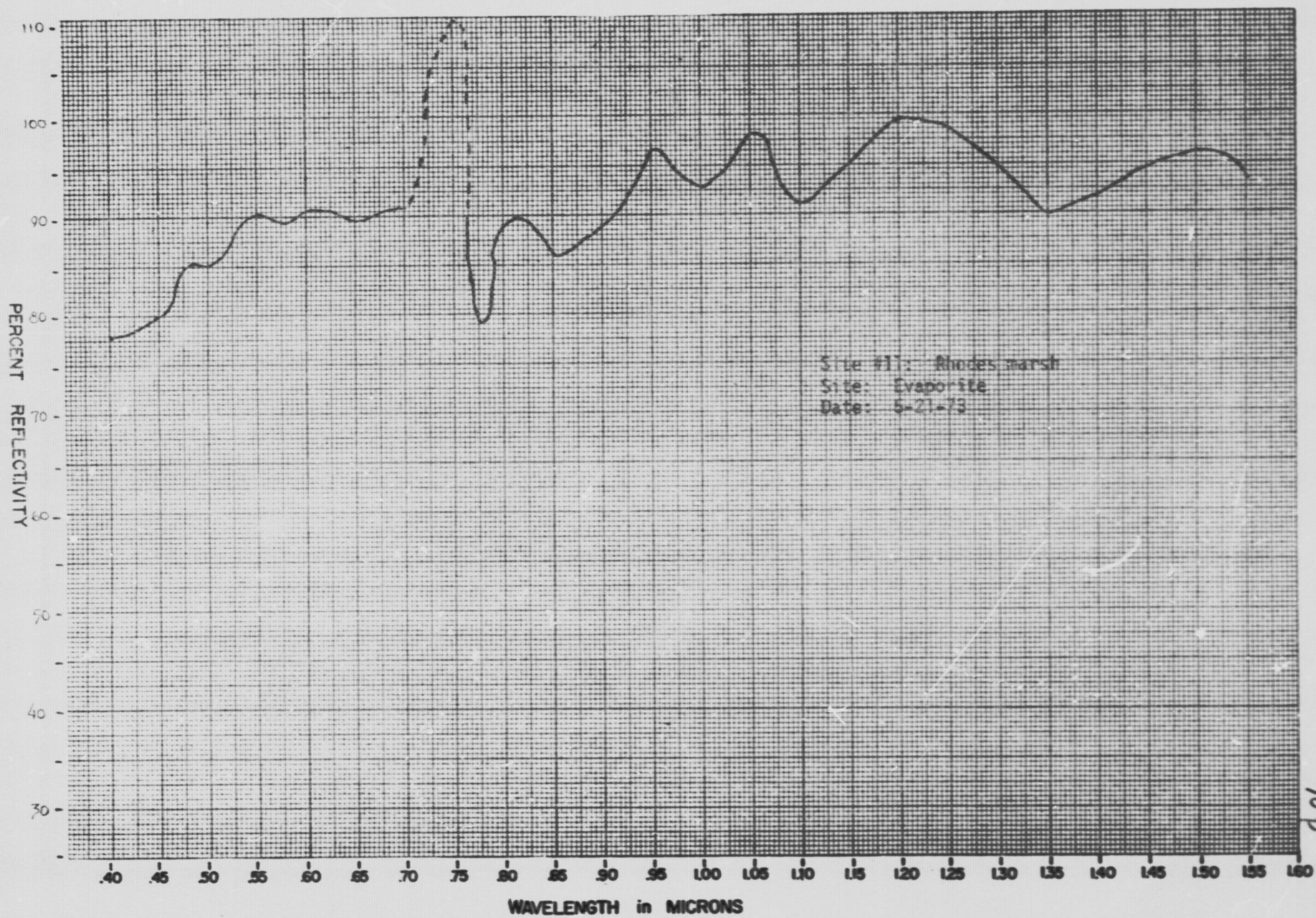
WAVELENGTH in MICRONS

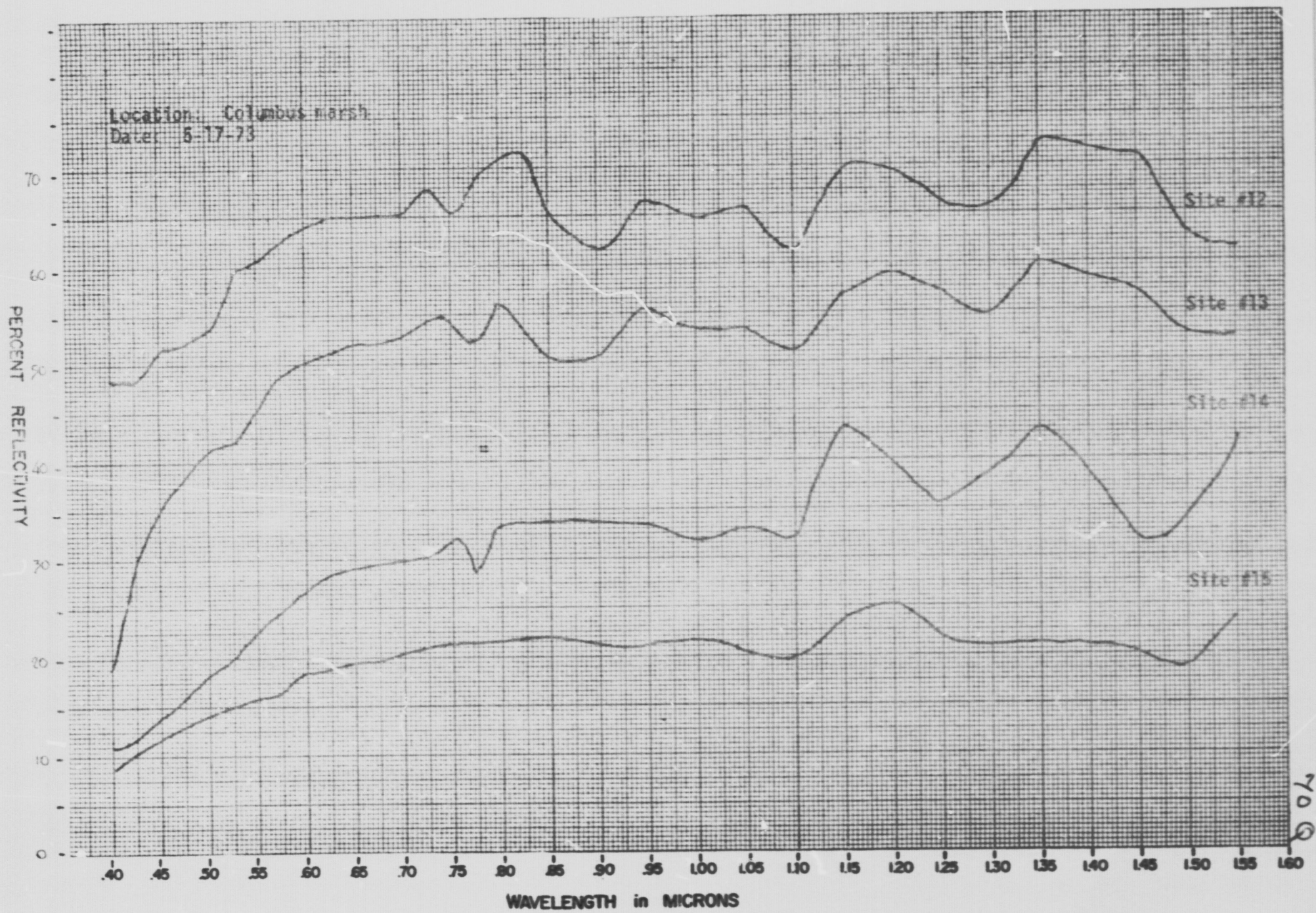
Site #8: East of Walker Lake
Red Oxidized chert
Date: 7-24-78

702

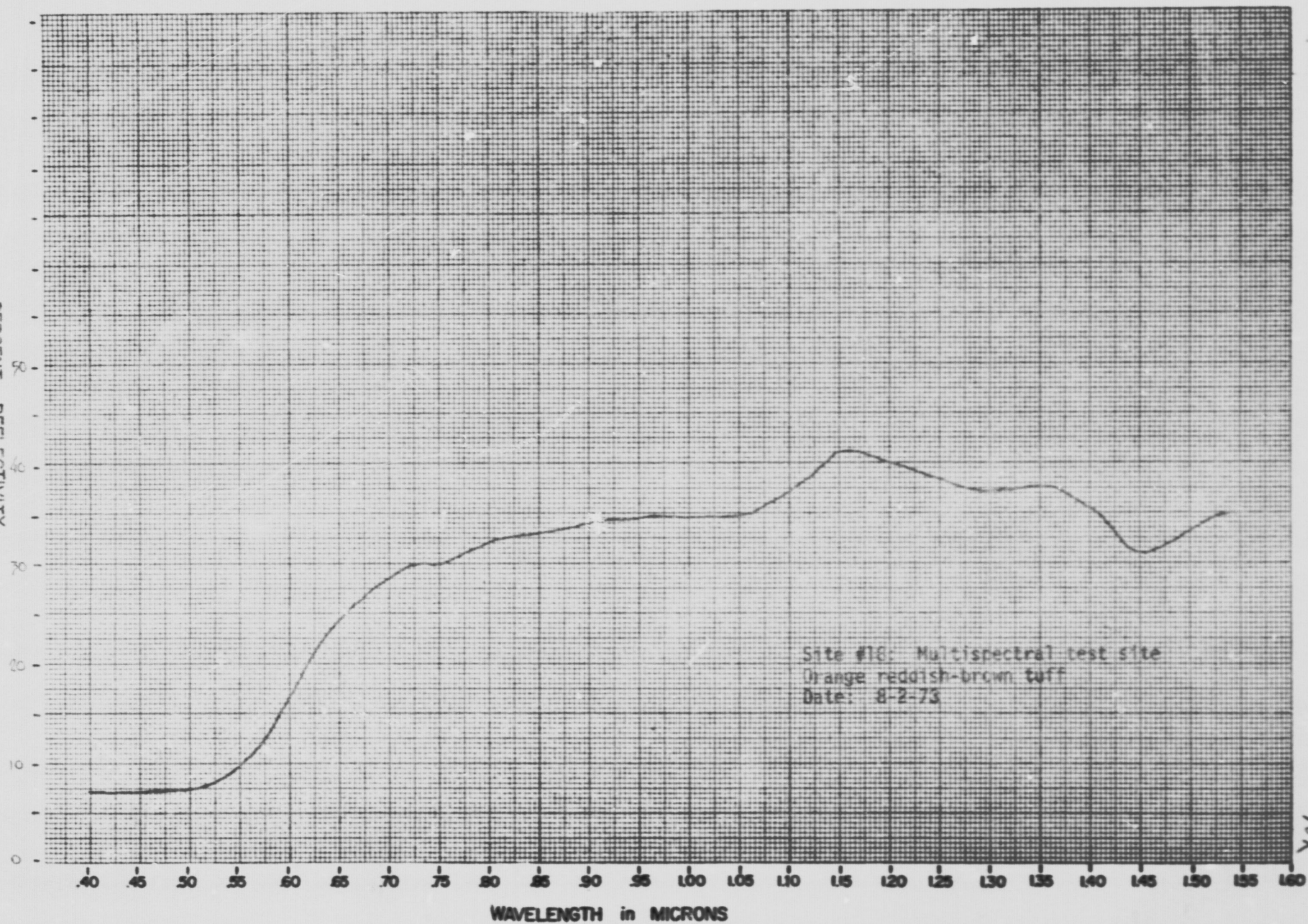






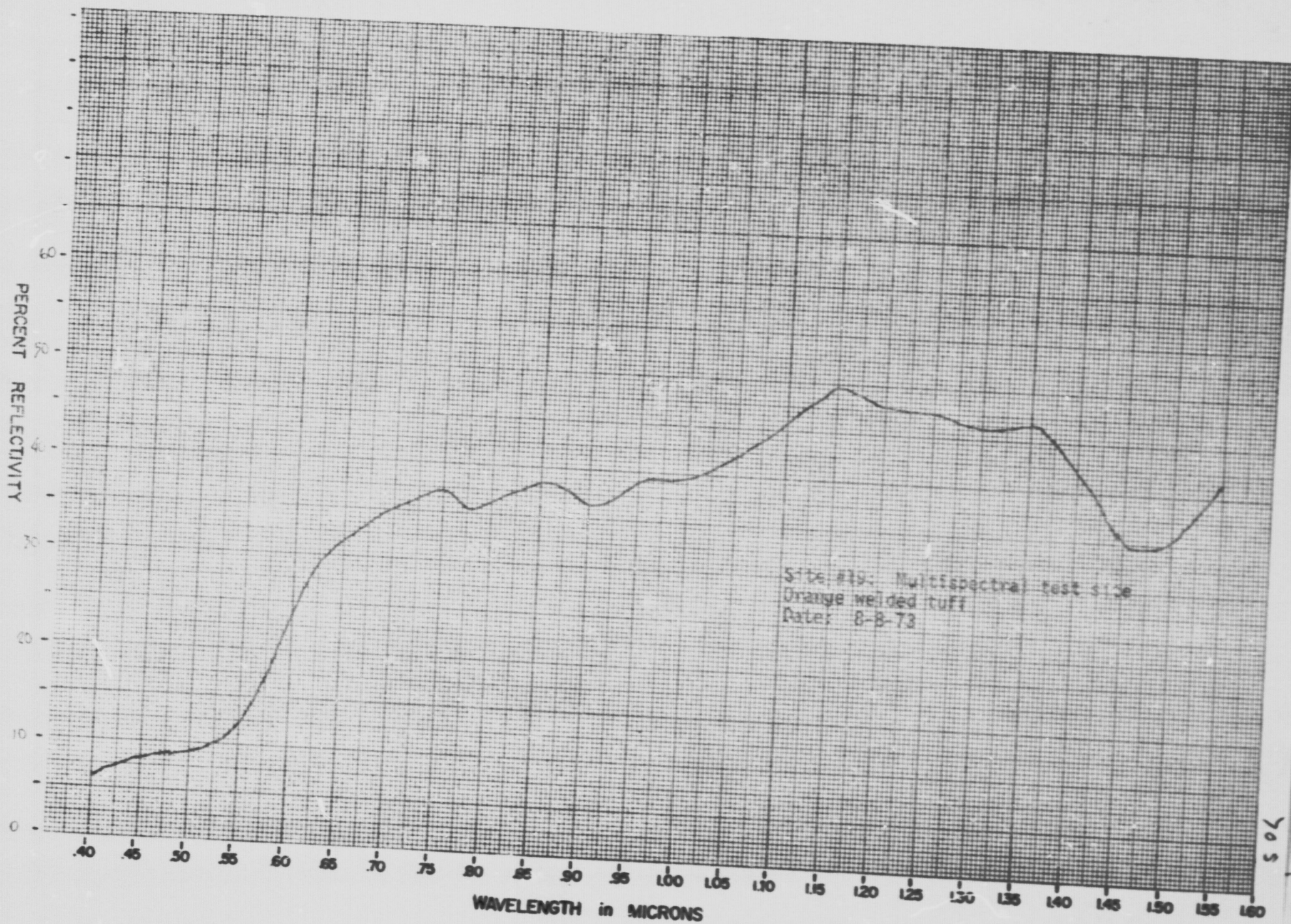


PERCENT REFLECTIVITY



WAVELENGTH in MICRONS

70K



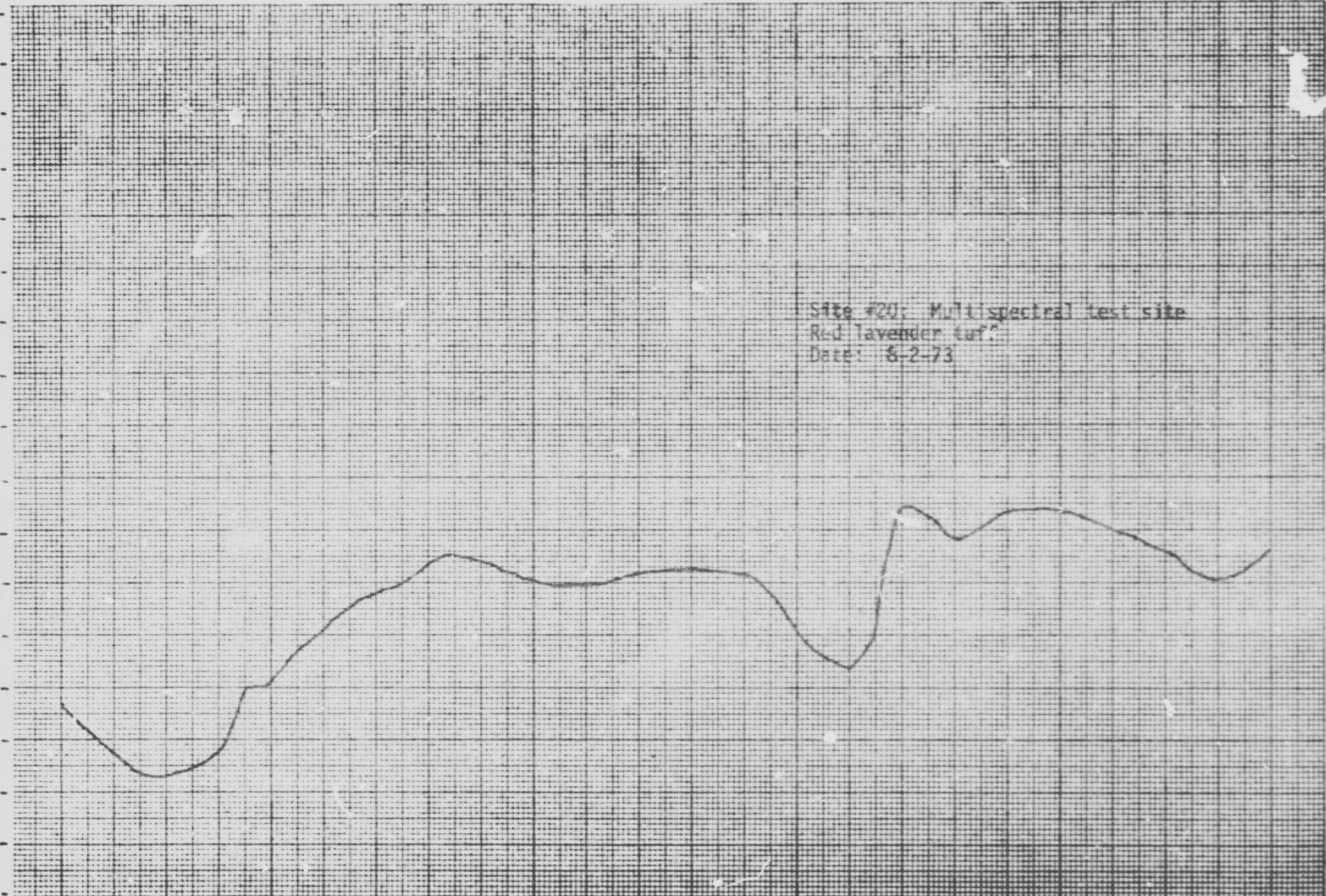
705

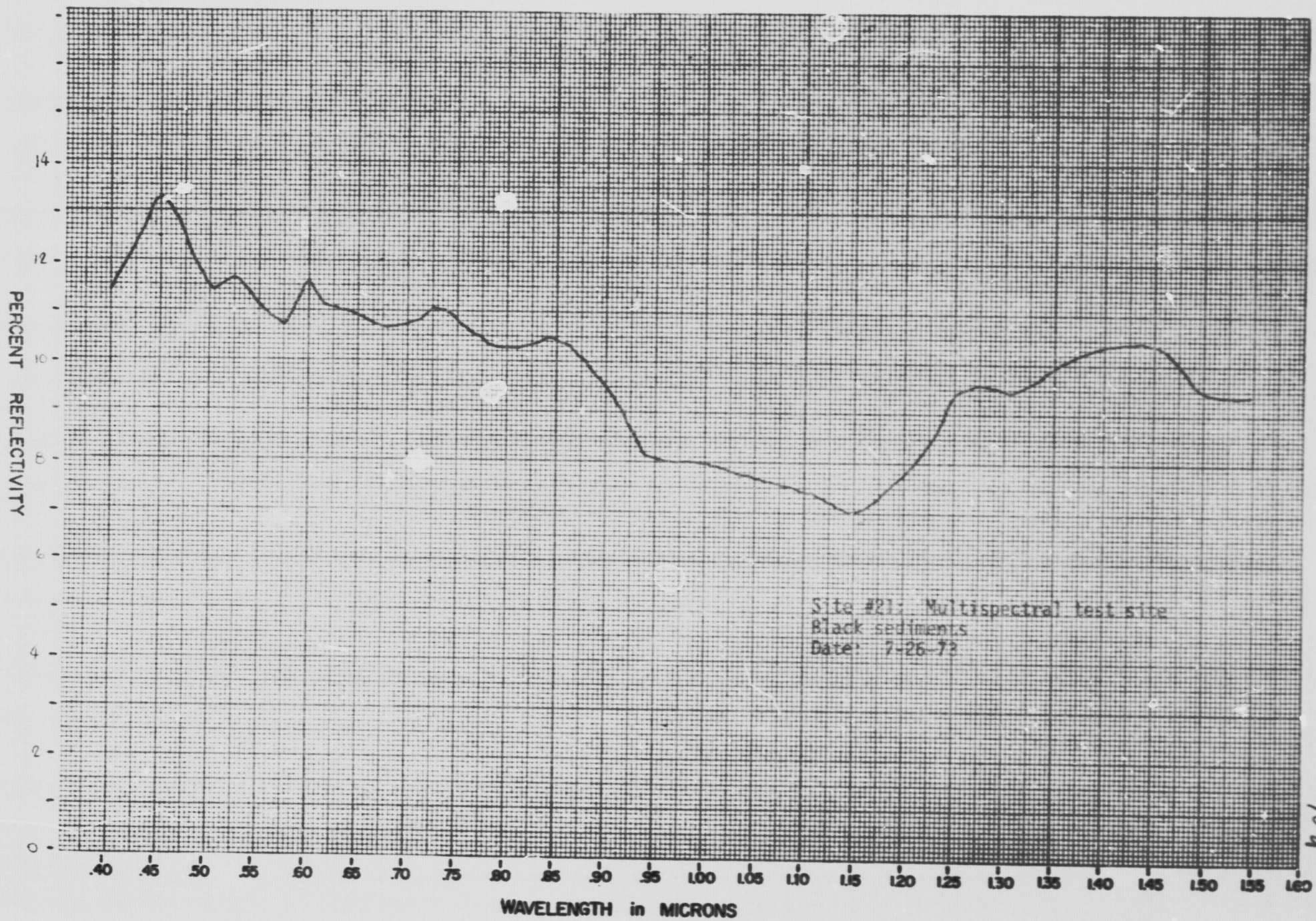
PERCENT REFLECTIVITY

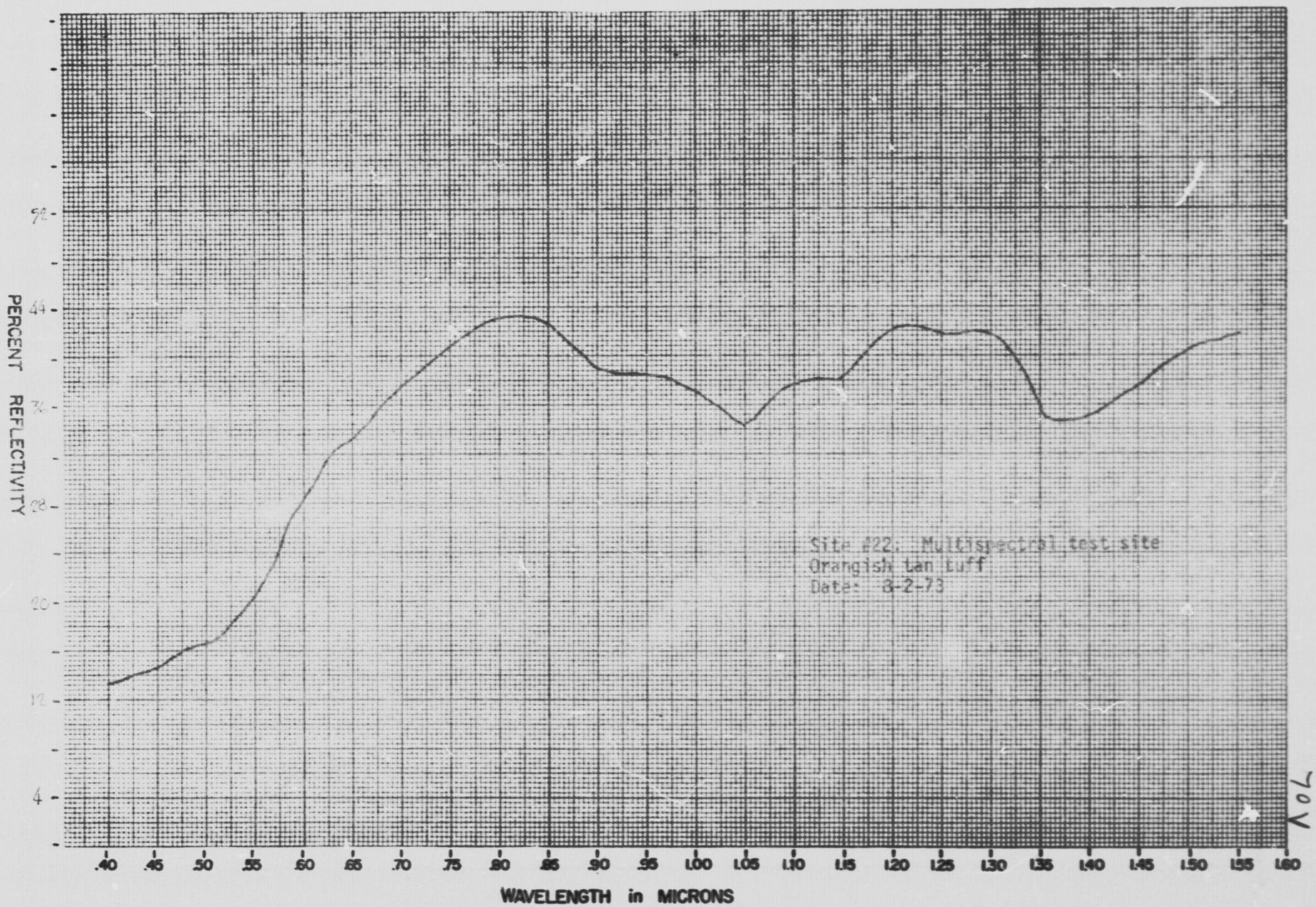
REPRODUCIBILITY OF THE
ORIGINAL PAGE IS POOR

Site #20: Multispectral test site
Red lavender turf
Date: 8-2-73

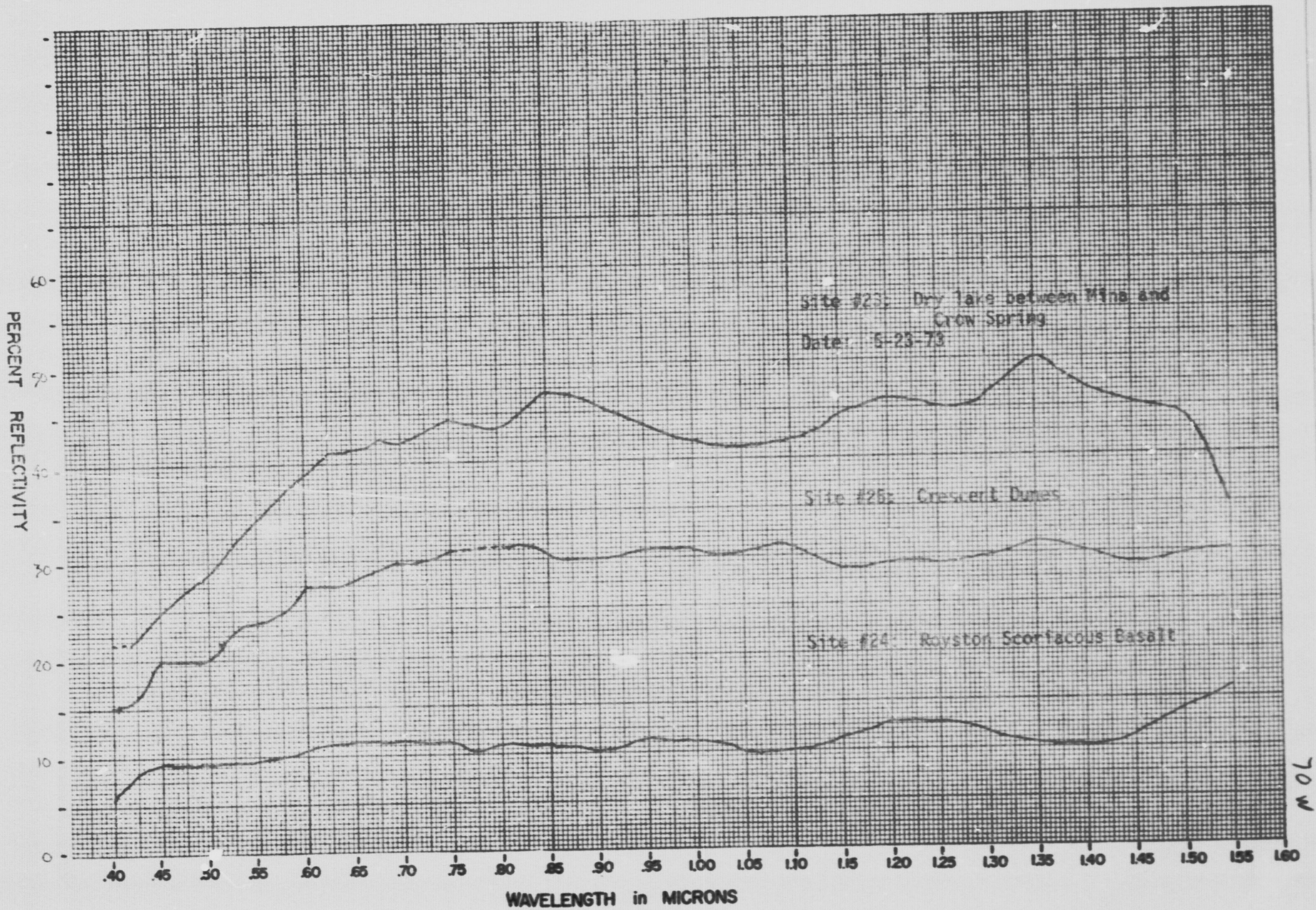
WAVELENGTH in MICRONS

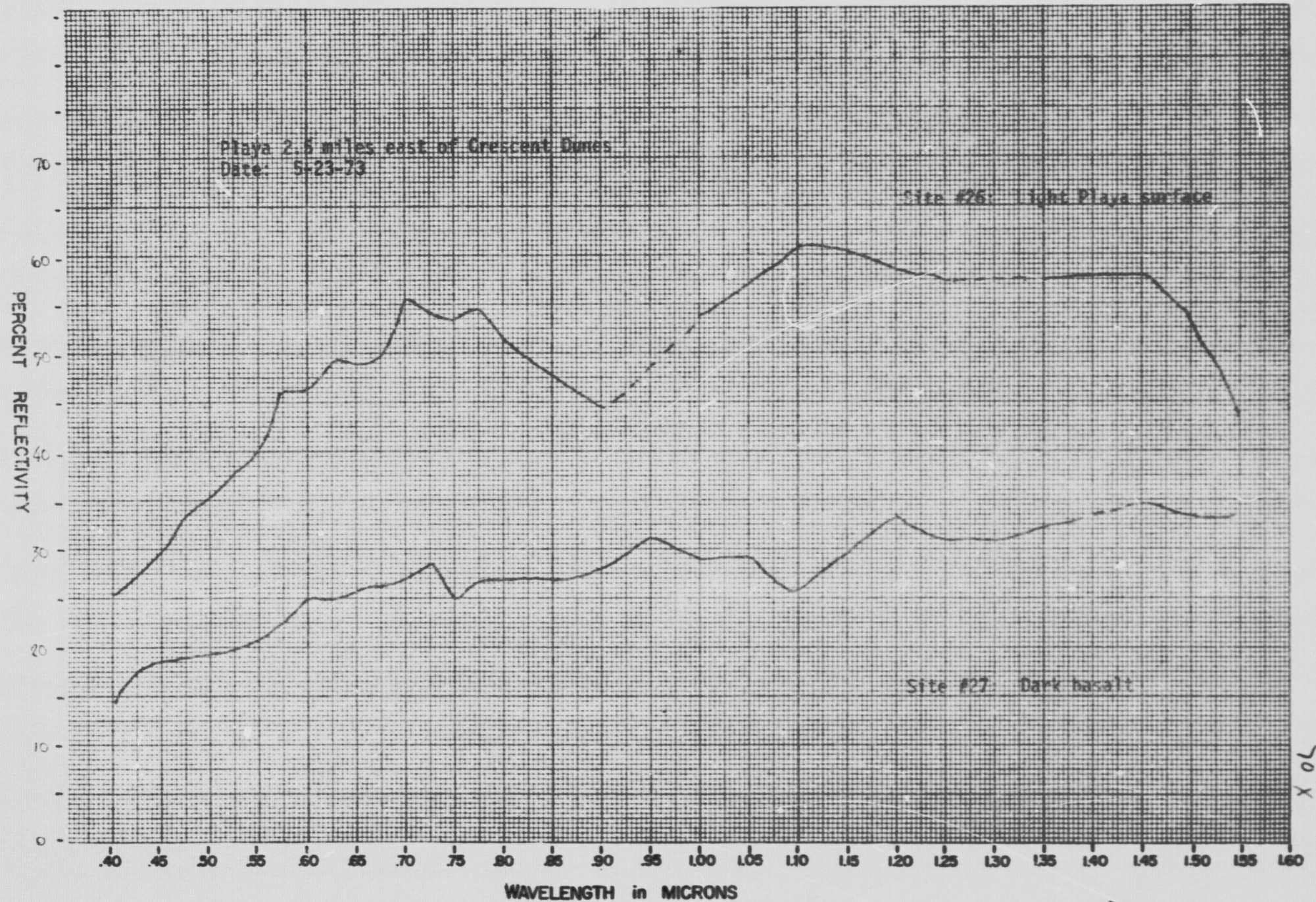


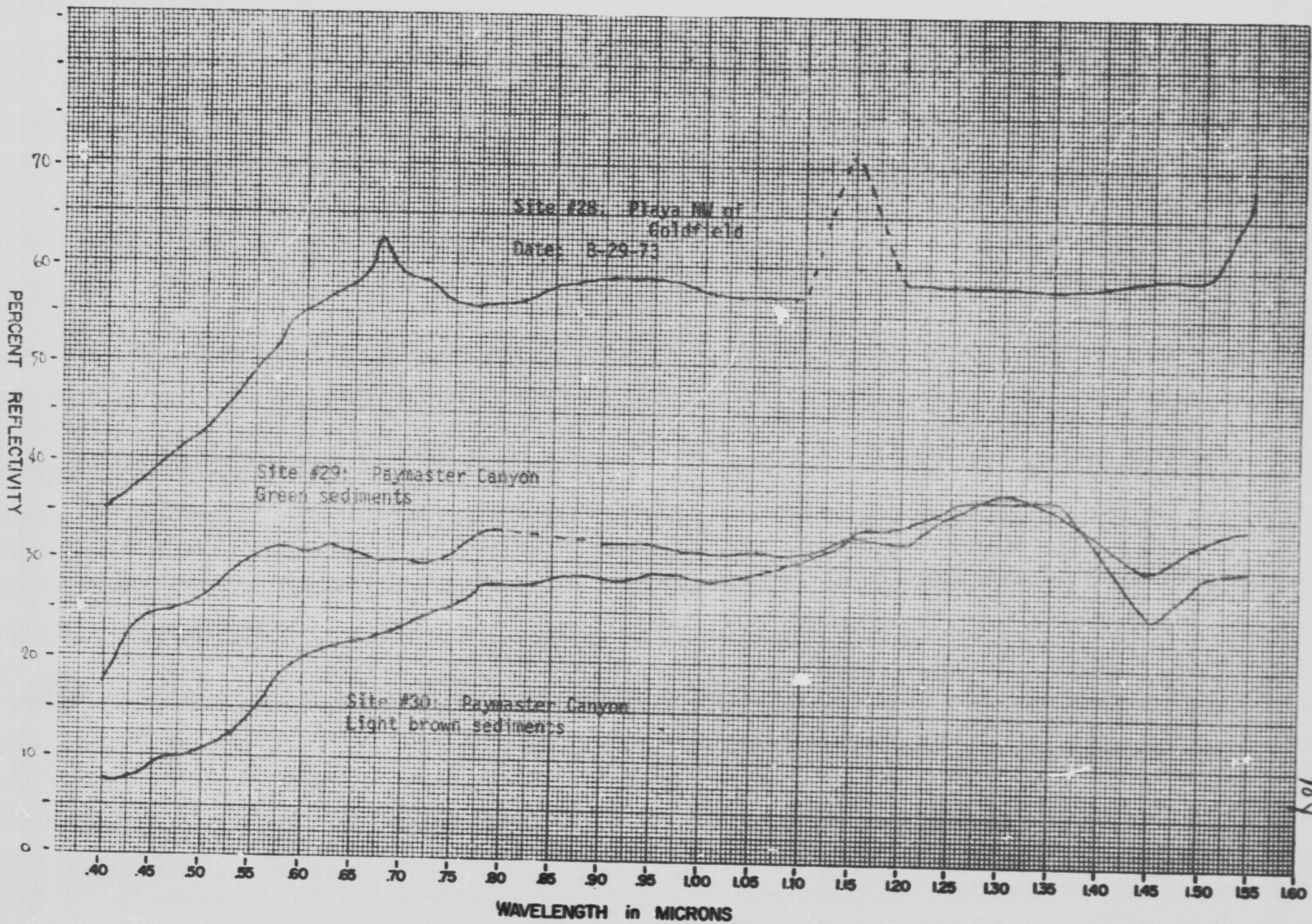


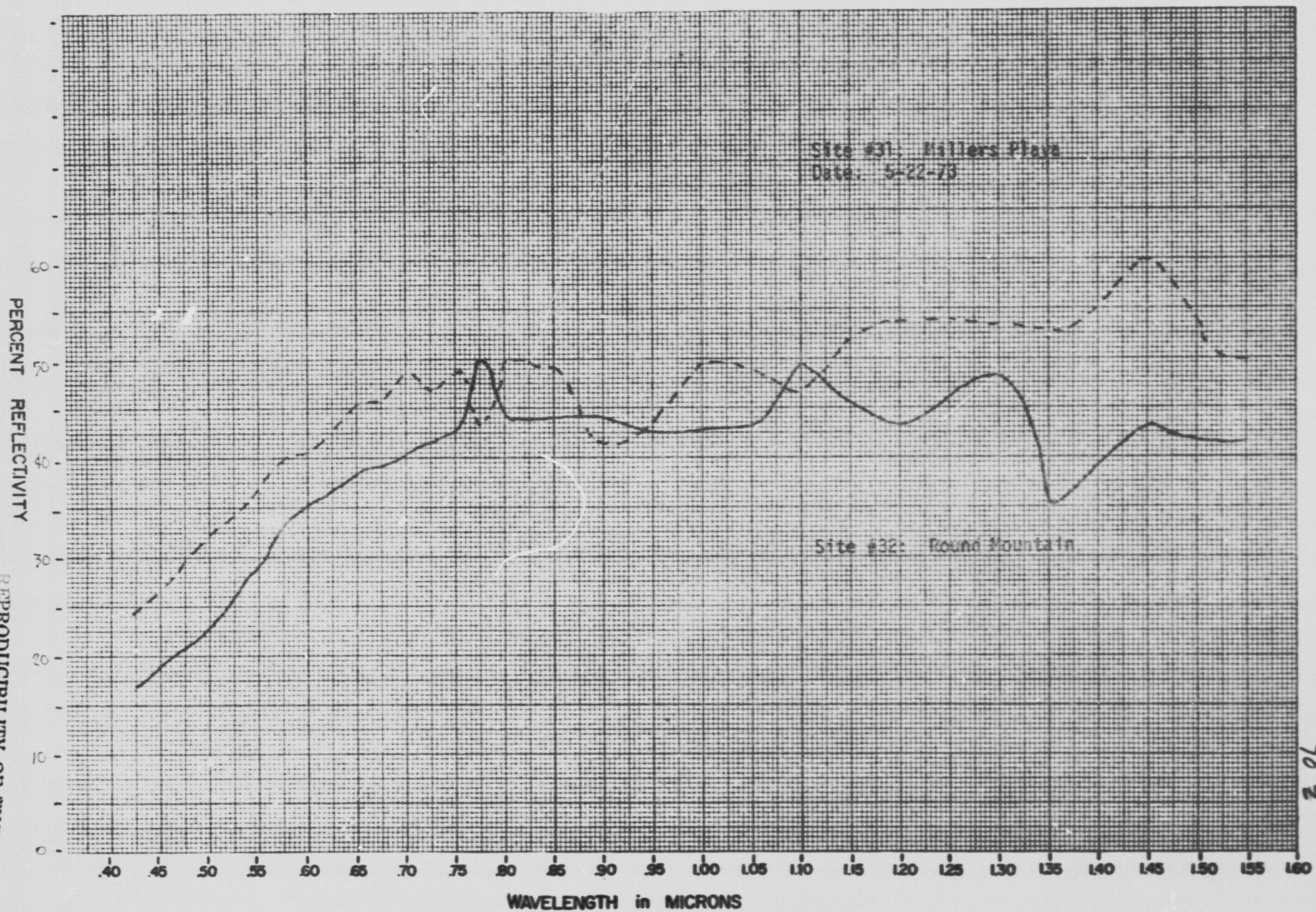


704

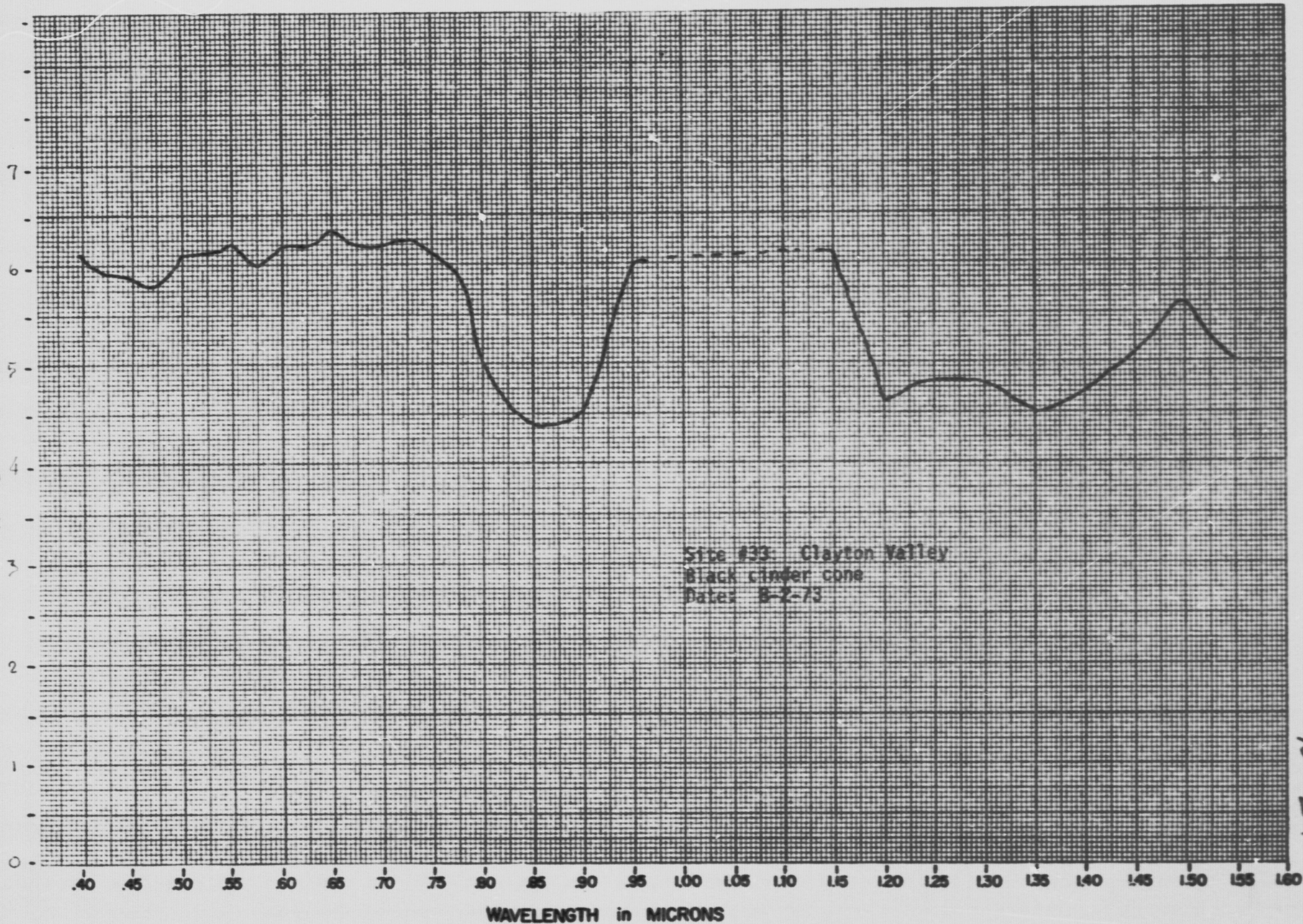




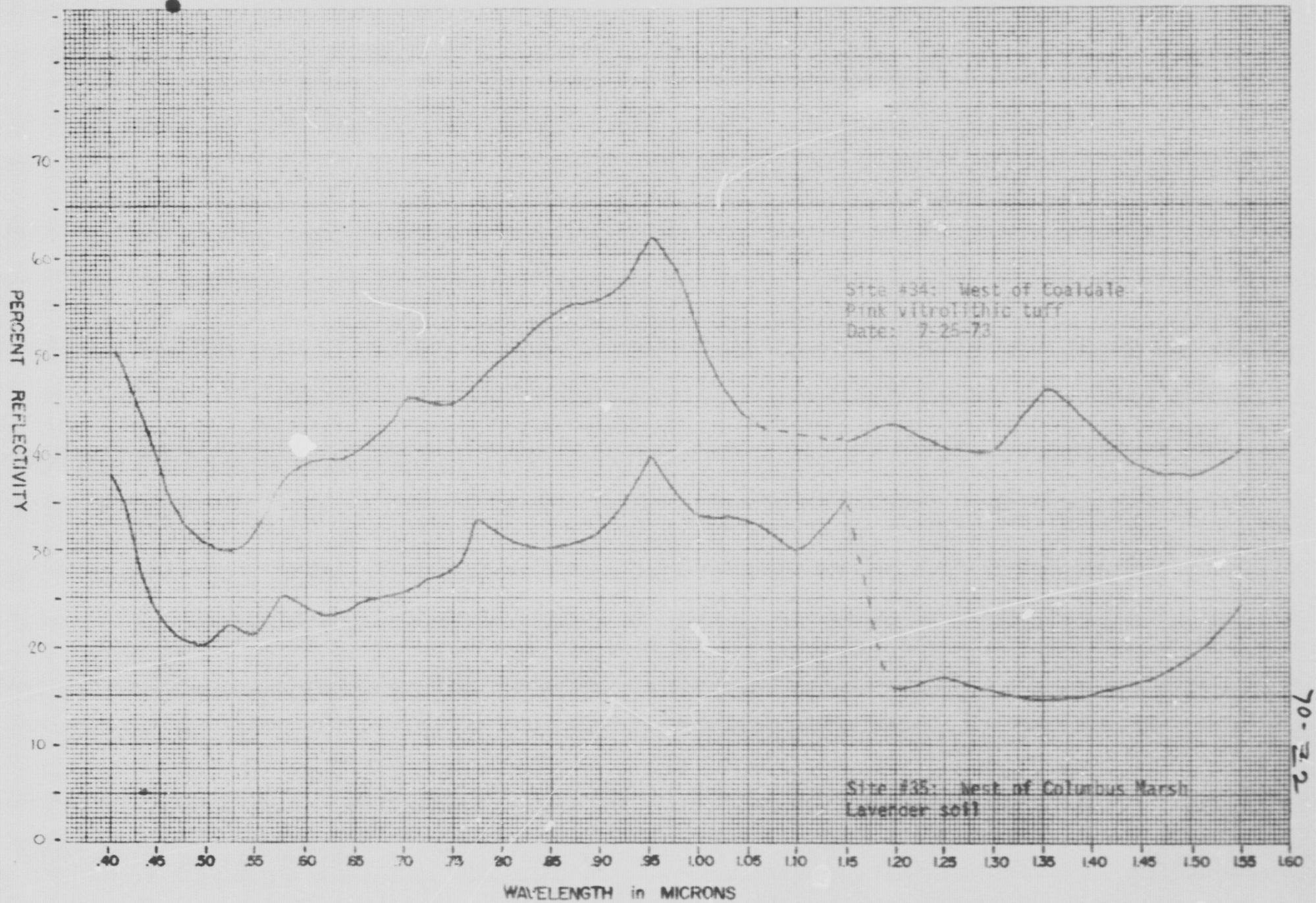




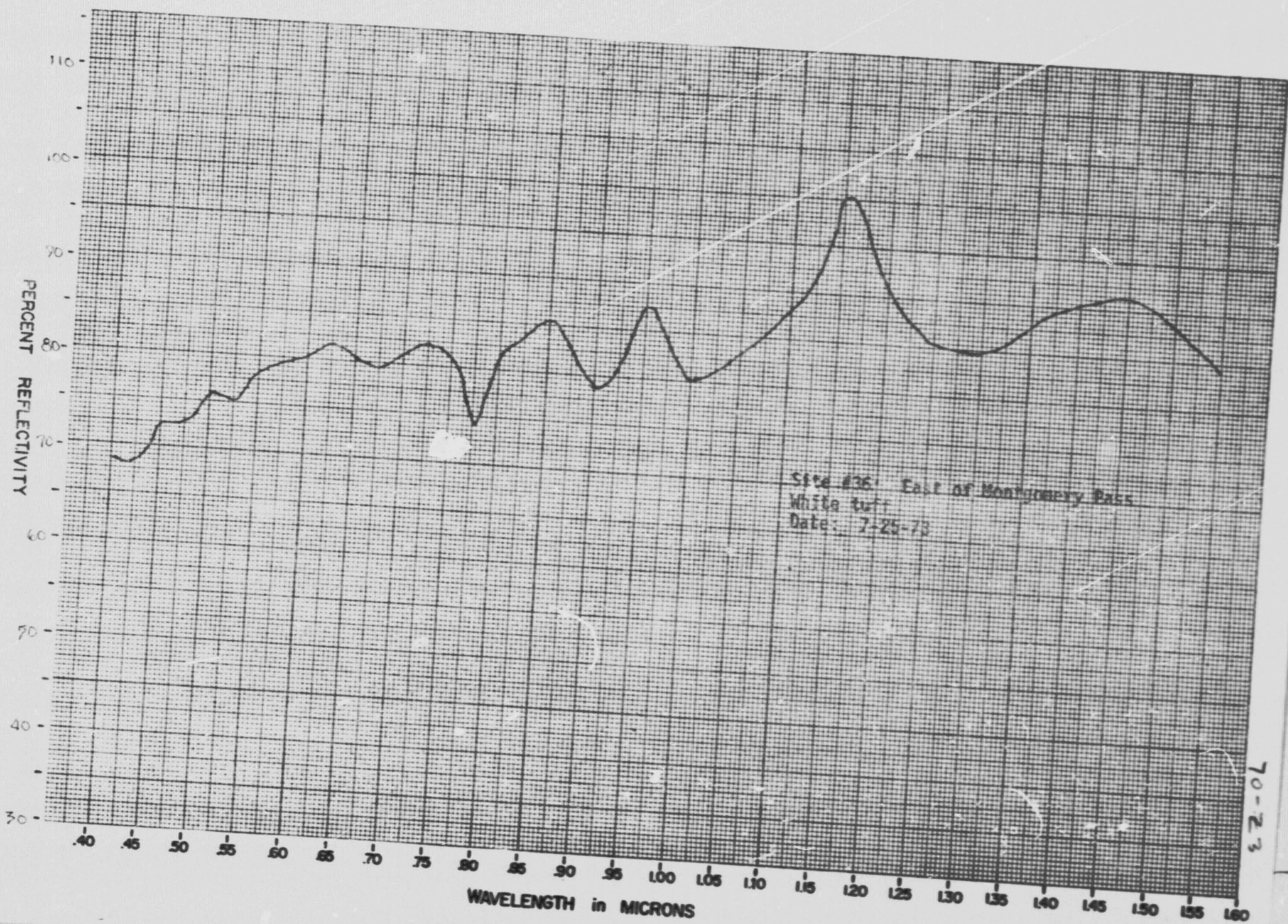
PERCENT REFLECTIVITY



70-71



70-22



PERCENT REFLECTIVITY

70

40

30

20

10

0

Site #37, Montgomery Pass
Red oxidized volcanics
Date: 7-25-78

WAVELENGTH in MICRONS

.40 .45 .50 .55 .60 .65 .70 .75 .80 .85 .90 .95 1.00 1.05 1.10 1.15 1.20 1.25 1.30 1.35 1.40 1.45 1.50 1.55 1.60

PERCENT REFLECTIVITY

50

40

30

20

10

0

.40

.45

.50

.55

.60

.65

.70

.75

.80

.85

.90

.95

1.00

1.05

1.10

1.15

1.20

1.25

1.30

1.35

1.40

1.45

1.50

1.55

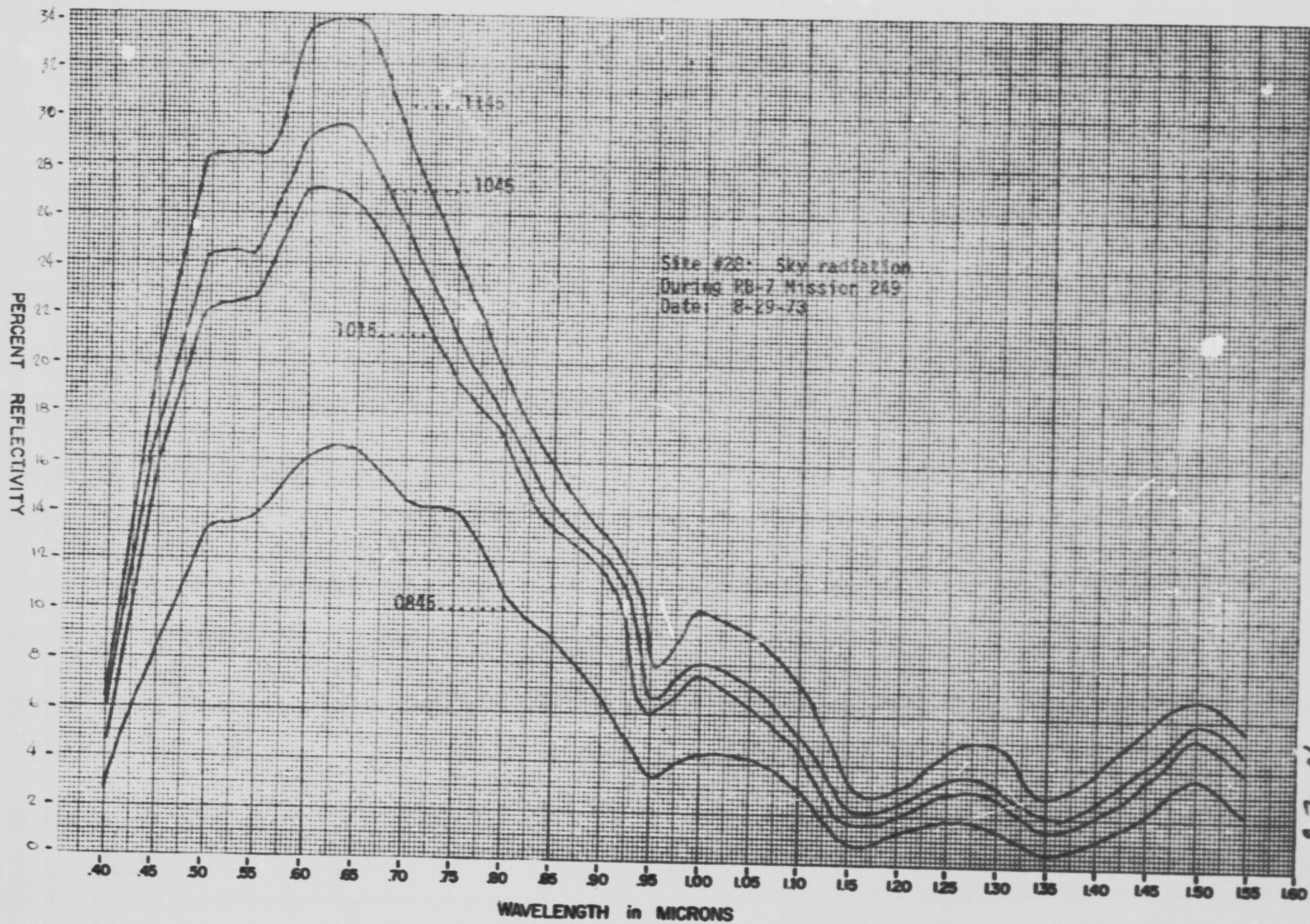
1.60

WAVELENGTH in MICRONS

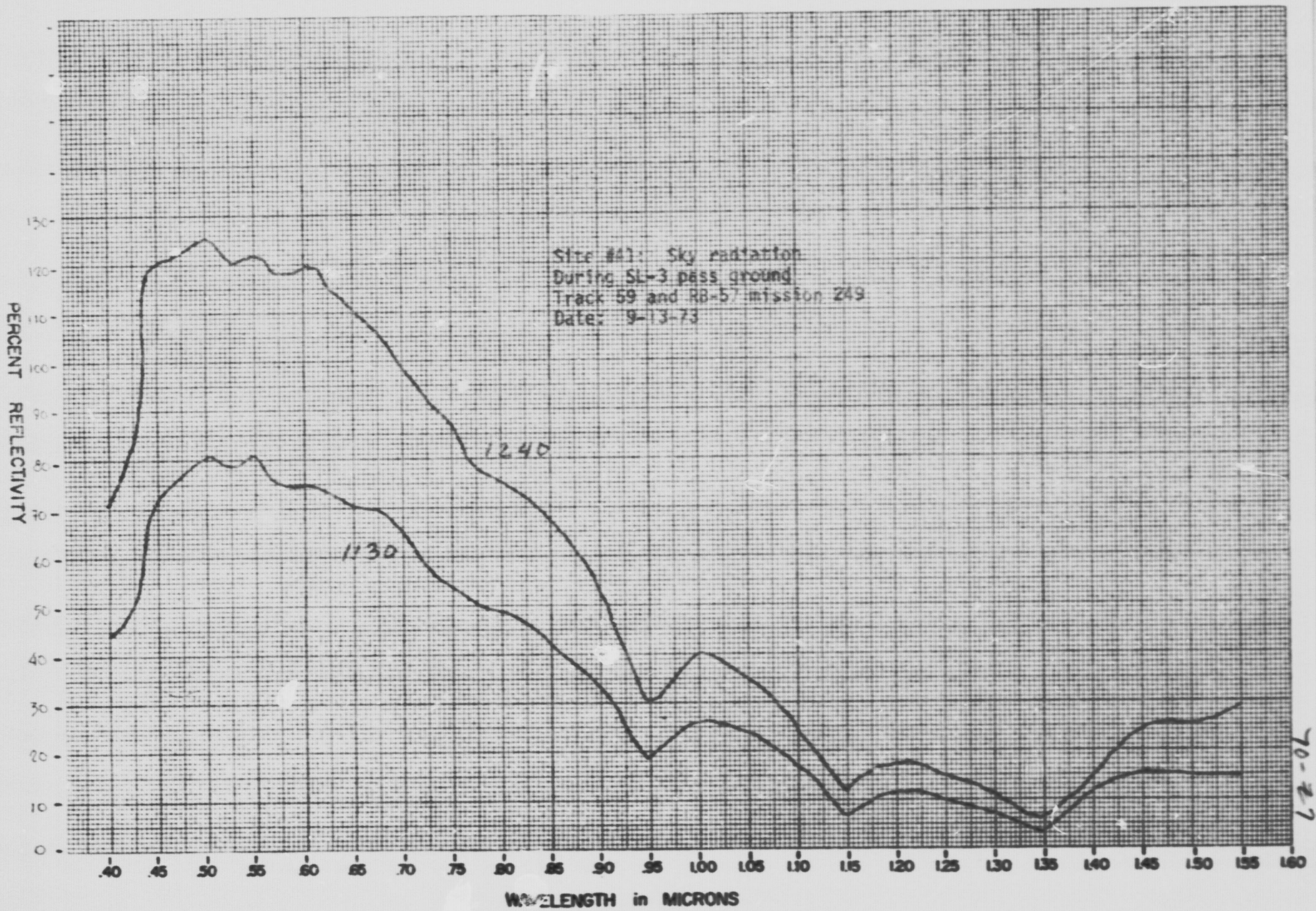
Site #38: Granite 7 mile north Benton Junction
Date: 8-1-73

Site #39: Clayton Valley
Green sediment
Date: 8-29-73

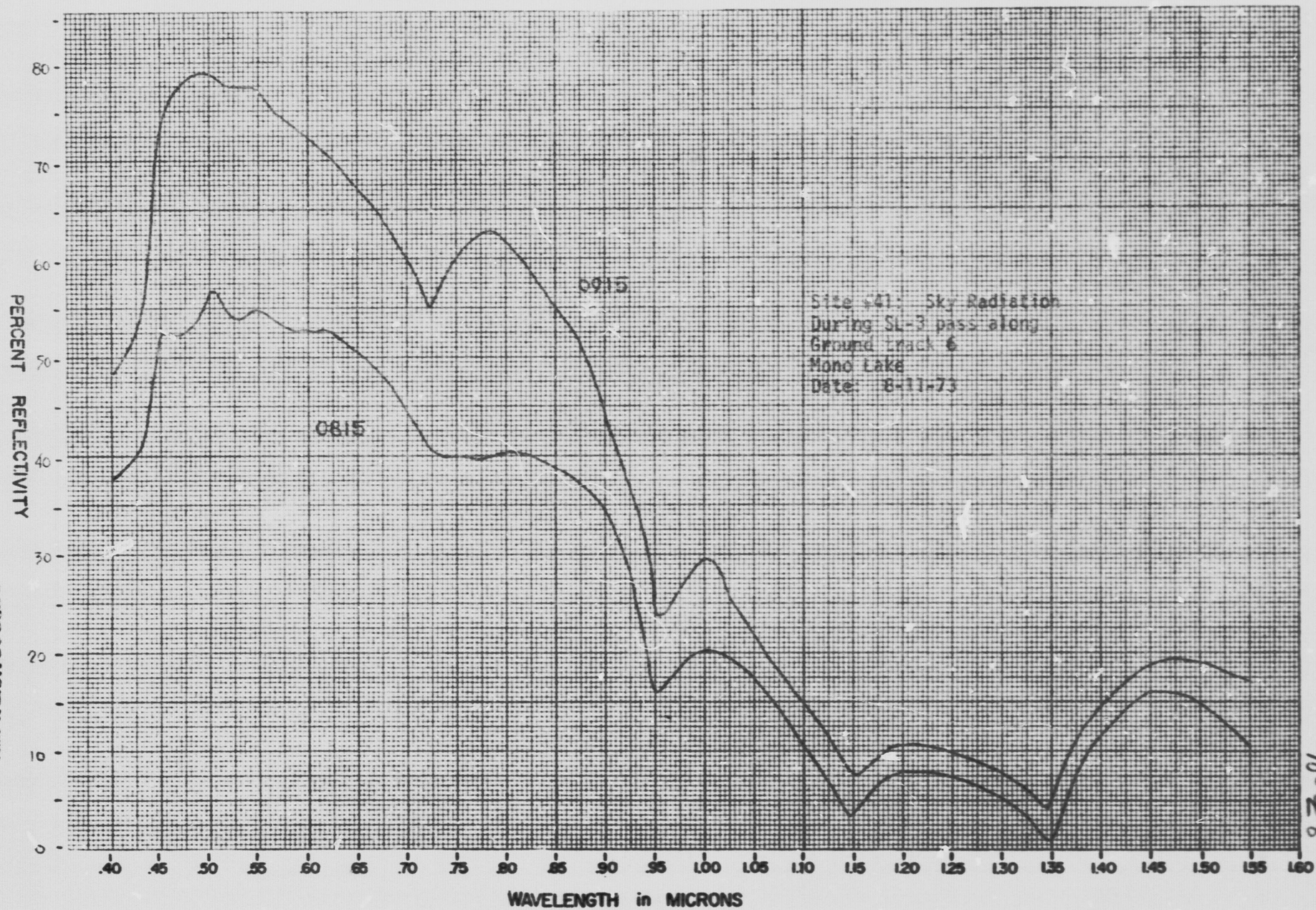
10-25

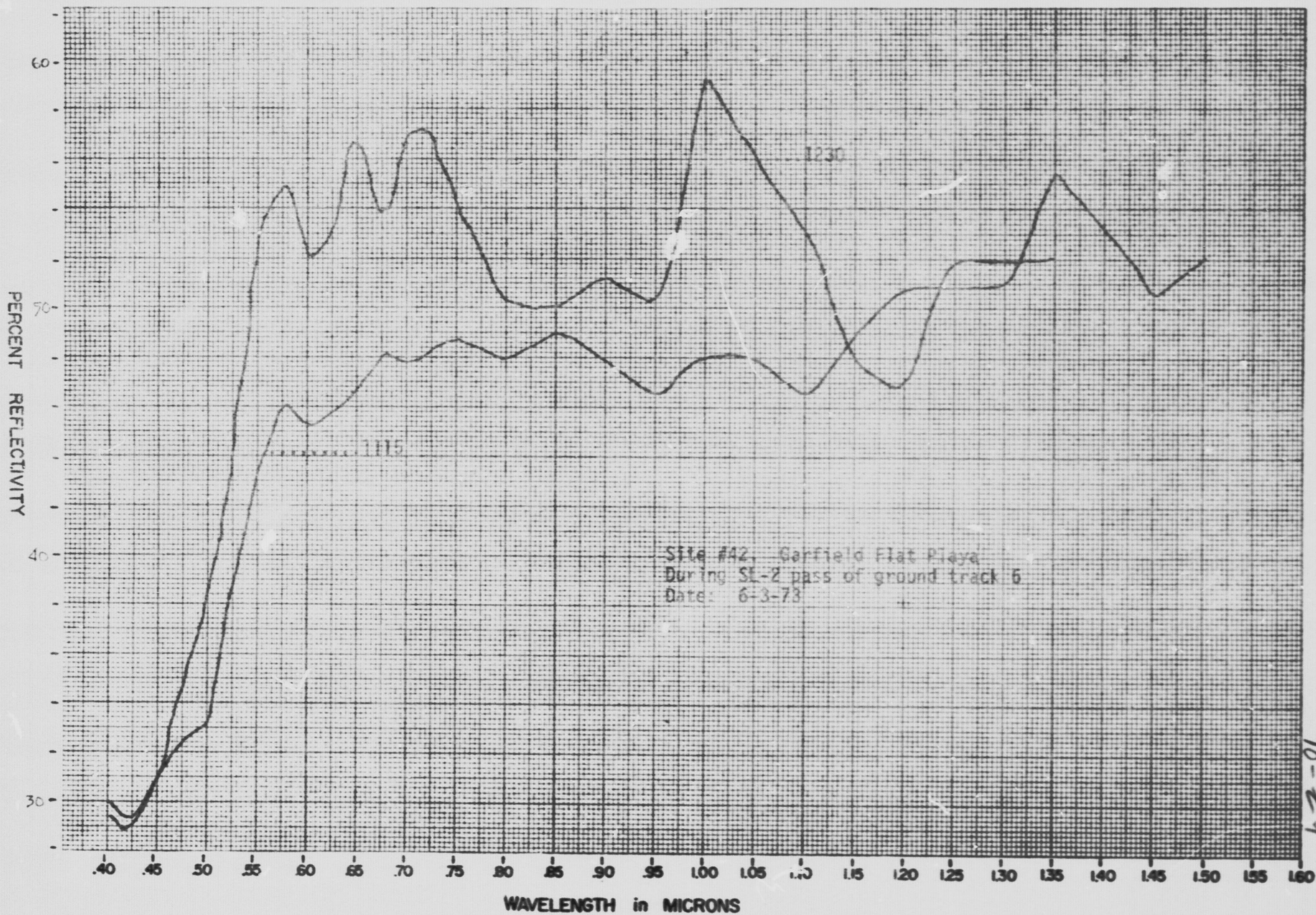


70-26

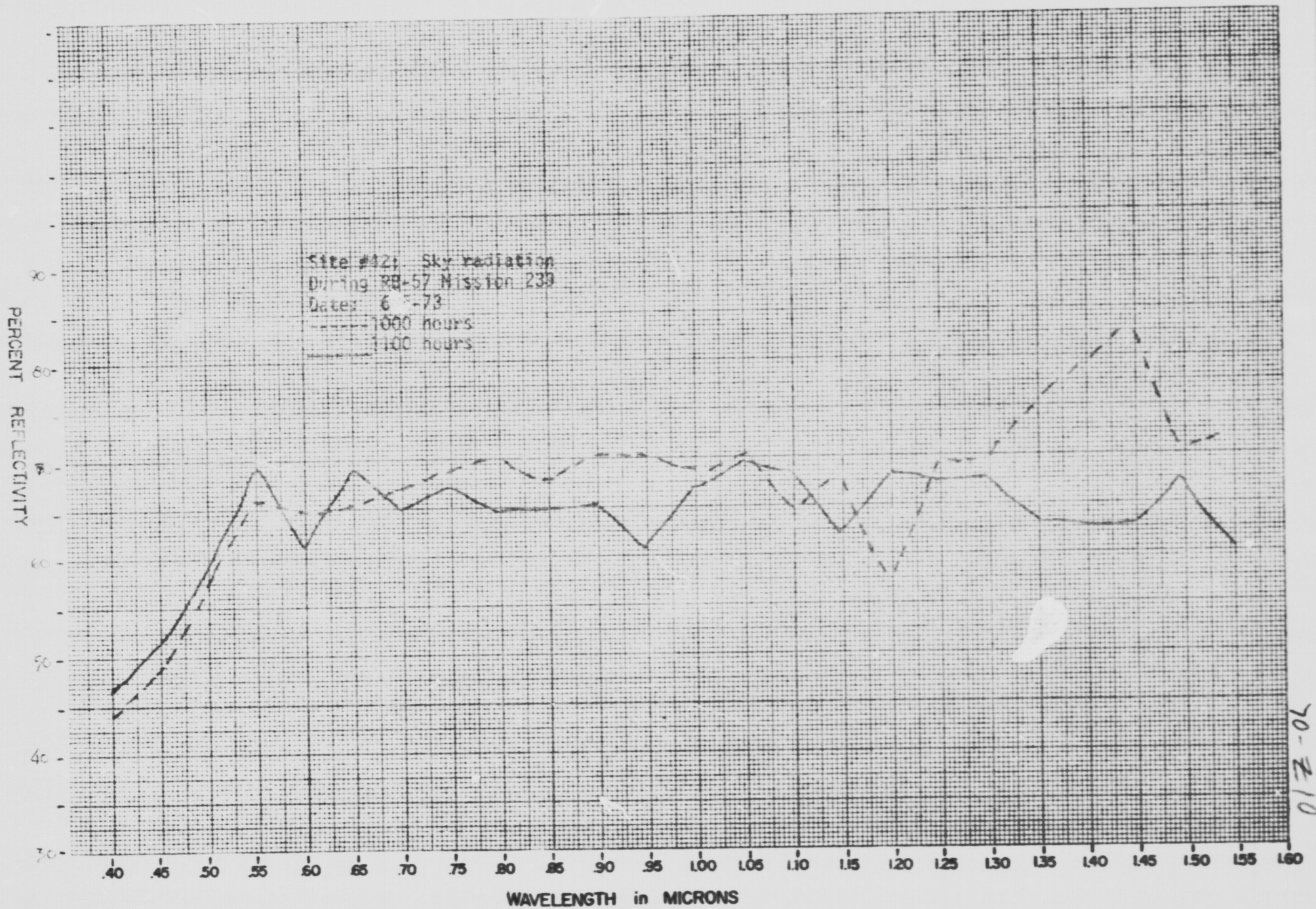


70-27





10-2-73



70-710